Functional Relationship between Merlin and the ERM Proteins

Advisor: Dr. Andrea I. McClatchey Alan M. Hebert

Functional Relationship Between Merlin and the ERM Proteins

Abstract

The ability to spatially restrict specific activities across the cell cortex functionally defines individual cells and tissues. This is achieved, in part, via the assembly of protein complexes that link the plasma membrane to the underlying cortical actin cytoskeleton. The neurofibromatosis type 2 (NF2) tumor suppressor Merlin and closely related ERM proteins (Ezrin, Radixin and Moesin) are a special class of such membrane:cytoskeleton associated proteins that function to organize specialized cortical domains. In addition to their high degree of similarity, mounting evidence suggests that Merlin/ERMs share a functional relationship, which is largely unexplored. Unlike Merlin, the ERMs are not known to inhibit cell proliferation; in fact, Ezrin is thought to *promote* tumor metastasis. Defining the relationship between Merlin and the ERMs is essential to appreciating their respective roles in cancer development.

Here I demonstrate a novel role for Merlin and the ERMs in generating cortical asymmetry in the absence of external cues. Our data reveal that Merlin functions to restrict the cortical distribution of Ezrin, which in turn positions the interphase centrosome in single epithelial cells and 3D organotypic cultures. In the absence of Merlin, ectopic cortical Ezrin yields mispositioned centrosomes, misoriented spindles and aberrant epithelial architecture. Furthermore, in tumor cells with centrosome amplification, the failure to restrict cortical Ezrin abolishes

centrosome clustering, yielding multipolar mitoses. Consistent with a functional relationship, I observe a strong genetic interaction between *Nf2* and *Ezrin* in the mouse intestine *in vivo.* Finally, I begin to address the basis of their functional interaction by testing whether they are coordinately regulated by the Ste-20 like kinase SLK. Altogether, these data uncover fundamental roles for Merlin/ERM proteins in spatiotemporally organizing the cell cortex *in vitro* and *in vivo* and suggest that Merlin's role in promoting cortical heterogeneity may contribute to tumorigenesis by disrupting cell polarity, spindle orientation and potentially genome stability.

TABLE OF CONTENTS

Acknowledgements

My time as a graduate student has been an incredibly transforming period in my life. I became a husband and father, as I aspired to make a scientific contribution to the field of Cancer Biology. Here, I have come to appreciate that science truly is a collaborative endeavor, not only among our fellow scientists but also through the support and sacrifices of our family and friends. It is only because of this support that I am able to submit a body of work that I take great pride in, which I hope will facilitate new ways of thinking about Cancer Biology.

None of this would be possible without the support and sacrifices of my family. First, I would like to thank my parents, who made graduate school at Harvard University a possibility for me. Mom and Dad, the values and determination you instilled in me from an early age are the tools I continue to fall back upon to confront any challenge. I will never forget the quiet sacrifices you made to support me in every aspect of my life. In particular, my wife Tanja has been by my side (sometimes carrying me) through the rigors that a laboratory science schedule demands. Tanja, I could not ask for a better friend, wife and mother of our children. You have been a tremendous source of strength when I needed it the most and I couldn't overstate my appreciation. To my daughters Dakota and Savannah, you are my daily inspiration and the reason I strive to be a better person. To my brother Michael, thank you for your companionship and encouragement. I'm proud to call you my brother. My grandparents Mary Ellen and Albert, you are a shining example of what family is all about. I value all of the guidance and support you have provided throughout my life. Finally, to my in-laws Zofia and Giro I can't thank you enough for raising such a wonderful daughter and saving the day when we needed help the most.

The central figure in my scientific growth has been and is my mentor Andi. As a graduate student and parent I presented a number of unique challenges that Andi took on with great patience and grace. When I became overwhelmed and discouraged Andi helped put me back on my feet and sent me off feeling confident that I could take on the next obstacle. Your faith and support of my work has given me the confidence to truly believe I can be a successful scientist and for that I am most grateful. I feel lucky to have been trained by someone with such a pure love and enthusiasm for science. Andi's intense work ethic reflects her passion for science and has been inspirational for me, who often thought that raising two kids was challenging. Thank you Andi for your continued support of my work and decisions, especially through the rough patches.

In addition to having Andi as a mentor I had the great fortune of working with a wonderful crew of hand picked, top tier scientists that comprise the McClatchey lab. To my friend and colleague Andrew, you have been an important catalyst to my development as a scientist. I value the friendship and scientific input you so generously provided me with over the years. I look fondly back on having beers at

Atwood's and talking science. I wish you the best of luck as you build your own lab at MD Anderson. I thank all the members of the McClatchey lab for their support and input over the years. Zach, thanks for the company during those late night experiments and for tolerating the inappropriate amount of '80s music I played; Samira, thank you for making me laugh when I felt down, listening when I needed to vent, but most of all for your friendship; Marcello, thank you for all of your guidance, support and friendship, you have been sorely missed by many here; Jessica, thank you for your input and your willingness to help; Jen, Banu, Christine and Annie thank you all for your many helpful contributions. Finally, Brian, it has been a pleasure to work with you for this short period. Thank you for the selfless hard work you have put in to strengthen our manuscript. I know you will take this work to new heights and look forward to seeing your progress.

Finally, I'd like to thank those who have helped guide me toward and prepare me for graduate school, most notably, my undergraduate mentor J. Stephen Horton who introduced me to bench science at Union College. Steve is an outstanding professor/mentor and is a major reason I am a scientist today. To Marc Kirschner, you believed in my scientific abilities and gave me the necessary tools and support to succeed at the next level. I would also like to thank my exceptional professors at Union College and great teachers at Lee High School.

Chapter 1

Introduction

Cortical organization

The cell cortex is defined by the dynamic interactions between plasma membrane proteins and/or lipids and the underlying cortical cytoskeleton (Fehon et al. 2010; Rauzi and Lenne 2011). The cortical cytoskeleton provides both physical support for cellular structures such as microvilli and a scaffold for membrane protein complexes that partition the membrane:cytoskeleton interface into physically and functionally distinct domains. The establishment of these domains is critical for cells to sense, interpret, and respond to signals from the extracellular milieu. In order to do this efficiently the membrane cytoskeleton must be highly dynamic. Adhesion between the cytoskeletion and overlaying plasma membrane is regulated by multiple weak, reversible interactions between membrane lipids and cytoskeletal proteins and by interaction of transmembrane receptors and associated protein complexes with the cortical cytoskeleton (Sheetz 2001; Sheetz et al. 2006).

The molecular basis of how the cortical cytoskeleton communicates with membrane complexes to control their activity and distribution is not well understood. There is, however, a well-defined role for the cortical cytoskeleton in controlling the internalization and processing of endocytic vesicles (Kaksonen et al. 2006). Regulated linkage between the actin cytoskeleton and associated membrane complexes could control receptor activity by dictating endocytic pathways. Indeed, endocytosis is critical for controlling EGFR activation, degradation and recycling (Sorkin and Goh 2009). In addition, it has been shown that the cortical cytoskeleton and associated membrane proteins can restrain receptors by forming molecular

fences that confine receptors, impeding their lateral movement and increasing the likelihood that they aggregate (Kusumi et al. 2005). Tethering or corralling membrane proteins to the cytoskeleton could also be used to bring them in close proximity to specific cytoplasmic components of signal transduction pathways. There is much to be gained by understanding the regulated linkage between the cell membrane and cortical cytoskeleton and this is the precise location where the neurofibromatosis type 2 tumor suppressor, Merlin and closely related ERM (Ezrin, Radixin and Moesin) proteins have their primary function in providing regulated linkage between the cell membrane and cortical cytoskeleton.

Cortical asymmetry

The ability to spatially restrict specific activities across the cell cortex functionally defines individual cells and tissues. Cortical asymmetry refers to the polarized distribution of membrane complexes and mechanical properties across the cortex. In addition to mechanical forces, cortical asymmetry in many cases is directed by extracellular positional cues including cell:cell and cell:ECM contacts (St Johnston and Ahringer 2010). These positional cues can also be generated intrinsically. For example, budding yeast can break symmetry in the absence of a polarizing cue (bud scar or chemoattractant gradient) in two ways. One depends on an actin-based positive feedback loop in which Cdc42 directs its own transport to form a polar cap. The second is actin-independent and requires Bem 1, a protein with multiple binding domains that initiates the formation of a signaling complex that includes Cdc42 (Slaughter et al. 2009). However, the molecular mechanisms by

which cells intrinsically generate polarity are unclear and it is not clear whether mammalian cells can do this.

Cortical forces are generated via Myosin II and actin filament assembly, which are spatially and temporally controlled in the cell. Determining how the cortical forces established by actomyosin networks are coupled to adhesion structures is critical for understanding important biological processes such as tissue morphogenesis. In single cells and single celled organisms cortical asymmetry can be triggered by external cues such as sperm entry or by the cortical scar that marks the site of an earlier cell division (Macara and Mili 2008; St Johnston and Ahringer 2010). For example, the *C. elegans* embryo contains a dynamic and contractile actomyosin network that is destabilized at the point of sperm entry. This, in turn, initiates a cortical flow of nonmuscle myosin and F-actin that drives asymmetry of the PAR proteins at the membrane (Munro et al. 2004).

In addition to actin and myosin mediated force generation at the cortex, inositol phospholipids play an important role in generating cortical asymmetry to orchestrate the establishment and maintenance of cellular architecture (Shewan et al. 2011). In particular, the establishment of apical-basal polarity is critical and phosphatidylinositides play an important role in generating these domains. For example, MDCK cells polarize in 3D culture where PIP_2 localizes apically and PIP_3 is restricted to the basolateral membrane (Gassama-Diagne et al. 2006; Martin-Belmonte et al. 2007). These two phospholipids play a key role in defining the apical and basolateral membranes, respectively since targeting exogenous PIP_3 to the apical surface leads to the accumulation of basolateral protein markers to the

apical surface and vice versa. How PIP_2 and PIP_3 asymmetry is established is not clear. However, the phosphatase PTEN and PI3-kinase are recruited to the apical and basolateral membrane, respectively via PAR-3 and DLG to perform their function (Laprise et al. 2004). While PIP_2 and PIP_3 can be regulated downstream of cortical polarity complexes the robust effects of targeting PIP_2 or PIP_3 to the opposite membrane suggest that this pathway may also feed back to regulate polarity complexes. Furthermore, it is unknown whether inositol phospholipids might play a role in generating cortical asymmetry in the absence of polarity cues.

The generation of cortical asymmetry is critical for a number of important biological functions including asymmetric cell division, morphogenesis, and positioning of receptors; disruption of these each of these processes has been linked to tumorigenesis.

FERM domain-containing proteins: linking the membrane and cytoskeleton

Protein 4.1 is one of the earliest recognized cortical organizing proteins (Anderson and Lovrien 1984; Anderson and Marchesi 1985; Mangeat 1988). It is the founding member of a superfamily of proteins that have highly conserved FERM (Four-point one, Ezrin, Radixin, Moesin) domains at the N-terminus of the molecule and, in many cases a spectrin/actin binding domain (Chishti et al. 1998). Protein 4.1 was originally identified as a structural component of the erythrocyte undercoat, where it serves to anchor the cytoskeleton to the membrane (Sun et al. 2002). It accomplishes this in part via binding spectrin and actin to promote their association, as well as tubulin and glycophorin C (Ohanian et al. 1984; Correas and Avila 1988;

Hemming et al. 1994). Indeed, mice null for Protein 4.1 R (erythrocyte) have abnormally shaped red blood cells (Shi et al. 1999). Thus, members of the Protein 4.1 superfamily appear to be critical regulators of membrane integrity and/or assembly via their FERM domain interactions

The FERM domain is a tri-lobed (F1, F2 and F3) structure responsible for anchoring to membrane proteins (Chishti et al. 1998; Pearson et al. 2000) and can be tethered to a number of different functional domains. Interestingly, 14 orthologous groups of FERM domain-containing proteins can be found in worms, flies and mammals but not yeast, suggesting a dramatic expansion of this superfamily occurred in response to the increased organizational challenges presented by multicellularity (Bretscher et al. 2002). In a subset of these proteins, including the ERMs and Merlin, the FERM domain is accompanied by disparate domains that link it to the cytoskeleton. At the membrane:cytoskeleton interface, the ERM proteins and Merlin are poised to receive and interpret signals from the extracellular milieu and transmit them to the cell interior.

The ERM proteins organize the cell cortex

ERM structure and regulation

Mounting evidence highlights the ERM proteins as architectural proteins and key organizers of specialized membrane domains. Through their ability to interact with transmembrane proteins, phospholipids, membrane associated cytoplasmic proteins and the actin cytoskeleton, the ERMs are poised to organize, regulate and stabilize membrane complexes. More recently, studies have revealed unexpectedly

diverse functions for the ERMs including villar organization in the gut (Saotome et al. 2004), control of cortical stiffening during mitosis (Carreno et al. 2008; Kunda et al. 2008), regulation of RhoA activity in epithelial cells (Speck et al. 2003), signaling (Neisch and Fehon 2011), and polarity (Jankovics et al. 2002; Polesello et al. 2002). Together, these data suggest that the ERMs orchestrate an array of complex biological processes by directly linking the membrane to the actin cytoskeleton. In doing so, the ERMs perform two central functions. First, they provide stability to the cortex and second they control the distribution and activity of membrane receptors in a highly dynamic fashion.

Structurally, the ERMs are characterized by the presence of an approximately 300 amino acid plasma membrane-associated FERM domain at the N-terminus. Following is the α-helical linking region that tethers the FERM domain to the C-terminal ERM-associated domain (C-ERMAD). The C-ERMAD, in turn, can associate with either the FERM domain or filamentous actin. Many studies conclude that ERM function is conformationally regulated by self-association of the C-ERMAD to the N-terminal FERM domain (Bretscher et al. 2002). Initially, studies discovered that the F-actin binding site, which was found to be at the end of the C-ERMAD, bound to the FERM domain in such a way that the F-actin binding site was masked (Turunen et al. 1994; Gary and Bretscher 1995). This discovery laid the foundation for a simple model that explains ERM activation. It is now thought that the ERMs exist in an "inactive" closed conformation where the actin-binding domain and membrane binding domains within the FERM domain are masked. Release of the C-ERMAD from the FERM domain exposes these protein-binding domains leading to an

"active" open conformation that can physically link the membrane and underlying cortical actin cytoskeleton (Figure 1.1) (Bretscher et al. 2002).

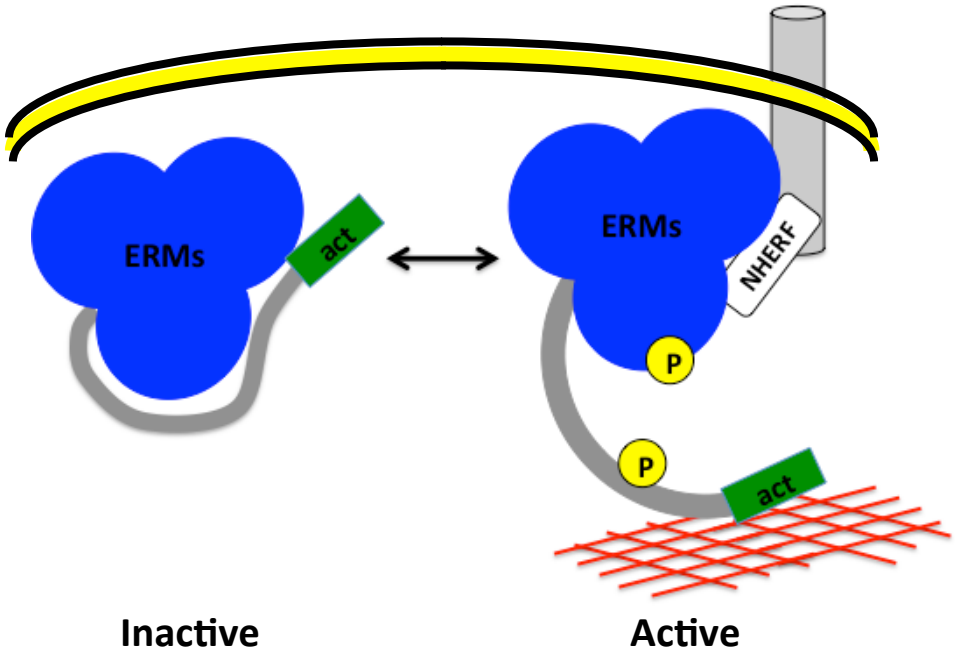

Figure 1.1 Regulation of ERM function. The ERM proteins contain an N-terminal FERM domain (blue), an alpha helical domain (grey bar) and a C-terminal tail actin binding domain (green). The hypophosphorylated ERMs are thought to be "inactive" where the C-terminal tail associates with the FERM domain, masking protein-binding domains. Upon phosphorylation, which can occur on the C-terminal tail or on the FERM domain (yellow), the ERMs are thought to adopt an open/"active" conformation where The FERM domain links membrane proteins either directly or via adapters (NHERF) to the actin cytoskeleton (red mesh).

Association of the ERMs with membrane proteins, lipids and the actin cytoskeleton is highly regulated, allowing cells to respond quickly to the demands of organizing higher order tissue structures. The first insights for understanding how the ERMs are dynamically regulated came with the discovery that Moesin is phosphorylated on T558 of its C-ERMAD during platelet activation (Nakamura et al. 1995). Follow up studies have shown that the equivalent residue in Ezrin and

Radixin (T576 and T564 respectively) can also lead to activation. To date, a number of kinases in mammalian cells are capable of phosphorylating ERMs on their regulatory threonine residue including Rho kinase, NIK, LOK, PKCα, PKCΘ and MST4 (Matsui et al. 1998; Simons et al. 1998; Ng et al. 2001; Belkina et al. 2009; ten Klooster et al. 2009). Additionally, *in vivo* studies in *D. melanogaster,* demonstrate the Ste20-like kinase Slik is important for phosphorylating this residue in its sole fly ERM ortholog, Moesin (Hipfner et al. 2004; Hughes and Fehon 2006; Carreno et al. 2008) highlighting this residue as a key point of activation.

Consistent with the complexity of biological functions that the ERMs control, additional mechanisms of ERM activation have been described, arguing against a simple active vs inactive conformation resulting from phosphorylation of a single residue. Indeed, phosphatidylinositol binding plays an important role in ERM activation/regulation. Binding of phosphatidylinositol 4,5-bisphosphate (PIP_2) to the FERM domain of ERM proteins is thought to facilitate ERM activation and promote interaction between ERMs and membrane binding partners (Nakamura et al. 1995; Niggli et al. 1995). This suggests a two-step model where recruitment of ERMs to PIP_2 may render the conserved threonine residue more accessible to phosphorylation (Fievet et al. 2004). Additional mechanisms of ERM activation have also been described suggesting that ERM regulation is even more complex. For example, cyclin-dependent kinase 5 (Cdk5) can directly phosphorylate residue T235 of Ezrin, which is located in the FERM domain and sits directly opposed to T567 (Pearson et al. 2000; Yang and Hinds 2003). The ERMs can also be substrates for

tyrosine kinases and can be phosphorylated on residues Y145 and Y353 by the epidermal growth factor receptor EGFR (Krieg and Hunter 1992).

The ERMs stabilize the cortex

One critical function for the ERMs is to provide cortical stability and recent studies of ERM function in mitosis illustrate this point perfectly. Cells undergo cortical retraction and rounding as they undergo mitosis. Recent studies have shown that *D. melanogaster* Moesin enhances cortical stiffness to promote cell rounding during mitosis (Carreno et al. 2008; Kunda et al. 2008). Briefly, loss of Moesin function in S2 cells results in multiple mitotic defects including cell shape abnormalities, mitotic spindle deformation, chromosome misalignment and delay of anaphase onset. These cells fail to undergo cortical retraction and exhibit severe membrane blebbing. This is consistent with the previous finding that the ERMs are critical for membrane bleb retraction (Charras et al. 2006). Atomic force measurements indicate that cortical rigidity fails during mitosis in cells that are depleted for Moesin. This suggests that Moesin mediated cortical stabilization is critical for proper mitotic spindle morphology and alignment of chromosomes. Indeed, these phenotypes can be rescued by stabilizing the cortex externally via treatment with the tetravalent lectin concanavallin A (Kunda et al. 2008), illustrating the importance of ERM mediated control of cortical stability.

In certain settings the role of ERM proteins in physically shaping the cortex may be via their ability to regulate Rho1 activity. *In vivo* studies in the fly demonstrate the sole ERM ortholog, Moesin is critical for maintaining the integrity of the

developing wing disc epithelium. In fact, loss of Moesin leads to an increase in Rho1 activity, while diminishing Rho1 activity in Moesin mutant tissue rescues both epithelial integrity and lethality (Speck et al. 2003), indicating that Moesin can facilitate epithelial morphology by antagonizing Rho rather than by providing a structural function. In addition, cell and molecular studies have shown that activation of RhoA induces phosphorylation of the ERM C-ERMAD, and translocation to the membrane:cytoskeleton interface (Matsui et al. 1998; Shaw et al. 1998), indicating a reciprocal relationship between the ERMs and Rho.

The ability to generate asymmetry at the cell cortex is a key feature of cell polarity. Indeed several studies argue that the ERMs play an important role in the establishment and maintenance of cell polarity, perhaps via their role in stabilizing the cortex (Micklem et al. 2000; Jankovics et al. 2002; Polesello et al. 2002; Speck et al. 2003; Pilot et al. 2006). For example, in *D. melanogaster*, the synaptotagmin ortholog Bitesize is recruited to the apical membrane domain through interactions with the apical polarity complex (Pilot et al. 2006). In the absence of Bitesize apico-basal polarity is established and adherens junctions form normally but epithelial organization subsequently breaks down. Pilot *et al* found that Bitesize stabilizes adherens junctions by binding and recruiting Moesin, which, in turn, stabilizes cortical actin. Here, cortical actin is required for the formation of stable adherens junctions, which are necessary for epithelial integrity and polarity. Together, these studies demonstrate that the ERMs can control a diverse number of biological processes via their ability to physically stabilize the cortex.

The ERMs control receptor distribution and regulation

In addition to their role in physically stabilizing the membrane, the ERMs can control the distribution and activation of a number of membrane receptors. For example, studies of immune cells have demonstrated that the ERM proteins can establish cortical asymmetry in round, suspended T-cells by directing membrane:cytoskeleton interactions and membrane receptor distribution (Burkhardt et al. 2008). T-cell activation requires the removal of the mucin CD43 from the immunological synapse between a T-cell and an antigen presenting cell, and this process requires Ezrin (Delon et al. 2001; Roumier et al. 2001; Shaw 2001). T-cells that express a dominant-negative form of Ezrin fail to exclude CD43 from the synapse and are not activated, demonstrating that ERM mediated changes in receptor distribution have important regulatory consequences

While the ERMs have been shown to directly associate with and regulate the activity of a number of membrane adhesion receptors including CD44, ICAM-2 and CD43 (Allenspach et al. 2001; Roumier et al. 2001; Legg et al. 2002), the ERM FERM domain also interacts with the PDZ domain containing membrane adapters NHERF-1and E3KARP (Reczek and Bretscher 1998; Yun et al. 1998). Indeed, NHERF-1 and E3KARP have been proposed to bind a number of membrane and cytoplasmic proteins, effectively increasing the complexity of membrane proteins and cytoplasmic complexes that the ERMs can regulate (Bretscher et al. 2000). For example, loss of Ezrin, the sole ERM expressed in the mouse intestinal epithelium, leads to both loss of apical membrane integrity and failure to localize the ERM-binding adapter NHERF-1 to the apical membrane (Saotome et al. 2004). This

suggests that brush border receptors that are localized or regulated by NHERF-1 are also likely affected. Consistent with this, intestinal function is compromised in these mice. Since NHERF-1 and E3KARP have been shown to directly activate ion transporters (Weinman et al. 2000), regulate endocytosis of plasma membrane proteins (Short et al. 1998; Cao et al. 1999; Maudsley et al. 2000), and restrict receptors to specific plasma membrane domains (Takeda et al. 2001) the ERMs are capable of orchestrating a wide range of biological processes.

The ERMs simultaneously perform multiple functions in vivo

Functional redundancy among the ERM proteins has made mammalian *in vivo* genetic studies difficult to interpret. However, in the mouse intestinal epithelium Ezrin is the sole ERM protein expressed, providing a valuable setting for studying mammalian ERMs. Individual cell and molecular studies have demonstrated a broad array of functions for the ERMs including stabilization of the membrane:cytoskeleton interface, controlling receptor distribution/function, regulating the small GTPase Rho and establishing cell-cell junctions. However, until recently it was unclear whether the ERMs could perform all of these functions *in vivo*. Members of our lab have previously characterized the phenotype of *Ezrin* deficiency in the developing and adult mouse intestinal epithelium (Saotome et al. 2004; Casaletto et al. 2011). These studies reveal that *Ezrin* is required for the integrity of the apical terminal web and associated apical junction in polarized epithelial cells. In the absence of this function *de novo* lumen formation and villus morphogenesis are compromised yielding villi that are fused (Saotome et al. 2004).

Interestingly, loss of *Ezrin* in an already fully developed adult intestinal epithelium yields villus fusion revealing a previously unrecognized step in intestinal homeostasis (Casaletto et al. 2011). These studies went on to show that Ezrin performs multiple molecular functions that collaborate to build the functional apical surface of the intestinal epithelium *in vivo*, supporting the hypothesis that ERMs can simultaneously coordinate the multiple cellular activities identified in separate cell and molecular studies.

In addition, *in vivo* studies using *C. elegans* and *D. melanogaster*, which contain a single ERM ortholog (ERM-1 and dMoesin respectively) support that the ERMs perform multiple molecular functions *in vivo.* Loss of the sole ERM ortholog, Moesin, in *D. melanogaster* leads to defective apical morphogenesis, increased Rho1 activation, and loss of epithelial integrity/morphology (Speck et al. 2003). Here, F-actin accumulates in ectopic sites within Moesin deficient cells of the wing imaginal epithelium and many of these cells lose polarity and extrude basally from the epithelial monolayer. Similarly, loss of the single ERM ortholog (*ERM-1)* in *C. elegans* yields defects in apical integrity throughout the developing intestinal epithelium (Gobel et al. 2004; Van Furden et al. 2004), which is critical for lumen morphogenesis *in vivo*. Thus the ERM proteins play an essential role in building the apical surface of polarized cells by organizing cortical complexes and linking them to the actin cytoskeleton.

The tumor suppressor Merlin

History of Neurofibromatosis

Neurofibromatosis (NF) was originally described in 1882 by German pathologist Friedrich von Recklinghausen following the autopsy of a patient that developed multiple tumors at the base of the skull, including bilateral schwannomas on the vestibulocochlear 8th cranial nerve (Wishart 1822; von Recklinghausen 1882). By the early 1900's physicians began to categorize sub-types of neurofibromatosis including "central" and "peripheral". The central sub-type was much like the one von Recklinghausen described which include Schwann cell tumors around cranial nerves and spinal nerve roots. These patients rarely developed dermal neurofibromas that are prominent in the more common peripheral neurofibromatosis (Henneberg 1903; Yohay 2006). However, for many years these diseases were considered to be the same. It wasn't until the 1980's that chromosomal linkage studies demonstrated that peripheral and central neurofibromatosis were two distinct diseases with different genetic causes. Today, they are known as neurofibromatosis type 1 (NF1) and type 2 (NF2) respectively.

Briefly, NF1 is more common (approximately 1 in 4,000 individuals will develop NF1) and displays a characteristic cutaneous phenotype including benign neurofibromas, which are mixed tumors composed of all cell types found in the peripheral nerves, hyperpigmented macules termed café-au-lait spots, axillary/inguinal freckling, and pigmented hamartomas of the iris, called Lisch nodules (Gerber et al. 2009). Patients develop NF1 upon inheriting an inactive copy of the *NF1* gene, which encodes the GTPase-activating protein Neurofibromin

(Evans et al. 2000; Yohay 2006). Neurofibromin is thought to function as a tumor suppressor by negatively regulating Ras signaling (Cichowski and Jacks 2001).

NF2 on the other hand is much less common (approximately 1 in 25,000-40,000 individuals will develop NF2). Mutations in the *NF2* tumor suppressor gene underlie neurofibromatosis type 2, a familial tumor syndrome that features the development of tumors of the central nervous system, particularly schwannomas and meningiomas (Baser et al. 2003). In 1993, the *NF2* tumor suppressor gene was identified by positional cloning and loss of heterozygosity studies without knowledge of the molecular basis for the disease (Rouleau et al. 1993; Trofatter et al. 1993). Surprisingly, Merlin was found to be closely related to the membrane:cytoskeletal associated ERM proteins, immediately raising the question of how a protein at this localization could control proliferation. The *NF2* encoded protein, referred to as Merlin, (Trofatter et al. 1993)(for Moesin/Ezrin/Radixin-like protein) is also known as schwannomin (Rouleau et al. 1993). While many studies have shown that Merlin does control proliferation, the mechanism by which it does this remains unclear.

Molecular studies of Merlin function

Initial functional studies of the *NF2*-encoded tumor suppressor, Merlin were naturally modeled after other tumor suppressors and focused on its role in controlling proliferation. These studies confirmed, as for other tumor suppressors, that overexpression of Merlin can block cell proliferation and oncogene-induced transformation (Tikoo et al. 1994; Lutchman and Rouleau 1995). Indeed, Merlin can

negatively regulate cyclin D1 levels, consistent with the cell cycle arrest phenotype observed upon Merlin overexpression (Xiao et al. 2002).However, the discovery that Merlin is closely related to the ERMs and localizes to the membrane:cytoskeleton interface suggests that its primary function is not to directly control cell cycle machinery. Therefore, Merlin represents a new type of tumor suppressor that is positioned at the membrane where it may function to receive and interpret extracellular signals. Furthermore, our understanding of ERM function has provided valuable insight as to how Merlin controls proliferation from the membrane:cytoskeleton interface.

As the ERM proteins are able to associate with and control the distribution/activation of certain membrane receptors many studies focused on Merlin-mediated receptor control to elucidate its role in proliferation. Indeed, a number of individual studies indicate that Merlin can regulate EGFR (Maitra et al. 2006; Curto et al. 2007), Hippo signaling (Hamaratoglu et al. 2006), transforming-growth-factor-β (LaJeunesse et al. 1998) and hepatocyte growth-factor receptor substrate (HRS) (Gutmann et al. 2001; Scoles et al. 2002). Other studies argue that Merlin controls contact dependent inhibition of proliferation via its interaction with CD44 (Morrison et al. 2001). Finally, Shaw *et al* proposed that Merlin functions to negatively regulate Rac, a Rho family small GTPase, which has been implicated in malignant transformation (Morrison et al. 2001; Shaw et al. 2001). Taken together, it is clear that Merlin can control a number of signaling pathways that regulate cell proliferation. Despite this knowledge there have been few significant advances for the treatment of NF2 patients and several key questions remain unresolved. One

key question is whether Merlin performs multiple independent functions, one of which is critical for its tumor suppressor function or whether Merlin controls a combination of pathways that contribute to tumor progression. To this end it will be most critical to define Merlin's primary and most fundamental function as a membrane organizer.

Contact-inhibition of proliferation

Many studies have shown that membrane association is critical for Merlin to suppress proliferation, which is consistent with the idea that Merlin controls proliferation in response to cell density. A hallmark feature of *Nf2* deficiency in cell culture is the failure to prevent proliferation upon cell:cell contact or loss of contact-dependent inhibition of proliferation. Studies from our lab demonstrated that Merlin is recruited to cadherin-containing complexes at the site of nascent cell:cell contacts to facilitate the formation of stable adherens junctions (Lallemand et al. 2003). Moreover, Curto *et al* showed that upon cell-cell contact Merlin coordinates the stabilization of adherens junctions with negative regulation of epidermal growth factor receptor (EGFR) signaling by restraining EGFR into a membrane compartment from which it can neither signal nor be internalized (Figure 1.2) (Curto et al. 2007). Merlin can also associate with the cell:ECM receptor CD44 so Merlin may sense environmental cues, other than contacting cells, to control proliferation (Morrison et al. 2001). Indeed, Morrison *et al* found that Merlin association with CD44 is also necessary for contact-dependent inhibition of

proliferation, however, the mechanism by which Merlin halts proliferation in this context is unknown (Morrison et al. 2001).

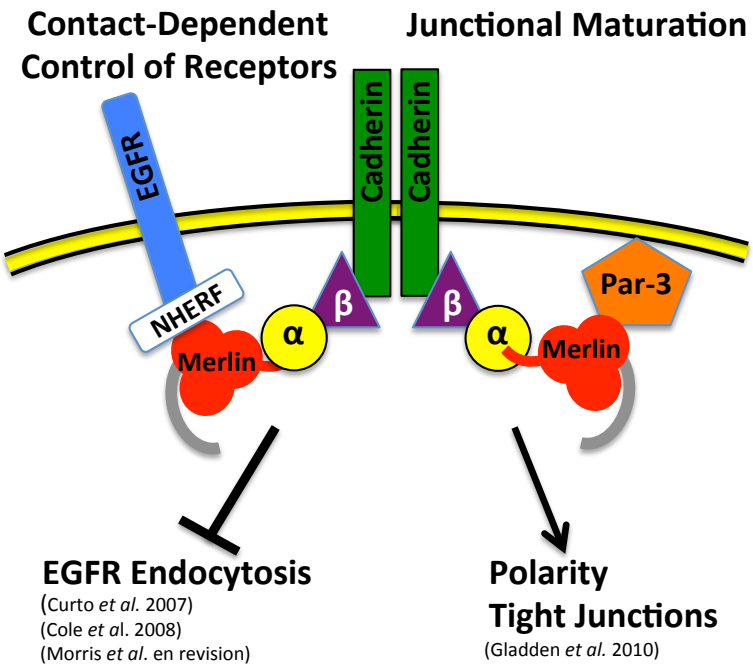

Figure 1.2 Merlin controls contact-dependent receptor activation and adherens junction maturation. **(Left)** Upon cell:cell contact Merlin (red) associates with cadherin-catenin containing complexes (green, purple, yellow) and sequesters EGFR (blue), via the PDZ domain containing adaptor protein NHERF, to a molecular compartment where it can neither signal nor be internalized. **(Right)** Merlin (red) promotes the establishment of adherens junctions by linking the polarity protein Par-3 (orange) directly to α-catenin (yellow), thereby providing an essential link between the adherens junction (green, purple, yellow) and the Par-3 polarity complex during junctional maturation.

In vivo studies of Merlin

A number of *in vivo* studies, particularly in the mouse, have advanced our knowledge of Merlin function. In the mouse, *Nf2* null embryos fail early during embryonic development without initiating gastrulation (McClatchey et al. 1997). The underlying defect in *Nf2* deficient embryos is not due to cell proliferation

abnormalities, but rather the absence of extra-embryonic structures that are required to generate a mesoderm-inducing signal, supporting the hypothesis that Merlin's primary function in this setting is not to control proliferation. Notably, Merlin is also required for normal development of *D. melanogaster* (Fehon et al. 1997).

Interestingly, heterozygous mutation of *Nf2* in the mouse yields various tumors including osteosarcomas and hepatocellular carcinoma that show loss of the wild-type *Nf2* allele (McClatchey et al. 1998). The unusually metastatic behavior of these tumors indicates that *Nf2* may have an unappreciated role in promoting metastasis. Though these mice do not develop the characteristic tumors that human NF2 patients do, inactivation of both *Nf2* alleles specifically in either Schwann cells or arachnoid cells does yield manifestations of human NF2 (Giovannini et al. 2000). Therefore, loss of the wild-type *Nf2* allele might be the rate-limiting step for development of these tumors in mice (Giovannini et al. 2000; Kalamarides et al. 2002). Taken together these studies suggest that Merlin's function as a tumor suppressor involves more than control of proliferation, so what else could Merlin be doing?

Most recently, *in vivo* studies from our lab have highlighted a role for Merlin in establishing adherens junctions (Figure 1.2), spindle orientation and tumorigenesis (Morris and McClatchey 2009; Benhamouche et al. 2010; Gladden et al. 2010) demonstrating that, like the ERMs, Merlin can perform multiple functions *in vivo*. In the mouse skin *Nf2* regulates epidermal development via the establishment of a junctional polarity complex. Notably, $Nf2^{-/-}$ basal cells within the

epidermis fail to form mature adherens junctions and randomly orient their mitotic spindles. Furthermore, Gladden et al found that Merlin can associate directly with α-catenin to link it to Par3, thereby linking the adherens junction and the Par3 polarity complex during junctional maturation. These studies clearly demonstrate that Merlin has functions beyond the control of mitogenic receptor signaling, which may explain the lack of effective treatments for NF2 patients (Plotkin et al. 2010). It appears that the inability to properly control receptor distribution/activity upon Merlin deficiency is the result of a greater and more fundamental inability to organize the cortex.

Functional relationship

The NF2 tumor suppressor, Merlin, and closely related ERM proteins are both membrane:cytoskeleton associated proteins that can organize the cell cortex by assembling and regulating protein complexes at the plasma membrane (McClatchey and Fehon 2009). Biologically, Merlin and the ERMs have well-established functions in cell proliferation and epithelial architecture, respectively. Despite many similarities and some interesting differences, most studies have focused on either Merlin or the ERMs without comparing them. Nevertheless, Merlin and the ERMs are co-expressed in most cell types, are regulated similarly, share binding partners (Gronholm et al. 1999; Meng et al. 2000; Nguyen et al. 2001), can physically interact with one another and display coordinate regulation (Hughes and Fehon 2006), indicating that they share a functional relationship (McClatchey 2003). Within cells Merlin and the ERMs have generally distinct but overlapping

subcellular distributions indicating that under certain conditions they may co-localize (McCartney and Fehon 1996; Bretscher et al. 2002). Defining the relationship between Merlin and the ERMs will be critical for understanding their respective roles in coordinating activities at the membrane and how ultimately their deregulation relates to tumorigenesis.

The high degree of structural similarity between Merlin and the ERMs suggests that they might share regulatory mechanisms and possibly cellular functions. However, some distinguishing features may explain their unique functions (Figure 1.3). Notably, while the ERMs contain a *bona fide* actin-binding domain on their C-ERMAD, Merlin does not. Alternatively, Merlin may associate with actin via a unique 17 amino acid stretch at its N-terminus, which is critical for its stable localization to the cortical cytoskeleton and for its ability to interact with α-catenin (Cole et al. 2008).

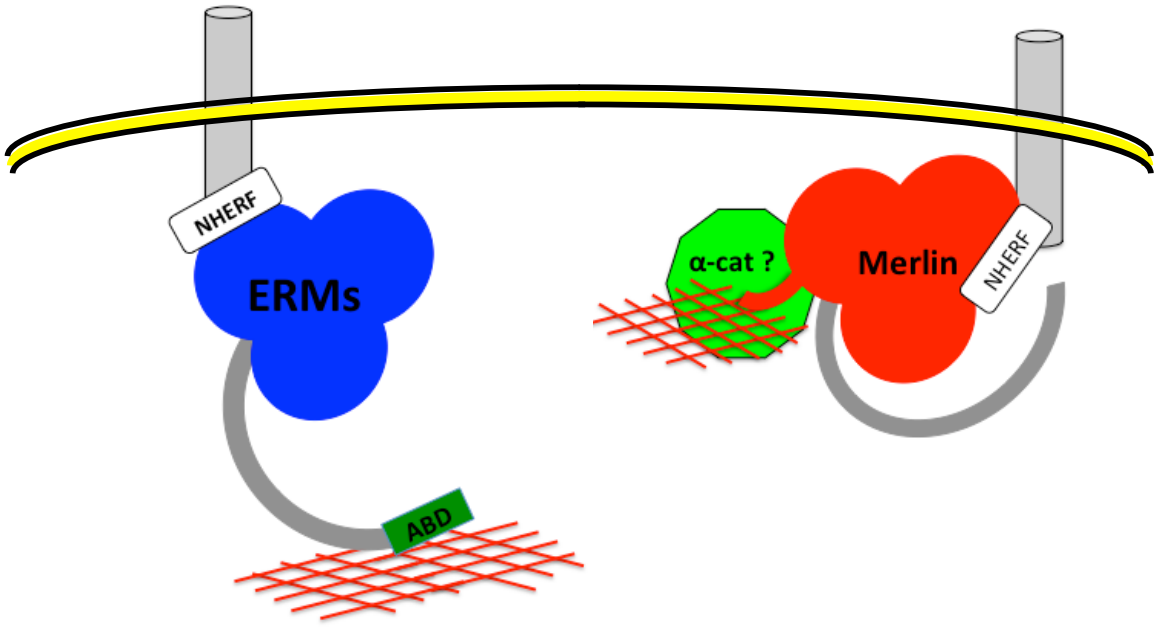

Figure 1.3 (Continued on next page)

Figure 1.3 (Continued). The ERM proteins (blue) and Merlin (red) are structurally similar but maintain some distinguishing features. The ERMs and Merlin can interact with transmembrane proteins (grey cylinders) either directly or via PDZ domain-containing adapters (NHERF). While the ERMs can directly associate with actin (red mesh) via a C-terminal actin binding domain (ABD) Merlin may associate with actin via a unique 17 amino acid stretch (red line) at its N-terminus, which is critical for its stable localization to the cortical cytoskeleton and for its ability to interact with α-catenin (green).

Modeling tissue morphogenesis *in vitro*

In vivo studies in *D. melanog*aster and *C. elegans* have been instrumental for understanding epithelial tissue morphogenesis and how individual proteins, including the ERMs, function to regulate it (Speck et al. 2003; Gobel et al. 2004; Van Furden et al. 2004). To obtain a more refined mechanistic understanding of epithelial morphogenesis and the molecules that regulate it cell culture models are often used. These models are well suited for studying signaling pathways and cellular processes involved in how cells arrange themselves. However, the vast majority of these studies use cells cultured in monolayers (2D) on tissue culture plastic or filters, which do not resolve well with the highly structured tissue architecture that exists *in vivo.* Though many important advances have been made using 2D cell culture models there can be considerable differences in their morphology, differentiation, and cell:cell/cell:ECM contacts, compared to those grown in more physiological relevant 3D environments (Cukierman et al. 2001; Birgersdotter et al. 2005; Griffith and Swartz 2006; Nelson and Bissell 2006). Alternatively, *in vivo* phenotypes are often complicated by secondary effects, such as the immune response, which inaccurately reflect specific protein function.

Therefore, it is not surprising that our molecular studies of proteins in 2D are difficult to resolve with the complexity of phenotypes we see *in vivo*.

A number of studies have recently emerged using 3D cell culture to study tissue morphogenesis. Typically these studies are performed using mammary epithelial cells (MCF-10A), Madin-Darbey canine kidney cells (MDCK), or human epithelial colorectal adenocarcinoma cells (CaCo2). Indeed, there are differences as to how each cell type develops from a single cell into a fully polarized epithelial cyst structure with a single lumen opposing the apical surface. MCF-10A cells proliferate to form cell masses that remove centrally localized cells via multiple cell death processes to generate cysts (Debnath et al. 2003). Alternatively, in Matrigel, CaCo2 cells, like MDCK cells, begin forming a lumen as early as the 2-cell stage and maintain the single lumen via a series of oriented cell divisions and apical abscission (Jaffe et al. 2008) (Figure 1.4).

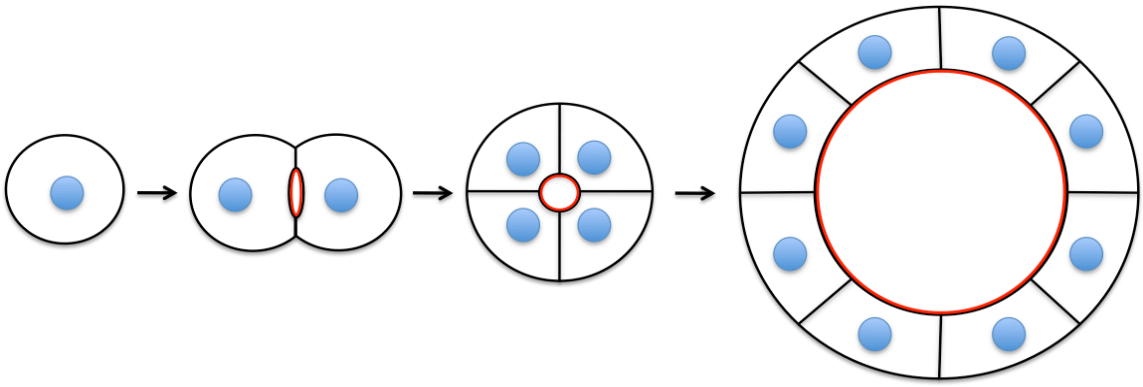

Figure 1.4 Schematic representation of cyst formation in 3D cell culture using CaCo2 cells. When embedded into ECM, single CaCo2 cells divide and build an apical surface (red) upon the first cell division at the site where cytokinesis takes place. Upon establishment of the first apical surface cells undergo a series of oriented cell divisions to maintain a single, central fluid-filled lumen that apposes the apical surface (red) of the epithelial cell monolayer.

Overview and objectives

Many Merlin interacting proteins have been identified and, not surprisingly, Merlin has been implicated in controlling many intracellular signaling pathways that control cell fate, shape, proliferation, survival and motility (Stamenkovic and Yu). Similarly, the ERMs, which have been thought of as mainly architectural proteins, appear to play complex roles in regulating signaling cascades and generating polarity (Jankovics et al. 2001; Polesello et al. 2002; Neisch and Fehon 2011). It is becoming increasingly clear that Merlin/ERM function and their functional relationship at the membrane:cytoskeleton interface is quite complex and for many reasons has been difficult to study. A major obstacle to understanding how Merlin and ERM function relates to tumor development and cancer is that we do not understand their fundamental function as membrane organizers. Indeed, few major medical advances have been made since *NF2* was discovered almost 20 years ago despite the identification of several mitogenic signaling pathways that Merlin is thought to control.

Here, I sought to evaluate Merlin and ERM mediated membrane organization as a single cell develops into an organized tissue structure using a 3D cell culture system. This work has provided new insight into the basic function of Merlin and the ERM proteins. We show that a key function of Merlin is to restrict cortical Ezrin positioning and identify a mechanism by which cells intrinsically generate cortical asymmetry in a cell-cycle correlated manner in the absence of external cues. Furthermore, these studies identify a novel cue for centrosome positioning and mitotic spindle orientation. To complement these studies, I developed an *in vivo*

model using the mouse intestinal epithelium and demonstrated a clear functional interaction between *Nf2* and *Ezrin*. Finally, we explored the possibility that Merlin and the ERMs are coordinately regulated by the single Ste20-like kinase SLK. This work has already informed our studies of Merlin and ERM function in many of the different tissue types we study and provides an important basis for understanding their most fundamental function as membrane organizers.

References

Allenspach, E.J., Cullinan, P., Tong, J., Tang, Q., Tesciuba, A.G., Cannon, J.L., Takahashi, S.M., Morgan, R., Burkhardt, J.K., and Sperling, A.I. 2001. ERM-dependent movement of CD43 defines a novel protein complex distal to the immunological synapse. *Immunity* **15**(5): 739-750.

Anderson, R.A. and Lovrien, R.E. 1984. Glycophorin is linked by band 4.1 protein to the human erythrocyte membrane skeleton. *Nature* **307**(5952): 655-658.

Anderson, R.A. and Marchesi, V.T. 1985. Regulation of the association of membrane skeletal protein 4.1 with glycophorin by a polyphosphoinositide. *Nature* **318**(6043): 295-298.

Baser, M.E., DG, R.E., and Gutmann, D.H. 2003. Neurofibromatosis 2. *Curr Opin Neurol* **16**(1): 27-33.

Belkina, N.V., Liu, Y., Hao, J.J., Karasuyama, H., and Shaw, S. 2009. LOK is a major ERM kinase in resting lymphocytes and regulates cytoskeletal rearrangement through ERM phosphorylation. *Proc Natl Acad Sci U S A* **106**(12): 4707-4712.

Benhamouche, S., Curto, M., Saotome, I., Gladden, A.B., Liu, C.H., Giovannini, M., and McClatchey, A.I. 2010. Nf2/Merlin controls progenitor homeostasis and tumorigenesis in the liver. *Genes Dev* **24**(16): 1718-1730.

Birgersdotter, A., Sandberg, R., and Ernberg, I. 2005. Gene expression perturbation in vitro--a growing case for three-dimensional (3D) culture systems. *Semin Cancer Biol* **15**(5): 405-412.

Bretscher, A., Chambers, D., Nguyen, R., and Reczek, D. 2000. ERM-Merlin and EBP50 protein families in plasma membrane organization and function. *Annu Rev Cell Dev Biol* **16**: 113-143.

Bretscher, A., Edwards, K., and Fehon, R.G. 2002. ERM proteins and merlin: integrators at the cell cortex. *Nat Rev Mol Cell Biol* **3**(8): 586-599.

Burkhardt, J.K., Carrizosa, E., and Shaffer, M.H. 2008. The actin cytoskeleton in T cell activation. *Annu Rev Immunol* **26**: 233-259.

Cao, T.T., Deacon, H.W., Reczek, D., Bretscher, A., and von Zastrow, M. 1999. A kinase-regulated PDZ-domain interaction controls endocytic sorting of the beta2-adrenergic receptor. *Nature* **401**(6750): 286-290.

Carreno, S., Kouranti, I., Glusman, E.S., Fuller, M.T., Echard, A., and Payre, F. 2008. Moesin and its activating kinase Slik are required for cortical stability and microtubule organization in mitotic cells. *J Cell Biol* **180**(4): 739-746.

Casaletto, J.B., Saotome, I., Curto, M., and McClatchey, A.I. 2011. Ezrin-mediated apical integrity is required for intestinal homeostasis. *Proc Natl Acad Sci U S A* **108**(29): 11924-11929.

Charras, G.T., Hu, C.K., Coughlin, M., and Mitchison, T.J. 2006. Reassembly of contractile actin cortex in cell blebs. *J Cell Biol* **175**(3): 477-490.

Chishti, A.H., Kim, A.C., Marfatia, S.M., Lutchman, M., Hanspal, M., Jindal, H., Liu, S.C., Low, P.S., Rouleau, G.A., Mohandas, N. et al. 1998. The FERM domain: a unique module involved in the linkage of cytoplasmic proteins to the membrane. *Trends Biochem Sci* **23**(8): 281-282.

Cichowski, K. and Jacks, T. 2001. NF1 tumor suppressor gene function: narrowing the GAP. *Cell* **104**(4): 593-604.

Cole, B.K., Curto, M., Chan, A.W., and McClatchey, A.I. 2008. Localization to the cortical cytoskeleton is necessary for Nf2/merlin-dependent epidermal growth factor receptor silencing. *Mol Cell Biol* **28**(4): 1274-1284.

Correas, I. and Avila, J. 1988. Erythrocyte protein 4.1 associates with tubulin. *Biochem J* **255**(1): 217-221.

Cukierman, E., Pankov, R., Stevens, D.R., and Yamada, K.M. 2001. Taking cell-matrix adhesions to the third dimension. *Science* **294**(5547): 1708-1712.

Curto, M., Cole, B.K., Lallemand, D., Liu, C.H., and McClatchey, A.I. 2007. Contact-dependent inhibition of EGFR signaling by Nf2/Merlin. *J Cell Biol* **177**(5): 893-903.

Debnath, J., Muthuswamy, S.K., and Brugge, J.S. 2003. Morphogenesis and oncogenesis of MCF-10A mammary epithelial acini grown in three-dimensional basement membrane cultures. *Methods* **30**(3): 256-268.

Delon, J., Kaibuchi, K., and Germain, R.N. 2001. Exclusion of CD43 from the immunological synapse is mediated by phosphorylation-regulated relocation of the cytoskeletal adaptor moesin. *Immunity* **15**(5): 691-701.

Evans, D.G., Sainio, M., and Baser, M.E. 2000. Neurofibromatosis type 2. *J Med Genet* **37**(12): 897-904.

Fehon, R.G., McClatchey, A.I., and Bretscher, A. 2010. Organizing the cell cortex: the role of ERM proteins. *Nat Rev Mol Cell Biol* **11**(4): 276-287.

Fehon, R.G., Oren, T., LaJeunesse, D.R., Melby, T.E., and McCartney, B.M. 1997. Isolation of mutations in the Drosophila homologues of the human Neurofibromatosis 2 and yeast CDC42 genes using a simple and efficient reverse-genetic method. *Genetics* **146**(1): 245-252.

Fievet, B.T., Gautreau, A., Roy, C., Del Maestro, L., Mangeat, P., Louvard, D., and Arpin, M. 2004. Phosphoinositide binding and phosphorylation act sequentially in the activation mechanism of ezrin. *J Cell Biol* **164**(5): 653-659.

Gary, R. and Bretscher, A. 1995. Ezrin self-association involves binding of an N-terminal domain to a normally masked C-terminal domain that includes the F-actin binding site. *Mol Biol Cell* **6**(8): 1061-1075.

Gassama-Diagne, A., Yu, W., ter Beest, M., Martin-Belmonte, F., Kierbel, A., Engel, J., and Mostov, K. 2006. Phosphatidylinositol-3,4,5-trisphosphate regulates the formation of the basolateral plasma membrane in epithelial cells. *Nat Cell Biol* **8**(9): 963-970.

Gerber, P.A., Antal, A.S., Neumann, N.J., Homey, B., Matuschek, C., Peiper, M., Budach, W., and Bolke, E. 2009. Neurofibromatosis. *Eur J Med Res* **14**(3): 102-105.

Giovannini, M., Robanus-Maandag, E., van der Valk, M., Niwa-Kawakita, M., Abramowski, V., Goutebroze, L., Woodruff, J.M., Berns, A., and Thomas, G. 2000. Conditional biallelic Nf2 mutation in the mouse promotes manifestations of human neurofibromatosis type 2. *Genes Dev* **14**(13): 1617-1630.

Gladden, A.B., Hebert, A.M., Schneeberger, E.E., and McClatchey, A.I. 2010. The NF2 Tumor Suppressor, Merlin, Regulates Epidermal Development through the Establishment of a Junctional Polarity Complex. *Dev Cell* **19**(5): 727-739.

Gobel, V., Barrett, P.L., Hall, D.H., and Fleming, J.T. 2004. Lumen morphogenesis in C. elegans requires the membrane-cytoskeleton linker erm-1. *Dev Cell* **6**(6): 865-873.

Griffith, L.G. and Swartz, M.A. 2006. Capturing complex 3D tissue physiology in vitro. *Nat Rev Mol Cell Biol* **7**(3): 211-224.

Gronholm, M., Sainio, M., Zhao, F., Heiska, L., Vaheri, A., and Carpen, O. 1999. Homotypic and heterotypic interaction of the neurofibromatosis 2 tumor suppressor protein merlin and the ERM protein ezrin. *J Cell Sci* **112 (Pt 6)**: 895-904.

Gutmann, D.H., Haipek, C.A., Burke, S.P., Sun, C.X., Scoles, D.R., and Pulst, S.M. 2001. The NF2 interactor, hepatocyte growth factor-regulated tyrosine kinase substrate (HRS), associates with merlin in the "open" conformation and suppresses cell growth and motility. *Hum Mol Genet* **10**(8): 825-834.

Hamaratoglu, F., Willecke, M., Kango-Singh, M., Nolo, R., Hyun, E., Tao, C., Jafar-Nejad, H., and Halder, G. 2006. The tumour-suppressor genes NF2/Merlin and Expanded act through Hippo signalling to regulate cell proliferation and apoptosis. *Nat Cell Biol* **8**(1): 27-36.

Hemming, N.J., Anstee, D.J., Mawby, W.J., Reid, M.E., and Tanner, M.J. 1994. Localization of the protein 4.1-binding site on human erythrocyte glycophorins C and D. *Biochem J* **299 (Pt 1)**: 191-196.

Henneberg, R., and Koch, M. 1903. Uber centrale neurofibromatose und die Geschwulste des Kleinhirnbruckenwinkels (Acusticusneurome. *Arch F Psychiatr* **36**.

Hipfner, D.R., Keller, N., and Cohen, S.M. 2004. Slik Sterile-20 kinase regulates Moesin activity to promote epithelial integrity during tissue growth. *Genes Dev* **18**(18): 2243-2248.

Hughes, S.C. and Fehon, R.G. 2006. Phosphorylation and activity of the tumor suppressor Merlin and the ERM protein Moesin are coordinately regulated by the Slik kinase. *J Cell Biol* **175**(2): 305-313.

Jaffe, A.B., Kaji, N., Durgan, J., and Hall, A. 2008. Cdc42 controls spindle orientation to position the apical surface during epithelial morphogenesis. *J Cell Biol* **183**(4): 625-633.

Jankovics, F., Sinka, R., and Erdelyi, M. 2001. An interaction type of genetic screen reveals a role of the Rab11 gene in oskar mRNA localization in the developing Drosophila melanogaster oocyte. *Genetics* **158**(3): 1177-1188.

Jankovics, F., Sinka, R., Lukacsovich, T., and Erdelyi, M. 2002. MOESIN crosslinks actin and cell membrane in Drosophila oocytes and is required for OSKAR anchoring. *Curr Biol* **12**(23): 2060-2065.

Kaksonen, M., Toret, C.P., and Drubin, D.G. 2006. Harnessing actin dynamics for clathrin-mediated endocytosis. *Nat Rev Mol Cell Biol* **7**(6): 404-414.

Kalamarides, M., Niwa-Kawakita, M., Leblois, H., Abramowski, V., Perricaudet, M., Janin, A., Thomas, G., Gutmann, D.H., and Giovannini, M. 2002. Nf2 gene inactivation in arachnoidal cells is rate-limiting for meningioma development in the mouse. *Genes Dev* **16**(9): 1060-1065.

Krieg, J. and Hunter, T. 1992. Identification of the two major epidermal growth factor-induced tyrosine phosphorylation sites in the microvillar core protein ezrin. *J Biol Chem* **267**(27): 19258-19265.

Kunda, P., Pelling, A.E., Liu, T., and Baum, B. 2008. Moesin controls cortical rigidity, cell rounding, and spindle morphogenesis during mitosis. *Curr Biol* **18**(2): 91-101.

Kusumi, A., Nakada, C., Ritchie, K., Murase, K., Suzuki, K., Murakoshi, H., Kasai, R.S., Kondo, J., and Fujiwara, T. 2005. Paradigm shift of the plasma membrane concept from the two-dimensional continuum fluid to the partitioned fluid: high-speed single-molecule tracking of membrane molecules. *Annu Rev Biophys Biomol Struct* **34**: 351-378.

LaJeunesse, D.R., McCartney, B.M., and Fehon, R.G. 1998. Structural analysis of Drosophila merlin reveals functional domains important for growth control and subcellular localization. *J Cell Biol* **141**(7): 1589-1599.

Lallemand, D., Curto, M., Saotome, I., Giovannini, M., and McClatchey, A.I. 2003. NF2 deficiency promotes tumorigenesis and metastasis by destabilizing adherens junctions. *Genes Dev* **17**(9): 1090-1100.

Laprise, P., Viel, A., and Rivard, N. 2004. Human homolog of disc-large is required for adherens junction assembly and differentiation of human intestinal epithelial cells. *J Biol Chem* **279**(11): 10157-10166.

Legg, J.W., Lewis, C.A., Parsons, M., Ng, T., and Isacke, C.M. 2002. A novel PKC-regulated mechanism controls CD44 ezrin association and directional cell motility. *Nat Cell Biol* **4**(6): 399-407.

Lutchman, M. and Rouleau, G.A. 1995. The neurofibromatosis type 2 gene product, schwannomin, suppresses growth of NIH 3T3 cells. *Cancer Res* **55**(11): 2270-2274.

Macara, I.G. and Mili, S. 2008. Polarity and differential inheritance--universal attributes of life? *Cell* **135**(5): 801-812.

Maitra, S., Kulikauskas, R.M., Gavilan, H., and Fehon, R.G. 2006. The tumor suppressors Merlin and Expanded function cooperatively to modulate receptor endocytosis and signaling. *Curr Biol* **16**(7): 702-709.

Mangeat, P.H. 1988. Interaction of biological membranes with the cytoskeletal framework of living cells. *Biol Cell* **64**(3): 261-281.

Martin-Belmonte, F., Gassama, A., Datta, A., Yu, W., Rescher, U., Gerke, V., and Mostov, K. 2007. PTEN-mediated apical segregation of phosphoinositides controls epithelial morphogenesis through Cdc42. *Cell* **128**(2): 383-397.

Matsui, T., Maeda, M., Doi, Y., Yonemura, S., Amano, M., Kaibuchi, K., and Tsukita, S. 1998. Rho-kinase phosphorylates COOH-terminal threonines of ezrin/radixin/moesin (ERM) proteins and regulates their head-to-tail association. *J Cell Biol* **140**(3): 647-657.

Maudsley, S., Zamah, A.M., Rahman, N., Blitzer, J.T., Luttrell, L.M., Lefkowitz, R.J., and Hall, R.A. 2000. Platelet-derived growth factor receptor association with Na(+)/H(+) exchanger regulatory factor potentiates receptor activity. *Mol Cell Biol* **20**(22): 8352-8363.

McCartney, B.M. and Fehon, R.G. 1996. Distinct cellular and subcellular patterns of expression imply distinct functions for the Drosophila homologues of moesin and the neurofibromatosis 2 tumor suppressor, merlin. *J Cell Biol* **133**(4): 843-852.

McClatchey, A.I. 2003. Merlin and ERM proteins: unappreciated roles in cancer development? *Nat Rev Cancer* **3**(11): 877-883.

McClatchey, A.I. and Fehon, R.G. 2009. Merlin and the ERM proteins--regulators of receptor distribution and signaling at the cell cortex. *Trends Cell Biol* **19**(5): 198-206.

McClatchey, A.I., Saotome, I., Mercer, K., Crowley, D., Gusella, J.F., Bronson, R.T., and Jacks, T. 1998. Mice heterozygous for a mutation at the Nf2 tumor suppressor locus develop a range of highly metastatic tumors. *Genes Dev* **12**(8): 1121-1133.

McClatchey, A.I., Saotome, I., Ramesh, V., Gusella, J.F., and Jacks, T. 1997. The Nf2 tumor suppressor gene product is essential for extraembryonic development immediately prior to gastrulation. *Genes Dev* **11**(10): 1253-1265.

Meng, J.J., Lowrie, D.J., Sun, H., Dorsey, E., Pelton, P.D., Bashour, A.M., Groden, J., Ratner, N., and Ip, W. 2000. Interaction between two isoforms of the NF2 tumor suppressor protein, merlin, and between merlin and ezrin, suggests modulation of ERM proteins by merlin. *J Neurosci Res* **62**(4): 491-502.

Micklem, D.R., Adams, J., Grunert, S., and St Johnston, D. 2000. Distinct roles of two conserved Staufen domains in oskar mRNA localization and translation. *EMBO J* **19**(6): 1366-1377.

Morris, Z.S. and McClatchey, A.I. 2009. Aberrant epithelial morphology and persistent epidermal growth factor receptor signaling in a mouse model of renal carcinoma. *Proc Natl Acad Sci U S A* **106**(24): 9767-9772.

Morrison, H., Sherman, L.S., Legg, J., Banine, F., Isacke, C., Haipek, C.A., Gutmann, D.H., Ponta, H., and Herrlich, P. 2001. The NF2 tumor suppressor gene product, merlin, mediates contact inhibition of growth through interactions with CD44. *Genes Dev* **15**(8): 968-980.

Munro, E., Nance, J., and Priess, J.R. 2004. Cortical flows powered by asymmetrical contraction transport PAR proteins to establish and maintain anterior-posterior polarity in the early C. elegans embryo. *Dev Cell* **7**(3): 413-424.

Nakamura, F., Amieva, M.R., and Furthmayr, H. 1995. Phosphorylation of threonine 558 in the carboxyl-terminal actin-binding domain of moesin by thrombin activation of human platelets. *J Biol Chem* **270**(52): 31377-31385.

Neisch, A.L. and Fehon, R.G. 2011. Ezrin, Radixin and Moesin: key regulators of membrane-cortex interactions and signaling. *Curr Opin Cell Biol* **23**(4): 377-382.

Nelson, C.M. and Bissell, M.J. 2006. Of extracellular matrix, scaffolds, and signaling: tissue architecture regulates development, homeostasis, and cancer. *Annu Rev Cell Dev Biol* **22**: 287-309.

Ng, T., Parsons, M., Hughes, W.E., Monypenny, J., Zicha, D., Gautreau, A., Arpin, M., Gschmeissner, S., Verveer, P.J., Bastiaens, P.I. et al. 2001. Ezrin is a downstream effector of trafficking PKC-integrin complexes involved in the control of cell motility. *EMBO J* **20**(11): 2723-2741.

Nguyen, R., Reczek, D., and Bretscher, A. 2001. Hierarchy of merlin and ezrin N- and C-terminal domain interactions in homo- and heterotypic associations and their relationship to binding of scaffolding proteins EBP50 and E3KARP. *J Biol Chem* **276**(10): 7621-7629.

Niggli, V., Andreoli, C., Roy, C., and Mangeat, P. 1995. Identification of a phosphatidylinositol-4,5-bisphosphate-binding domain in the N-terminal region of ezrin. *FEBS Lett* **376**(3): 172-176.

Ohanian, V., Wolfe, L.C., John, K.M., Pinder, J.C., Lux, S.E., and Gratzer, W.B. 1984. Analysis of the ternary interaction of the red cell membrane skeletal proteins spectrin, actin, and 4.1. *Biochemistry* **23**(19): 4416-4420.

Pearson, M.A., Reczek, D., Bretscher, A., and Karplus, P.A. 2000. Structure of the ERM protein moesin reveals the FERM domain fold masked by an extended actin binding tail domain. *Cell* **101**(3): 259-270.

Pilot, F., Philippe, J.M., Lemmers, C., and Lecuit, T. 2006. Spatial control of actin organization at adherens junctions by a synaptotagmin-like protein Btsz. *Nature* **442**(7102): 580-584.

Plotkin, S.R., Halpin, C., McKenna, M.J., Loeffler, J.S., Batchelor, T.T., and Barker, F.G., 2nd. 2010. Erlotinib for progressive vestibular schwannoma in neurofibromatosis 2 patients. *Otol Neurotol* **31**(7): 1135-1143.

Polesello, C., Delon, I., Valenti, P., Ferrer, P., and Payre, F. 2002. Dmoesin controls actin-based cell shape and polarity during Drosophila melanogaster oogenesis. *Nat Cell Biol* **4**(10): 782-789.

Rauzi, M. and Lenne, P.F. 2011. Cortical forces in cell shape changes and tissue morphogenesis. *Curr Top Dev Biol* **95**: 93-144.

Reczek, D. and Bretscher, A. 1998. The carboxyl-terminal region of EBP50 binds to a site in the amino-terminal domain of ezrin that is masked in the dormant molecule. *J Biol Chem* **273**(29): 18452-18458.

Rouleau, G.A., Merel, P., Lutchman, M., Sanson, M., Zucman, J., Marineau, C., Hoang-Xuan, K., Demczuk, S., Desmaze, C., Plougastel, B. et al. 1993. Alteration in a new gene encoding a putative membrane-organizing protein causes neuro-fibromatosis type 2. *Nature* **363**(6429): 515-521.

Roumier, A., Olivo-Marin, J.C., Arpin, M., Michel, F., Martin, M., Mangeat, P., Acuto, O., Dautry-Varsat, A., and Alcover, A. 2001. The membrane-microfilament linker ezrin is involved in the formation of the immunological synapse and in T cell activation. *Immunity* **15**(5): 715-728.

Saotome, I., Curto, M., and McClatchey, A.I. 2004. Ezrin is essential for epithelial organization and villus morphogenesis in the developing intestine. *Dev Cell* **6**(6): 855-864.

Scoles, D.R., Nguyen, V.D., Qin, Y., Sun, C.X., Morrison, H., Gutmann, D.H., and Pulst, S.M. 2002. Neurofibromatosis 2 (NF2) tumor suppressor schwannomin and its interacting protein HRS regulate STAT signaling. *Hum Mol Genet* **11**(25): 3179-3189.

Shaw, A.S. 2001. FERMing up the synapse. *Immunity* **15**(5): 683-686.

Shaw, R.J., Henry, M., Solomon, F., and Jacks, T. 1998. RhoA-dependent phosphorylation and relocalization of ERM proteins into apical membrane/actin protrusions in fibroblasts. *Mol Biol Cell* **9**(2): 403-419.

Shaw, R.J., Paez, J.G., Curto, M., Yaktine, A., Pruitt, W.M., Saotome, I., O'Bryan, J.P., Gupta, V., Ratner, N., Der, C.J. et al. 2001. The Nf2 tumor suppressor, merlin, functions in Rac-dependent signaling. *Dev Cell* **1**(1): 63-72.

Sheetz, M.P. 2001. Cell control by membrane-cytoskeleton adhesion. *Nat Rev Mol Cell Biol* **2**(5): 392-396.

Sheetz, M.P., Sable, J.E., and Dobereiner, H.G. 2006. Continuous membrane-cytoskeleton adhesion requires continuous accommodation to lipid and cytoskeleton dynamics. *Annu Rev Biophys Biomol Struct* **35**: 417-434.

Shewan, A., Eastburn, D.J., and Mostov, K. 2011. Phosphoinositides in cell architecture. *Cold Spring Harb Perspect Biol* **3**(8): a004796.

Shi, Z.T., Afzal, V., Coller, B., Patel, D., Chasis, J.A., Parra, M., Lee, G., Paszty, C., Stevens, M., Walensky, L. et al. 1999. Protein 4.1R-deficient mice are viable but have erythroid membrane skeleton abnormalities. *J Clin Invest* **103**(3): 331-340.

Short, D.B., Trotter, K.W., Reczek, D., Kreda, S.M., Bretscher, A., Boucher, R.C., Stutts, M.J., and Milgram, S.L. 1998. An apical PDZ protein anchors the cystic fibrosis transmembrane conductance regulator to the cytoskeleton. *J Biol Chem* **273**(31): 19797-19801.

Simons, P.C., Pietromonaco, S.F., Reczek, D., Bretscher, A., and Elias, L. 1998. C-terminal threonine phosphorylation activates ERM proteins to link the cell's cortical lipid bilayer to the cytoskeleton. *Biochem Biophys Res Commun* **253**(3): 561-565.

Slaughter, B.D., Smith, S.E., and Li, R. 2009. Symmetry breaking in the life cycle of the budding yeast. *Cold Spring Harb Perspect Biol* **1**(3): a003384.

Sorkin, A. and Goh, L.K. 2009. Endocytosis and intracellular trafficking of ErbBs. *Exp Cell Res* **315**(4): 683-696.

Speck, O., Hughes, S.C., Noren, N.K., Kulikauskas, R.M., and Fehon, R.G. 2003. Moesin functions antagonistically to the Rho pathway to maintain epithelial integrity. *Nature* **421**(6918): 83-87.

St Johnston, D. and Ahringer, J. 2010. Cell polarity in eggs and epithelia: parallels and diversity. *Cell* **141**(5): 757-774.

Stamenkovic, I. and Yu, Q. Merlin, a "magic" linker between extracellular cues and intracellular signaling pathways that regulate cell motility, proliferation, and survival. *Curr Protein Pept Sci* **11**(6): 471-484.

Sun, C.X., Robb, V.A., and Gutmann, D.H. 2002. Protein 4.1 tumor suppressors: getting a FERM grip on growth regulation. *J Cell Sci* **115**(Pt 21): 3991-4000.

Takeda, T., McQuistan, T., Orlando, R.A., and Farquhar, M.G. 2001. Loss of glomerular foot processes is associated with uncoupling of podocalyxin from the actin cytoskeleton. *J Clin Invest* **108**(2): 289-301.

ten Klooster, J.P., Jansen, M., Yuan, J., Oorschot, V., Begthel, H., Di Giacomo, V., Colland, F., de Koning, J., Maurice, M.M., Hornbeck, P. et al. 2009. Mst4 and Ezrin induce brush borders downstream of the Lkb1/Strad/Mo25 polarization complex. *Dev Cell* **16**(4): 551-562.

Tikoo, A., Varga, M., Ramesh, V., Gusella, J., and Maruta, H. 1994. An anti-Ras function of neurofibromatosis type 2 gene product (NF2/Merlin). *J Biol Chem* **269**(38): 23387-23390.

Trofatter, J.A., MacCollin, M.M., Rutter, J.L., Murrell, J.R., Duyao, M.P., Parry, D.M., Eldridge, R., Kley, N., Menon, A.G., Pulaski, K. et al. 1993. A novel moesin-, ezrin-, radixin-like gene is a candidate for the neurofibromatosis 2 tumor suppressor. *Cell* **75**(4): 826.

Turunen, O., Wahlstrom, T., and Vaheri, A. 1994. Ezrin has a COOH-terminal actin-binding site that is conserved in the ezrin protein family. *J Cell Biol* **126**(6): 1445-1453.

Van Furden, D., Johnson, K., Segbert, C., and Bossinger, O. 2004. The C. elegans ezrin-radixin-moesin protein ERM-1 is necessary for apical junction remodelling and tubulogenesis in the intestine. *Dev Biol* **272**(1): 262-276.

von Recklinghausen, F. 1882. Ueber die Multiplen Fibrome der Haut und ihre Beziehung zu den Multiplen Neuromen. *Berlin: Hirschwald*: 138.

Weinman, E.J., Minkoff, C., and Shenolikar, S. 2000. Signal complex regulation of renal transport proteins: NHERF and regulation of NHE3 by PKA. *Am J Physiol Renal Physiol* **279**(3): F393-399.

Wishart, J.H. 1822. Case tumors in the skull, dura mater, and brain. *Edinburgh Med Surg J* **18**: 5.

Xiao, G.H., Beeser, A., Chernoff, J., and Testa, J.R. 2002. p21-activated kinase links Rac/Cdc42 signaling to merlin. *J Biol Chem* **277**(2): 883-886.

Yang, H.S. and Hinds, P.W. 2003. Increased ezrin expression and activation by CDK5 coincident with acquisition of the senescent phenotype. *Mol Cell* **11**(5): 1163-1176.

Yohay, K. 2006. Neurofibromatosis types 1 and 2. *Neurologist* **12**(2): 86-93.

Yun, C.H., Lamprecht, G., Forster, D.V., and Sidor, A. 1998. NHE3 kinase A regulatory protein E3KARP binds the epithelial brush border Na+/H+ exchanger NHE3 and the cytoskeletal protein ezrin. *J Biol Chem* **273**(40): 25856-25863.

Chapter 2

Merlin and the ERM proteins establish cortical asymmetry and centrosome position

Alan M. Hebert[1] and Andrea I. McClatchey[1]

[1]Massachusetts General Hospital Center for Cancer Research and
Harvard Medical School Department of Pathology
149 13th St. Charlestown, MA 02129

Publications and Contributions: This chapter is adapted from a manuscript submitted to the journal *Genes & Development* on April 13th 2012. All figures in this chapter were contributed by A. M. Hebert.

Abstract

The ability to generate asymmetry at the cell cortex underlies cell polarization and asymmetric cell division. Here we demonstrate a novel role for the tumor suppressor Merlin and closely related ERM proteins in generating cortical asymmetry in the absence of external cues. Our data reveal that Merlin functions to restrict the cortical distribution of the actin regulator Ezrin, which in turn positions the interphase centrosome in single epithelial cells and 3D organotypic cultures. In the absence of Merlin ectopic cortical Ezrin yields mispositioned centrosomes, misoriented spindles and aberrant epithelial architecture. Furthermore, in tumor cells with centrosome amplification, the failure to restrict cortical Ezrin abolishes centrosome clustering, yielding multipolar mitoses. These data uncover fundamental roles for Merlin/ERM proteins in spatiotemporally organizing the cell cortex and suggest that Merlin's role in promoting cortical heterogeneity may contribute to tumorigenesis by disrupting cell polarity, spindle orientation and potentially genome stability.

Introduction

The ability to spatially restrict specific activities across the cell cortex functionally defines individual cells and tissues. Cortical asymmetry is achieved via the polarized distribution of membrane protein complexes and mechanical properties across the cortex. In single cells and single-celled organisms cortical asymmetry can be triggered by external cues such as sperm entry or by the cortical scar that marks the site of an earlier division (Macara and Mili 2008; St Johnston and Ahringer 2010). In multicellular tissues cortical asymmetry is guided by cell-cell and/or cell-ECM interaction (St Johnston and Ahringer 2010). Much less is known about how or even whether cells can intrinsically establish cortical asymmetry in the absence of external cues.

A central consequence of cortical asymmetry in single- and multi-cellular organisms is the orientation and morphology of the mitotic spindle, which dictates whether divisions will be symmetric or asymmetric and yield faithful chromosome segregation (Siller and Doe 2009; Pereira and Yamashita 2011). In multicellular organisms aberrant spindle orientation can cause defective tissue architecture and stem cell gain/loss while aberrant spindle morphology can yield chromosome missegregation and aneuploidy - phenotypes that are all known to contribute to tumorigenesis (Bettencourt-Dias et al. 2011; Morin and Bellaiche 2011). Both the physical properties of the cell cortex and communication between the cortex and centrosomes at the spindle poles are known to be critical for spindle orientation and function (Sandquist et al. 2011). The molecular mechanisms by which cortical cues

direct spindle orientation and function must involve the dynamic spatiotemporal organization of the cell cortex.

The cell cortex is defined by dynamic interactions between plasma membrane proteins and/or lipids and the underlying cortical cytoskeleton (Fehon et al. 2010; Rauzi and Lenne 2011). The ERM proteins (Ezrin, Radixin and Moesin) and closely related neurofibromatosis type 2 (NF2) tumor suppressor, Merlin, have emerged as key scaffolds that can assemble protein complexes at the membrane:cytoskeleton interface and play important roles in cortical organization (McClatchey and Fehon 2009). For example, by linking plasma membrane proteins and/or lipids directly to cortical actin, activated ERM proteins can physically stabilize the cell cortex during mitotic rounding, membrane bleb retraction and the establishment of the apical and apical junctional region of epithelial cells (Gobel et al. 2004; Saotome et al. 2004; Van Furden et al. 2004; Charras et al. 2006; Pilot et al. 2006; Kunda et al. 2008; Luxenburg et al. 2011). ERM proteins can also control the distribution and activity of the numerous membrane receptors with which they interact (McClatchey and Fehon 2009). Similarly, functional studies indicate that cortical Merlin can both control the distribution of certain membrane receptors and regulate cortical features such as cell junctions, polarity and spindle orientation (Lallemand et al. 2003; Maitra et al. 2006; Curto et al. 2007; Cole et al. 2008; Lallemand et al. 2009; Gladden et al. ; Yi et al. 2011). Merlin and the ERM proteins share strong evolutionary conservation and are thought to be derived from a common ancestor. They are co-expressed in most cell types, share binding partners, hetero-oligomerize and display coordinated regulation, yet they often exhibit

distinct cortical localizations (McClatchey and Fehon 2009). Moreover, in contrast to the ERM proteins, Merlin is an established tumor suppressor in flies, mice and humans (Rouleau et al. 1993; Trofatter et al. 1993; LaJeunesse et al. 1998; McClatchey et al. 1998). Indeed, the nature of the functional relationship between Merlin and the ERM proteins is not clear and we lack a fundamental understanding of how Merlin/ERM proteins organize the cell cortex.

Here we show that cortical Ezrin undergoes a progressive cell cycle-correlated redistribution in single epithelial cells in the absence of external cues. Moreover, Merlin functions to restrict the cortical distribution of Ezrin, which, in turn, intrinsically and actively positions the interphase centrosome and ensuing mitotic spindle in both single cells and derivative 3D organotypic cultures. Notably, Merlin-mediated restriction of Ezrin is dependent upon the Merlin-interacting protein α-catenin, even in single cells, revealing a novel junction independent function for α-catenin in establishing cortical asymmetry. In the absence of Merlin, ectopic Ezrin yields mispositioned centrosomes, aberrant mitotic spindle orientation and defective epithelial architecture. The importance of Merlin-mediated restriction of cortical Ezrin is exemplified by the fact that in tumor cells that contain supernumerary centrosomes loss of Merlin yields centrosome unclustering and multipolar spindles, suggesting that Ezrin is a key component of the poorly understood phenomenon of centrosome clustering. Thus Ezrin and Merlin are central components of a program whereby the intrinsic spatiotemporal organization of the cell cortex governs polarity, centrosome position, and mitotic spindle orientation and function.

Results

Cell cycle-dependent distribution of cortical Ezrin in single cells

To follow the localization of Ezrin and Merlin as individual cells establish apical-basal polarity during epithelial morphogenesis we employed the well-established model of Caco2 intestinal epithelial cyst formation in Matrigel (Jaffe et al. 2008). Consistent with previous reports, we found that Ezrin concentrated at the cleavage furrow and nascent apical lumen at the 2-cell-stage and remained apically concentrated as the 2-cell structures developed into fully polarized cysts with a single central lumen (Figure 2.1A; Jaffe et al. 2008). Surprisingly, however, we found that Ezrin also concentrated into a distinct cap-like structure at the membrane of single spherical cells *prior to* the first cell division (Figure 2.1B). At early times after plating, Ezrin localized uniformly around the cortex of single cells indicating that the Ezrin 'cap' is not a remnant of the apical surface established in 2D and instead forms *de novo* via the progressive restriction of Ezrin to a small cortical domain (Figure 2.1B).

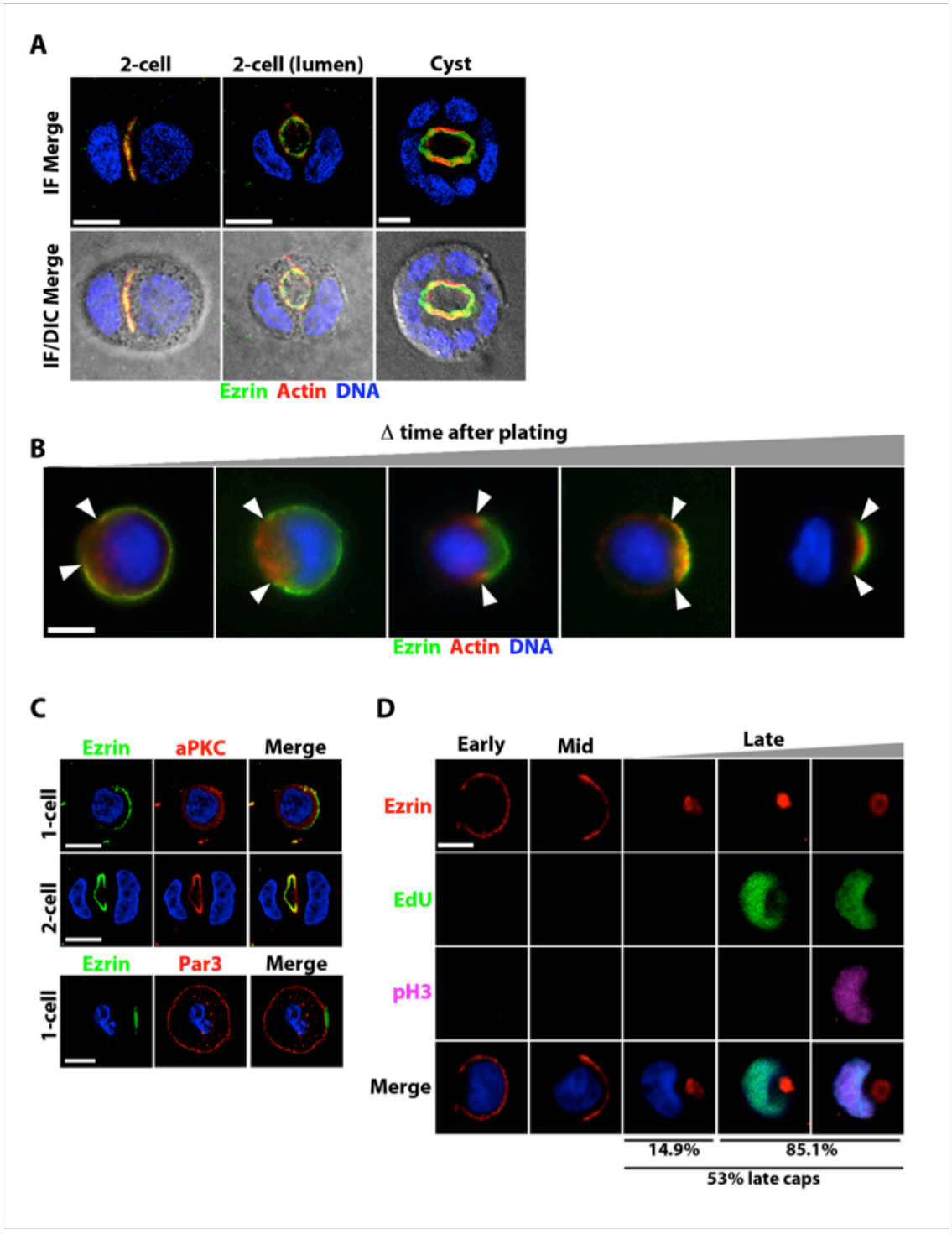

Figure 2.1 (Continued on next page)

Figure 2.1 (Continued). Restricted cortical distribution of Ezrin in single Caco2 cells. **(A)** Ezrin localizes to the cleavage furrow and nascent apical lumen in developing Caco2 cysts. Single Caco2 cells were embedded in Matrigel for 16 hr (2-cell stage) or 6 days (cysts), and stained for Ezrin (green), actin (red) and DNA (blue). Unless otherwise indicated, all images shown are single confocal sections through the middle of each structure. Corresponding differential interference contrast (DIC) images are also shown. **(B)** Cortical Ezrin is progressively restricted into a cap-like structure (arrowheads) that colocalizes with markedly enriched cortical actin in single Caco2 cells. Cells were stained as in A and imaged using a widefield fluorescence microscope. **(C)** The Ezrin cap does not contain apical polarity proteins. Embedded Caco2 cells were stained for Ezrin (green), DNA (blue) and aPKC or Par-3 (red). **(D)** The Ezrin cap forms prior to S-phase. Embedded Caco2 cells were incubated with EdU for 14 hr and stained for Ezrin (red), EdU (green), pH3 (purple) and DNA (blue). Of the ~53% of cells that had a mature Ezrin cap in this experiment, 85.1% stained positively for EdU and/or pH3 and 14.9% stained negatively for EdU/pH3. In contrast, cells with an immature Ezrin cap rarely stained positively for EdU/pH3. Bars, 10μm.

Ezrin can directly interact with actin and stabilize the cortical actin cytoskeleton. Consistent with this, we found that cortical actin is markedly concentrated directly beneath the mature Ezrin cap (Figure 2.1B). In contrast, α-tubulin exhibited a uniform distribution in Ezrin cap-containing cells (Figure 2.2A). Importantly, apical markers such as aPKC and Par3 were not concentrated at the Ezrin cap (Figure 2.1C), indicating that it does not represent a *bona fide* apical surface. Similarly, E-cadherin was uniformly localized around the cortex in capping cells in the absence of adherens junctions (Figure 2.2B). Thus Ezrin forms a distinct cortical domain in single epithelial cells prior to the establishment of apico-basal polarity and in the absence of external cues.

To determine whether the dynamic restriction of Ezrin into a cap is linked to the cell cycle, we labeled single Caco2 cells with EdU- and phospho-histone H3 (pH3) that mark cells that have entered S-phase or mitosis, respectively. At a time when about half (~53%) of the cells have a mature cap, the majority (85%) of those cells were EdU- or EdU/pH3-positive and a small percentage (15%) were EdU/pH3-negative; in contrast, nearly all cells that exhibited a partial restriction of cortical Ezrin were EdU/pH3-negative (Figure 2.1D; Figure 2.2C). These data indicate that the restriction of cortical Ezrin occurs during G1 and is largely completed by S-phase. Thus the formation of a cortical Ezrin cap is a very early indication of a cell's pending entry into S-phase.

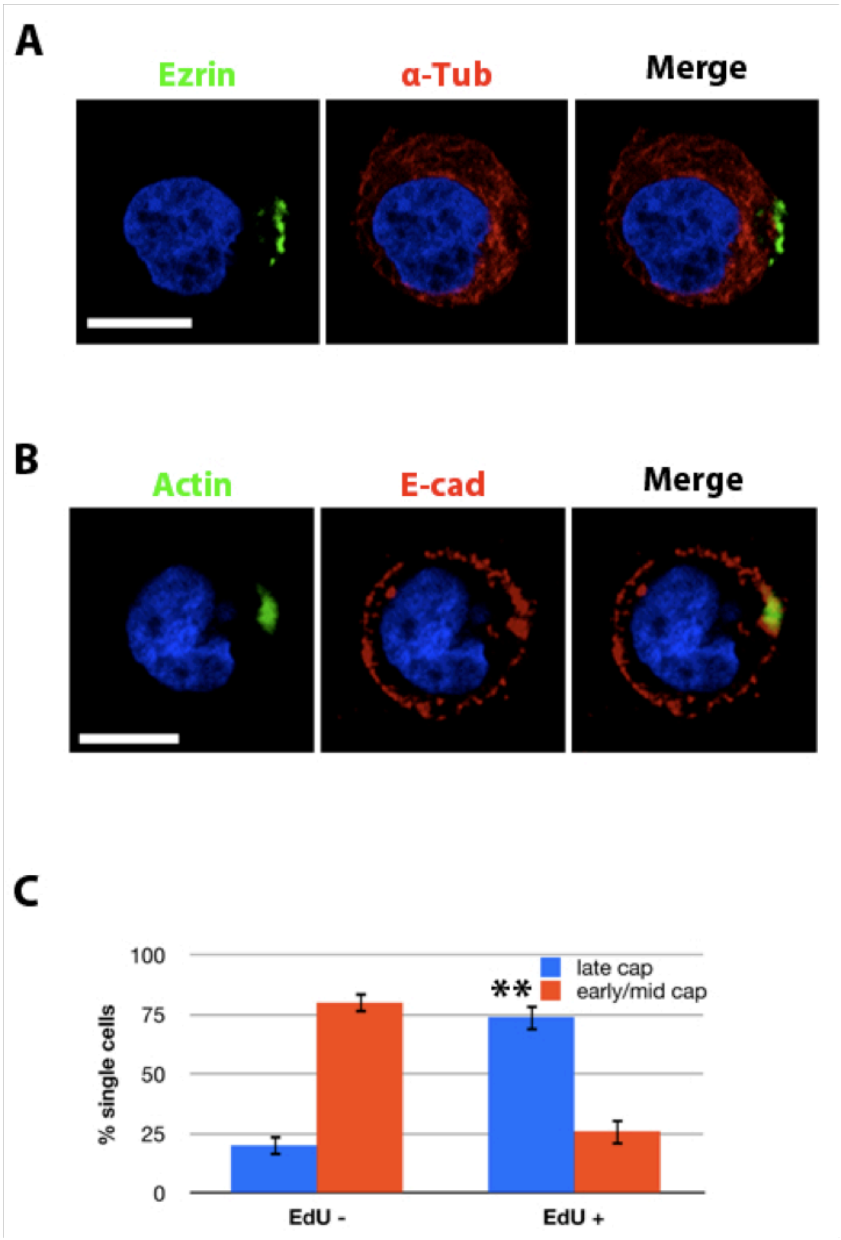

Figure 2.2 Restricted cortical distribution of Ezrin in single Caco2 cells. **(A)** Microtubules are not concentrated at or beneath the Ezrin cap. Embedded Caco2 cells, cultured as in Figure 1C, were stained for Ezrin (green), DNA (blue), and α-tubulin (red). **(B)** E-cadherin localizes ubiquitously around the cell membrane in single cells containing an Ezrin 'cap'. Embedded Caco2 cells, cultured as in Figure 1C, were stained for Actin (green) to mark the Ezrin cap, E-cadherin (red), and DNA (blue). **(C)** The cortical Ezrin cap forms prior to S-phase. Cells depicted in Figure 1C were categorized as having either late-stage or early/mid stage Ezrin caps then scored for the presence or absence of EdU incorporation indicative of S-phase entry. Values shown represent mean ± SEM from at least 3 experiments.

Requirements for Ezrin cap formation

Since the Ezrin cap coincides with a marked concentration of cortical actin and Ezrin can bind directly to actin (Algrain et al. 1993; Turunen et al. 1994), we examined the dependency of Ezrin cap formation upon the actin cytoskeleton. Treatment of cells with cytochalasin D, jasplakinolide or latrunculin A - drugs that disrupt actin by different mechanisms - completely abolished cap formation in single cells; in contrast, cells treated with the microtubule-depolymerizing agent nocodazole did form mature caps (Figure 2.3A). Polarization of the single-celled *C. elegans* oocyte is driven by actomyosin-powered cortical flow of membrane proteins (Munro et al. 2004); however, neither inhibitors of myosin II (blebbistatin) or Rho-kinase, which acts upstream of myosin II (Y27632), perturbed Ezrin cap formation (Figure 2.3A).

The ERM proteins are activated by a phosphorylation-mediated conformational change that unmasks the amino-(N)-terminal Four-point-one-ERM (FERM) and carboxy-(C)-terminal actin-binding domains; phosphorylation of residues within the FERM and C-terminal domains may cooperate to effect and sustain ERM activation (Pearson et al. 2000; Yang and Hinds 2003). An antibody that specifically detects phosphorylation of the well-studied T567 C-terminal residue recognized cortical Ezrin during all stages of cap formation, suggesting that the cap is composed of activated Ezrin (Figure 2.3B). The Ste20-like kinases SLK and Mst4 can both phosphorylate this residue; in fact, Mst4-mediated phosphorylation of Ezrin is important for brush border formation in Caco2 cells (Hipfner et al. 2004; Carreno et al. 2008; Kunda et al. 2008; ten Klooster et al. 2009). However,

elimination of Mst4 did not perturb Ezrin cap formation (Figure 2.3C). A more in depth analysis of SLK is described in Chapter 4.

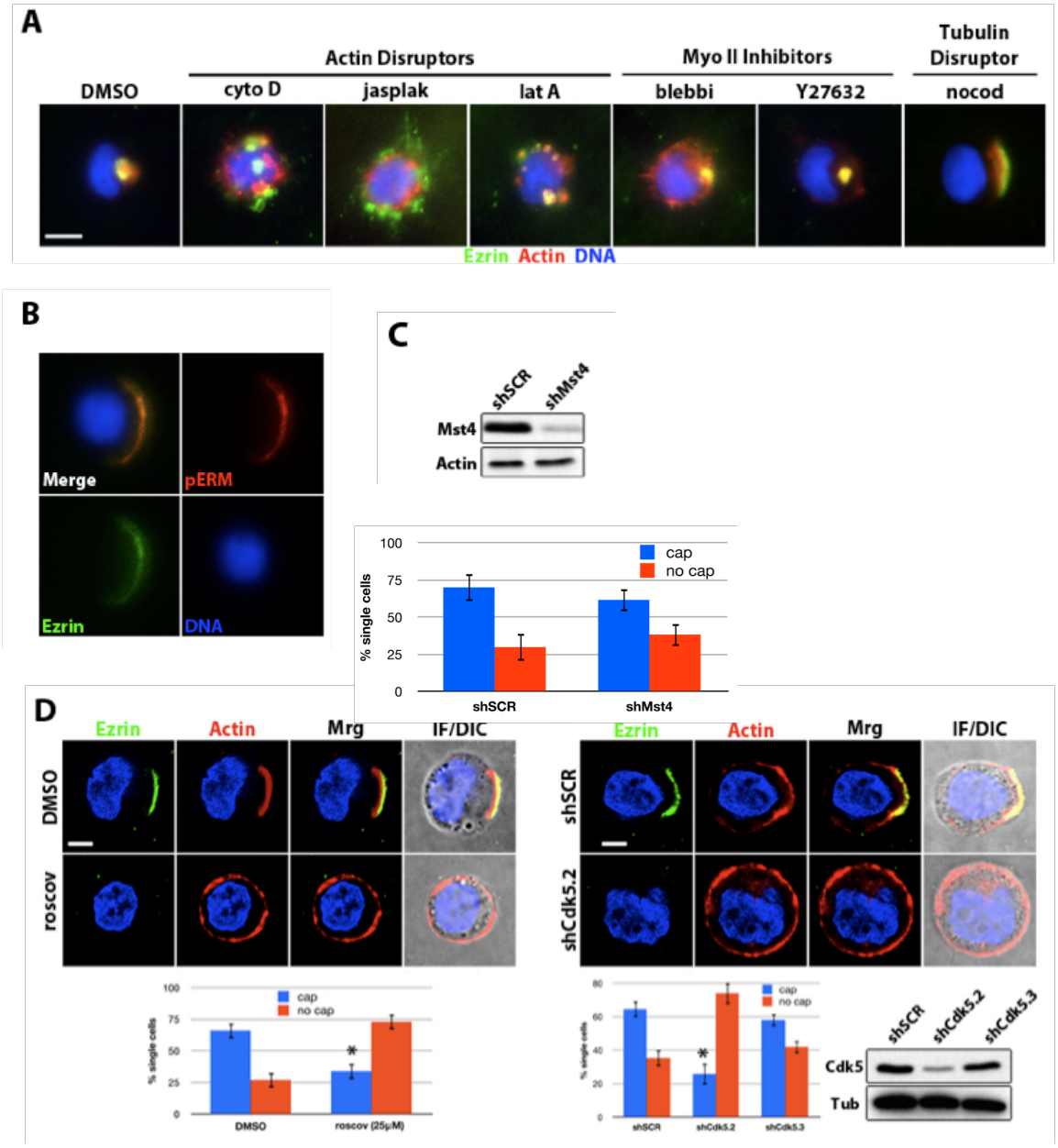

Figure 2.3 (Continued on next page)

Figure 2.3 (Continued). Regulation of Ezrin cap formation. **(A)** Ezrin cap formation is dependent upon actin. Single embedded Caco2 cells were cultured with vehicle (DMSO), actin-disrupting compounds (cytochalasin D, cytoD; jasplakinolide, jasplak; latrunculin A, latA), myosin II inhibitors (blebbistatin, blebbi; Rho-kinase inhibitor, Y27632) or the microtubule depolymerizing drug nocodazole (nocod) and stained for Ezrin (green), actin (red) and DNA (blue). Cells were imaged using a widefield fluorescence microscope. **(B)** The Ezrin cap contains active phosphorylated ERM (pERM). Single embedded Caco2 cells were fixed with TCA to preserve the pERM epitope and stained for Ezrin (green), pERM (red) and DNA (blue). **(C)** Mst4 is not necessary for Ezrin cap formation. Cells infected with lentiviruses expressing control (scrambled; shSCR) or Mst4-targeted shRNAs were subject to immunoblotting or IF analysis of Ezrin cap formation. Values shown are mean ± SEM. **(D)** The pan-Cdk inhibitor roscovitine prevents cortical Ezrin localization and cap formation. Single embedded Caco2 cells were cultured with 25 μM roscovitine for 14 hr then stained for Ezrin (green), actin (red) and DNA (blue). Values shown are mean ± SEM; *$p<0.05$. **(E)** Cdk5 is required for Ezrin cortical localization and cap formation. Cells were stably infected with lentiviruses expressing control (shSCR) or two short hairpins targeting Cdk5 (shCdk5.2, shCdk5.3). Most shCdk5.2 expressing cells do not form Ezrin caps while shCdk5.3 expressing cells exhibit a mild defect in cap-formation, consistent with the weak knockdown achieved with shCdk5.3. Values shown are mean ± SEM; *$p<0.05$. Bars 10μm.

The N-terminal residue T235 directly apposes T567 in crystal structures of self-associated ERMs and can be phosphorylated by the cyclin-dependent kinase Cdk5 (Pearson et al. 2000; Yang and Hinds 2003). Indeed, treatment with the pan-Cdk inhibitor roscovitine dramatically perturbed Ezrin cap formation and largely eliminated the cortical localization of Ezrin (Figure 2.3D). The absence of pH3-positive cells confirmed the activity of roscovitine in these experiments (Figure 2.4A). Moreover, elimination of the expression of Cdk5, which is inhibited by roscovitine, or its major activator p35, also dramatically decreased the proportion of single cells with an Ezrin cap (Figure 2.3E; Figure 2.4B). Like those treated with roscovitine, the majority of single Cdk5-deficient cells failed to concentrate Ezrin at the membrane at all, consistent with the notion that Cdk5 is required for Ezrin activation. Unlike roscovitine-treated cells, however, Cdk5-deficient cells progressed normally into S-phase, indicating that Ezrin cap formation is not dependent upon or required for S-phase progression (not shown). Thus Cdk5-mediated Ezrin activation may be a prerequisite for the cell-cycle dependent reorganization of the cell cortex prior to mitosis. Notably, in both roscovitine-treated and Cdk5-deficient cells actin is uniformly localized around the cortex (Figure 2.3D,E) suggesting that the concentration of actin into a cap requires cortical Ezrin.

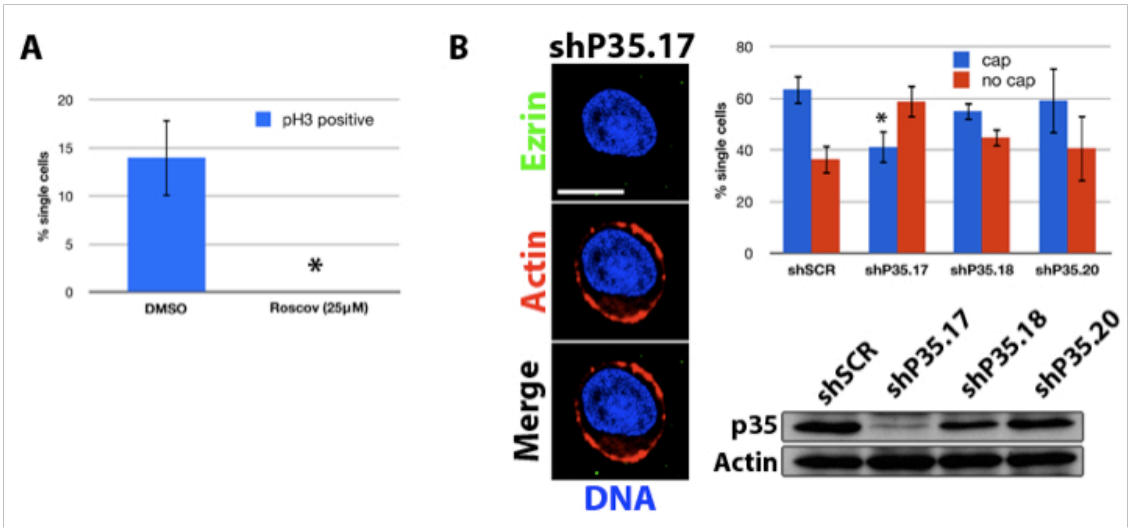

Figure 2.4 Regulation of Ezrin cap formation. **(A)** Roscovitine-treatment blocks cell cycle progression. Single embedded Caco2 cells were cultured for 14 hr in DMSO or 25 μM roscovitine and stained for pH3 and DNA. Nuclei of single Caco2 cells were scored for the presence or absence of pH3 staining indicative of mitotic entry. Values shown represent mean ± SEM from at least 3 independent experiments. **(B)** p35 is required for Ezrin cortical localization and cap formation. Cells were stably infected with lentiviruses expressing control (shSCR) or three short hairpins targeting p35 (shp35.17, shp35.18 and shp35.20). Single cells were embedded and cultured for 14 hr and stained for Ezrin (green), Actin (red) and DNA (blue). The shp35.17 hairpin yielded strong knockdown of p35 (immunoblot) and shp35.17-expressing cells exhibited defective cap formation, largely failing to concentrate Ezrin at the cortex at all. In contrast, cells expressing shSCR, shp35.18 and shp35.20 retain p35 expression and form normal Ezrin caps. Values shown represent mean ± SEM from at least 3 independent experiments. Bar 10μ m.

Ezrin cap formation is dependent on Merlin

Substantial evidence suggests that the ERM proteins and Merlin share a functional and conserved relationship, but the nature of that relationship is obscure (McClatchey and Fehon 2009). We found that in cells forming an Ezrin cap, exogenous wild-type Merlin does not colocalize with Ezrin and instead decorates the entire cell cortex (Figure 2.5A). In contrast, a mutant version of Merlin ($Nf2^{18-595}$) that does not stably localize to the cortical cytoskeleton (Cole et al. 2008) remains cytoplasmic throughout Ezrin cap formation (Figure 2.5A). Thus Merlin and Ezrin exhibit distinct cortical distributions in single cells prior to division.

Strikingly, we found that elimination of *NF2* expression completely prevented Ezrin cap formation (Figure 2.5B). However, in contrast to roscovitine treatment or elimination of Cdk5, loss of Merlin yielded either uniform cortical localization of Ezrin or the appearance of multiple cortical Ezrin patches, suggesting that rather than influencing Ezrin activation, Merlin normally functions to restrict the localization of active Ezrin at the membrane. In fact, re-expression of either wild-type or myristoylated, membrane-tethered Merlin ($NF2^{myr}$) rescued Ezrin cap formation (Figure 2.5C). In contrast, Ezrin cap formation was not rescued by $Nf2^{18-595}$ (Figure 2.5D). The N-terminal 17 amino acids of Merlin precede the FERM domain and are necessary for both localization to the cortical cytoskeleton and for the direct association of Merlin with the actin-binding protein α-catenin (Gladden et al. 2010). Notably, Ezrin neither has this N-terminal motif nor interacts with α-catenin (Gladden et al. 2010). The requirement of these residues for the cortical localization of Merlin in single Caco2 cells suggests that α-catenin could link Merlin

to the cortical cytoskeleton even in the absence of adherens junctions. Indeed, Merlin fails to stably localize to the cortex of single cells in the absence of α-catenin (Figure 2.5F). Moreover, Ezrin cap formation in single cells is completely dependent upon α-catenin (Figure 2.5E). These data identify a novel junction-independent function for α-catenin and suggest that the α-catenin-dependent localization of Merlin to the cortex of single cells functions to restrict cortical Ezrin distribution prior to mitosis.

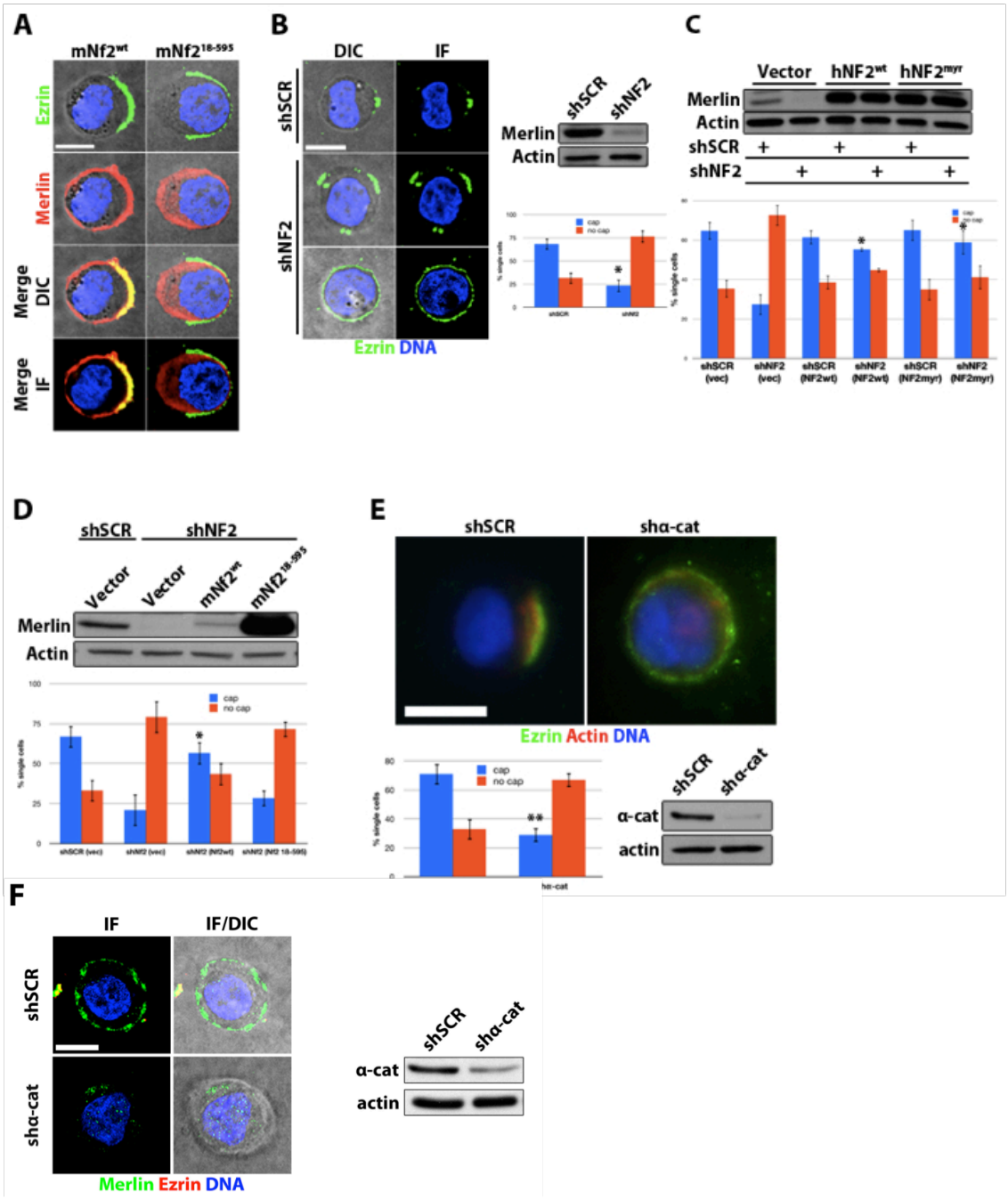

Figure 2.5 (Continued on next page)

Figure 2.5 (Continued). Merlin is required for Ezrin cap formation. **(A)** Merlin exhibits uniform cortical localization in cells harboring a mature Ezrin cap. Cells expressing FLAG-tagged versions of wild-type mouse Merlin ($mNf2^{wt}$) or $mNf2^{18\text{-}595}$ were stained for Ezrin (green), Merlin (red) and DNA (blue). **(B)** Endogenous Merlin is required for Ezrin cap formation. Caco2 cells stably expressing control (shSCR) or *NF2*-targeted shRNAs (shNF2) were stained for Ezrin (green) and DNA (blue). Immunoblot confirms the loss of Merlin. **(C)** Ezrin capping is rescued by reintroduction of wild-type or membrane-tethered Merlin. CaCo2 cells stably expressing shSCR or shNF2 were infected with lentiviruses expressing shNF2-resistant wild-type ($hNF2^{wt}$) or myristoylated ($hNF2^{myr}$) human Merlin. Immunoblot confirms the loss of endogenous Merlin and expression of exogenous $hNF2^{wt}$ and $hNF2^{myr}$. Values shown are mean ± SEM; *$p<0.05$. **(D)** $mNf2^{18\text{-}595}$ does not rescue Ezrin cap formation. Cells stably expressing shSCR or shNF2 were infected with lentiviruses expressing $mNf2^{wt}$ or $mNf2^{18\text{-}595}$. Immunoblot confirms loss of Merlin and expression of exogenous $mNf2^{wt}$ and $mNf2^{18\text{-}595}$. Values shown are mean ± SEM; *$p<0.05$. **(E)** α-catenin is required for Ezrin cap formation. Cells expressing control (shSCR) or α-catenin-targeted (shα-cat) shRNAs were stained for Ezrin (green), actin (red) and DNA (blue) and monitored for Ezrin cap formation. Immunoblot confirms the loss α-catenin protein. **(F)** Embedded Caco2 cells expressing control (shSCR) or α-catenin-targeted (shα-cat) shRNAs were cultured for 14 hr, fixed, permeabilized and stained for Merlin (green), Ezrin (red) and DNA (blue). Merlin retained stable cortical localization in shSCR-expressing cells but not in shα-cat-expressing cells. Immunoblot confirms diminished shα-cat expression. Values shown are mean ± SEM; **$p<0.01$. Bars, 10μm.

ERMs and Merlin are essential for centrosome positioning

As single Caco2 cells undergo the first mitosis in Matrigel the cleavage furrow is converted to junctional and then apical surface and subsequent mitotic spindles orient relative to that central apical lumen (Jaffe et al. 2008). It is not known whether a single cell actively orients the first mitotic spindle in the absence of an external cue or apical domain. The mitotic spindle forms after centrosome duplication and migration of one centrosome to the opposite pole (Nigg 2007). Centrosomes use astral microtubules to communicate with the cell cortex, but little is known about the molecular basis of this communication (Sandquist et al. 2011). During Ezrin cap formation cells contain single centrosomes (Figure 2.6A, left); however, most cells harboring a mature Ezrin cap had undergone centrosome duplication, which occurs at the G1-S transition (Figure 2.6A, middle). We noted that prior to duplication the single centrosome is always positioned beneath the Ezrin-decorated cortex and centrosome duplication occurs immediately beneath the cap as soon as it is mature (Figure 2.6A). Subsequently, mitotic spindles always orient with one centrosome proximal to the Ezrin cap (Figure 2.6B). During cytokinesis Ezrin relocalizes to the cleavage furrow, from which the nascent apical lumen forms; during the ensuing interphase centrosomes again localize in close apposition to Ezrin at the new apical surface (Figure 2.6A, right). Thus there is a tight correlation between the cortical distribution of Ezrin and the position of the centrosome(s) throughout the cell cycle.

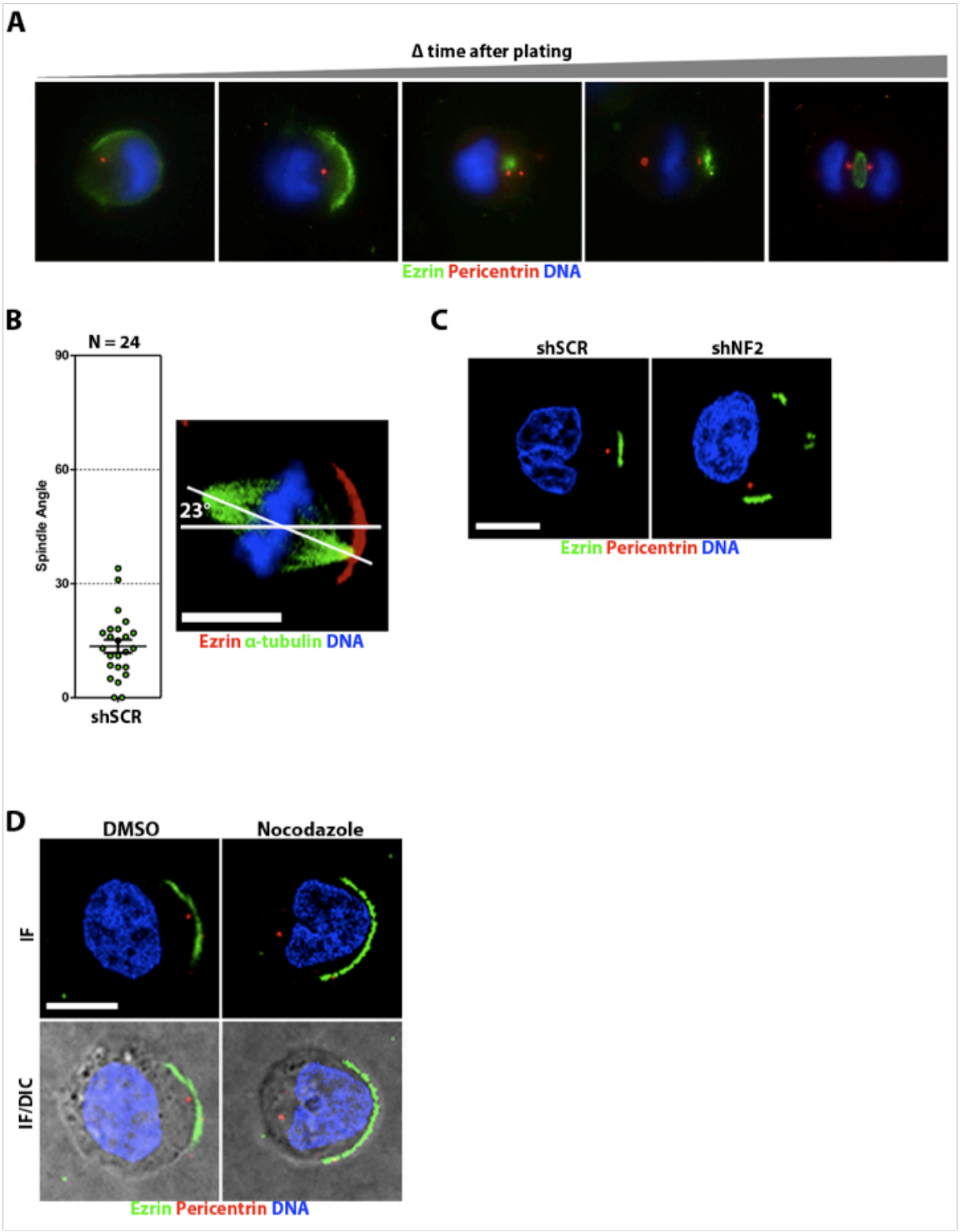

Figure 2.6 (Continued on next page)

Figure 2.6 (Continued). Cortical Ezrin controls centrosome position. **(A)** Correlation between cortical Ezrin and centrosome position. Cells were stained for Ezrin (green), Pericentrin (red) and DNA (blue) and imaged using a widefield fluorescence microscope. **(B)** In single cells one spindle pole always localizes beneath the Ezrin cap. Cells were stained for Ezrin (red), α-Tubulin (green) and DNA (blue). The angles between the spindle axis (dotted line) and a line connecting the center of the Ezrin cap to the center of the spindle (dashed line) were measured using Zen software and depicted by scatter plot (left). **(C)** Centrosomes localize beneath ectopic cortical Ezrin. Control (shSCR), shCdk5- or shNF2-expressing cells were stained for Ezrin (green), Pericentrin (red) and DNA (blue). **(D)** Microtubules are required for the positioning of centrosomes beneath cortical Ezrin. Cells were treated with vehicle (DMSO) or nocodazole (20 μM) and stained for Ezrin (green), Pericentrin (red) or DNA (blue). Bars, 10μm.

To determine whether Ezrin provides a cortical cue for centrosome positioning we examined the position of centrosomes in shNF2-expressing cells, in which cortical Ezrin fails to be restricted to a single cap-like domain. In these cells centrosomes were located in close proximity to the cell cortex and specifically to areas of the cortex that were decorated by ectopic Ezrin (Figure 2.6C). In contrast, in cells that express shCdk5 and have no cortical Ezrin, centrosomes often failed to exhibit a clear cortical association (not shown). Finally, consistent with the notion that astral microtubules mediate communication between centrosomes and the Ezrin-decorated cortex, we found that although nocodazole treatment did not prevent Ezrin cap formation, it eliminated the positioning of the centrosome beneath the Ezrin cap; nocodazole-treated cells, like shCdk5-expressing cells, exhibited a random and often non-cortical localization of centrosomes (Figure 2.6D). Together these results suggest that Ezrin provides an intrinsic cortical cue for positioning the centrosome and that cortical Merlin functions to restrict and position that cue.

Coordination of cell cycle and polarity cues

Although Ezrin cap formation is perturbed in shNF2-expressing cells, some Ezrin did relocalize to the cleavage furrow and nascent lumen (Figure 2.7A). However, in contrast to control cells, Ezrin was not restricted to the cleavage furrow and nascent apical lumen at the 2-cell stage in the absence of Merlin and instead exhibited ectopic cortical localization (Figure 2.7A). Centrosomes were also not

restricted to the area beneath the nascent lumen and were instead observed in proximity to ectopic cortical Ezrin (Figure 2.7A).

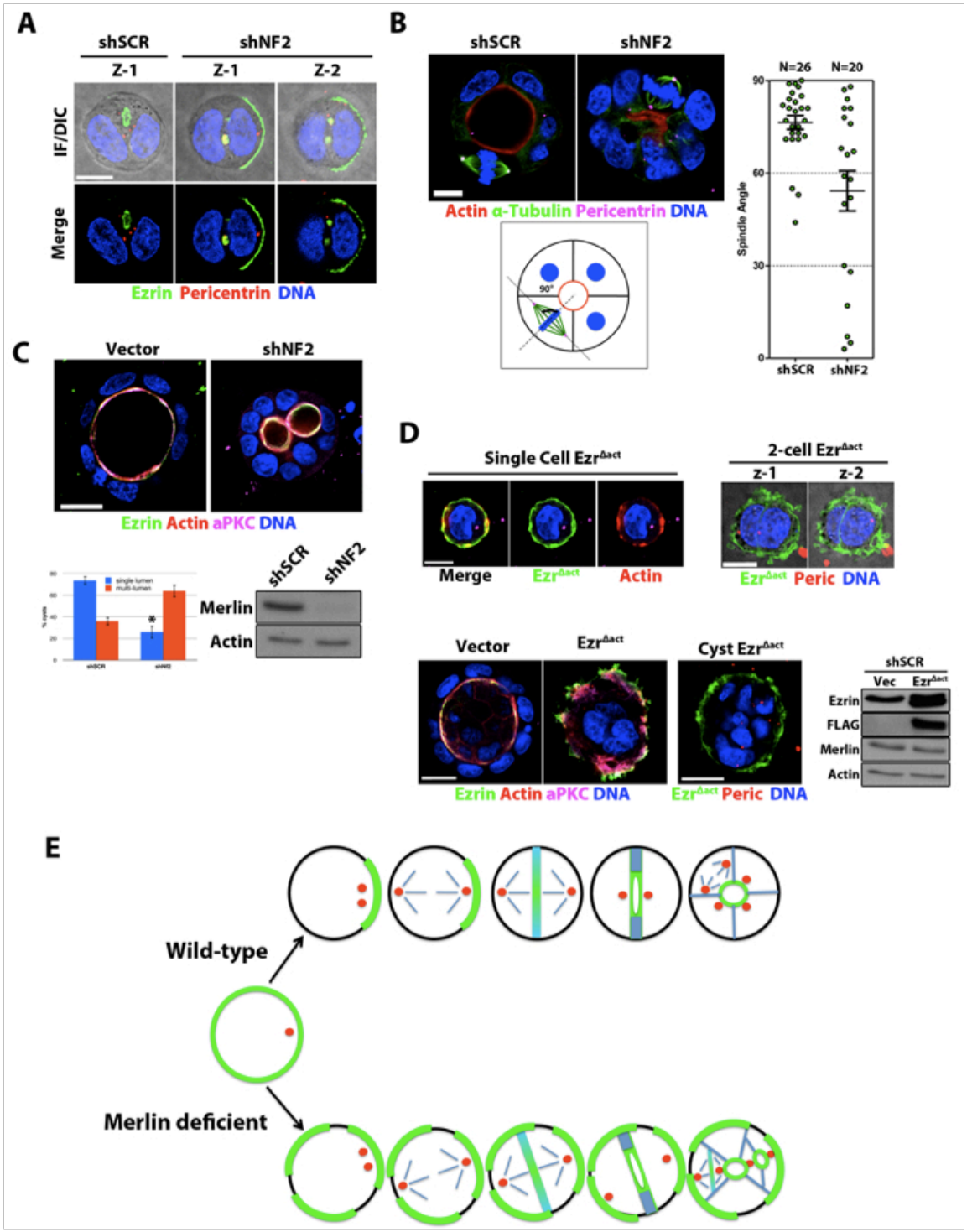

Figure 2.7 (Continued on next page)

Figure 2.7 (Continued). Merlin/ERMs are required for the development of cysts containing a single central lumen. **(A)** Ectopic Ezrin persists after the first cell division in developing shNF2-expressing cysts. 2-cell-stage cysts expressing shSCR or shNF2 were stained for Ezrin (green), Pericentrin (red) and DNA (blue). In contrast to controls, Ezrin is not restricted to the cleavage furrow/nascent lumen in the absence of Merlin. Two optical Z sections are shown so that centrosomes from both cells can be seen. The cell on the left lacks ectopic Ezrin and the centrosome positions normally beneath the nascent lumen; the centrosome in the cell on the right is closely associated with ectopic cortical Ezrin. **(B)** Ectopic cortical Ezrin is associated with aberrant spindle orientation. shSCR- and shNF2-expressing cells were stained for actin (red), α-tubulin (green), Pericentrin (magenta) and DNA (blue). Confocal images spanning both spindle poles were used to measure the angle between the spindle axis and a line connecting the apical surface of the cyst to the center of the spindle using Zen software (schematic). Values shown are mean ± SEM. **(C)** Loss of Merlin yields cysts with multiple lumens. Cysts were stained for Ezrin (green), actin (red), aPKC (magenta) and DNA (blue). Control cells (shSCR) developed into cysts with a single lumen but cells expressing shNF2 develop into cysts with multiple lumens. Immunoblot confirms the loss of Merlin expression. Values shown are mean ± SEM. **(D)** Dominant negative Ezrin interferes with capping, centrosome positioning and cyst formation. Cells infected with control or FLAG-Ezr$^{\wedge act}$ were cultured for 14 hr (1- and 2-cell structures) or 6 days (cysts). Single cells were stained for FLAG-Ezr$^{\wedge act}$ (green), actin (red), Pericentrin (magenta) and DNA (blue) while 2-cell and cyst structures were stained for Ezrin (green, detects Ezrin and FLAG-Ezr$^{\wedge act}$) or FLAG-Ezr$^{\wedge act}$ (green), Pericentrin (red) and DNA (blue). Ezr$^{\wedge act}$-expressing cysts fail to form lumens and localize Ezr$^{\wedge act}$, actin and aPKC, which are normally apical, to the outer membrane that contacts the Matrigel. Immunoblot confirms the expression of Ezr$^{\wedge act}$. Bars, 10 μm (1-/2-cell structures) or 20 μm (cysts). Values shown are mean ± SEM; *$p<0.05$. **(E)** Schematic showing how the restriction of cortical Ezrin (green) positions the interphase centrosome (red) and ensuing mitotic spindle in single control cells and in the derivative cyst with a single lumen (top). In the absence of Merlin (bottom), ectopic cortical Ezrin yields mispositioned centrosomes, misoriented spindles and cysts with multiple lumens.

Ectopic Ezrin and defective centrosome positioning were associated with abnormal spindle orientation in cysts composed of two or more cells. In control cysts, centrosome duplication occurs apically and is followed by the migration of one centrosome to the opposite basolateral pole of the cell; in contrast to single cells, this is followed by a 90° rotation of the developing spindle such that cells divide symmetrically around the central lumen (Rodriguez-Fraticelli et al. 2010). In contrast, spindles in shNF2-expressing cells were randomly oriented at all times (Figure 2.7B). Other studies have concluded that misorientation of the mitotic spindle leads to the formation of multiple lumens in 3D cyst models (Jaffe et al. 2008; Durgan et al. 2011; Rilla et al. 2011; Bray et al. 2012). Indeed, mature *NF2*-deficient cysts exhibit multiple lumens (Figure 2.7C), a phenotype that can be rescued by exogenous expression of $NF2^{wt}$ and $NF2^{myr}$ but not by $Nf2^{18\text{-}595}$ (Figure 2.8A, B). Notably, elimination of α-catenin expression also led to the formation of multiple lumens, consistent with the role of α-catenin in cortically localizing Merlin (Figure 2.8C). Thus Merlin-mediated restriction of cortical Ezrin is critical for centrosome positioning and spindle orientation, which is, in turn, necessary for the formation of an epithelial cyst with a single central lumen (Figure 2.7E).

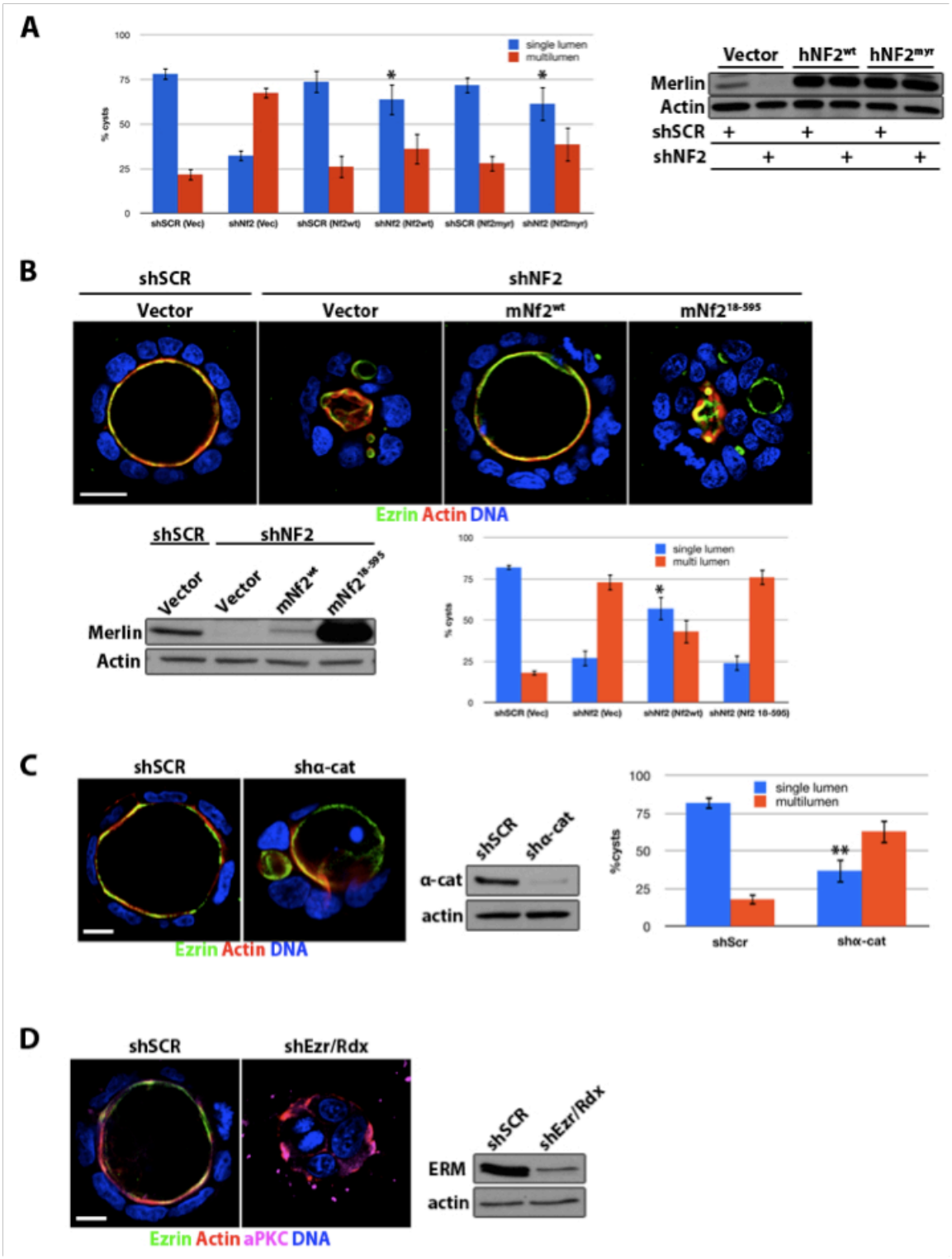

Figure 2.8 (Continued on next page)

Figure 2.8 (Continued). Merlin/ERMs are required for the development of cysts containing a single central lumen. **(A)** Reintroduction of human wild-type ($hNF2^{wt}$) or myristoylated membrane-tethered Merlin ($hNF2^{myr}$) rescues the multiple lumen phenotype in shNF2-expressing cells. Caco2 cells expressing shSCR or shNF2 were infected with empty vector, $hNF2^{wt}$ and $hNF2^{myr}$ and embedded as single cells and cultured for 6 days. Cysts were stained for Ezrin (green), Actin (red) and DNA (blue). Cysts were scored for the presence of single or multiple lumens and quantified (left). Values shown represent mean ± SEM from at least 3 independent experiments. Merlin expression was confirmed by immunoblot (right). **(B)** Exogenous expression of mouse wild-type Merlin ($mNf2^{wt}$) but not a mutant version ($mNf2^{18\text{-}595}$) that does not stably localize to the cortical cytoskeleton rescues the multiple lumen phenotype. Cells stably expressing shSCR or shNF2 were infected with empty vector, $mNf2^{wt}$ and $mNf2^{18\text{-}595}$ then embedded as single cells and cultured for 6 days. Cysts (top) were stained for Ezrin (green), Actin (red) and DNA (blue) and scored for the presence of single or multiple lumens. Values shown represent mean ± SEM from at least 3 independent experiments. Merlin expression was confirmed by immunoblot (bottom left). Bar 20μm. **(C)** Loss of α-catenin yields multiple lumens. Cysts cultured as in (A and B) and expressing shSCR or shα-cat (left) were stained for Ezrin (green), Actin (red) and DNA (blue). Cysts were scored for the presence of single or multiple lumens and quantified (right). Values shown represent mean ± SEM from at least 3 independent experiments. Expression of α-catenin was confirmed by immunoblot (middle). Bar 10μm. **(D)** Loss of Ezrin and Radixin prevents lumen formation. Cysts cultured as in (A and B) expressing shSCR or two independent hairpins targeting Ezrin and Radixin (shEzr/Rdx), the only two ERMs expressed by Caco2 cells, were stained for Ezrin (green), Actin (red), aPKC (magenta) and DNA (blue). Cysts that lack ERM expression do not form lumens (left). Expression of Ezrin and Radixin was confirmed by immunoblot (middle). Bar 10μm.

Consistent with this model, elimination of ERM function, either via expression of a well-characterized dominant negative version of Ezrin ($Ezr^{\Delta act}$) that can neither bind to nor stabilize actin or of shRNAs targeting both Ezrin and Radixin yielded loss of Ezrin capping and cysts that lacked lumens altogether (Figure 2.7D; Figure 2.8D). This is consistent with the known function of Ezrin in establishing apical integrity and lumen formation *in vivo* (Saotome et al. 2004). Notably, actin and the apical marker aPKC were concentrated on the outer surface of the ERM-deficient cyst apposed to the extracellular matrix, consistent with a reversal of polarity (Figure 2.7D). However, centrosomes and spindles were randomly positioned, even in these outer cells that form a pseudo-apical surface, consistent with the notion that active Ezrin itself is the essential cue for centrosome positioning (Figure 2.7D; not shown).

Merlin/ERM proteins promote centrosome clustering

Centrosome amplification is a feature of many cancer cells and can lead to the formation of multipolar spindles and chromosomal aneuploidy (Godinho et al. 2009). However, in many cancer cells supernumerary centrosomes are clustered such that cells retain the ability to form bipolar spindles. The mechanisms by which centrosome clustering occurs are not well-understood but recent studies suggest a key role for the force-generating properties of the cortical actin cytoskeleton (Kwon et al. 2008). We hypothesized that failure to restrict cortical Ezrin would prevent centrosome clustering and yield multipolar spindles. In fact, a significant fraction of Caco2 cells have supernumerary centrosomes but they cluster well, yielding

predominantly bipolar spindles (Figure 2.9A). However, shNF2-expressing Caco2 cells often exhibited defective centrosome clustering and multipolar spindles in 3D cultures and with even greater frequency in 2D cultures (Figure 2.9A). To determine whether Merlin is required for centrosome clustering in other tumor cell types, we eliminated NF2 expression in BT-549 mammary tumor cells that also harbor supernumerary centrosomes (Kwon et al. 2008); again, loss of Merlin prevented centrosome clustering and yielded a dramatic increase in multipolar spindle formation (Figure 2.9B).

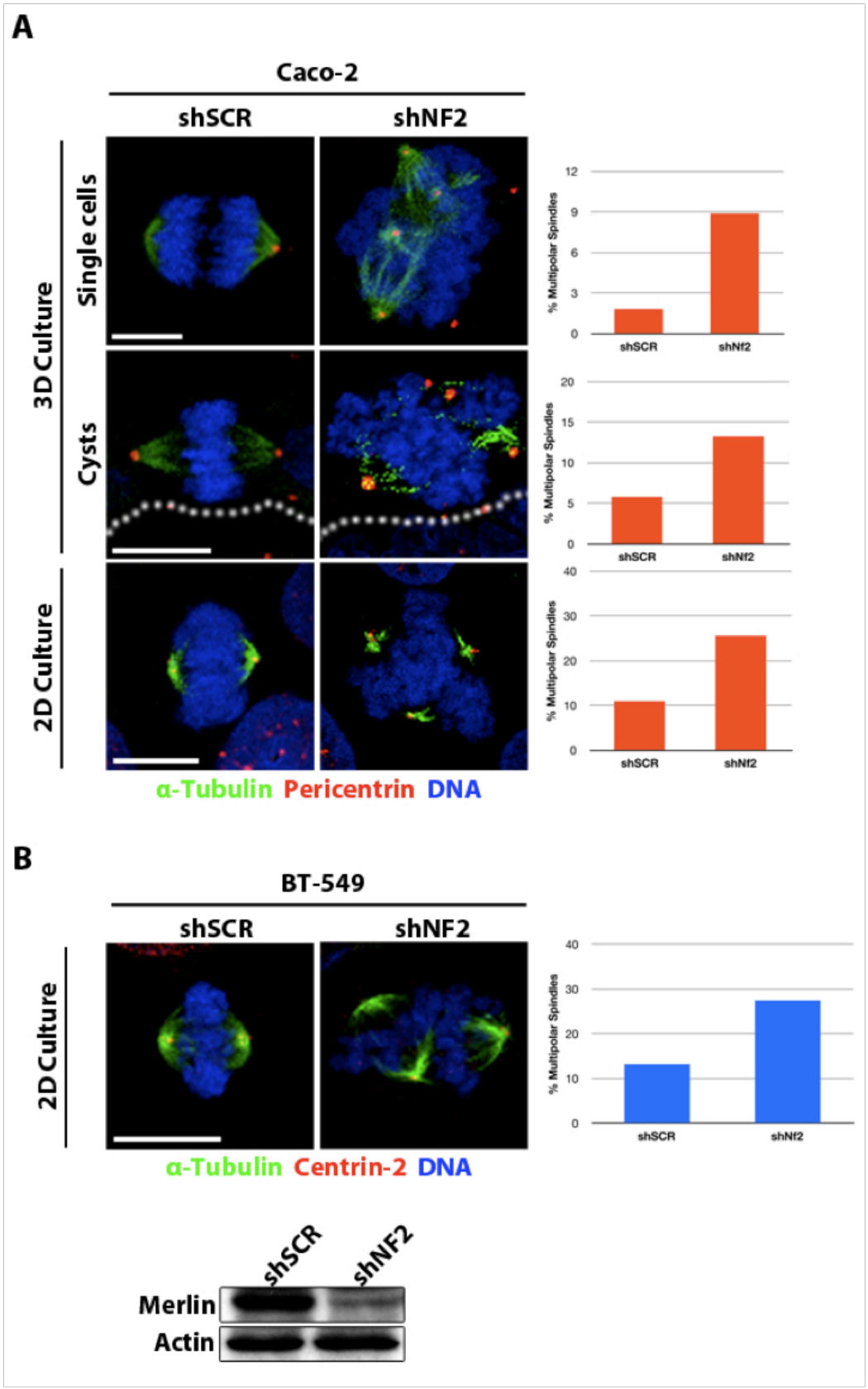

Figure 2.9 (Continued on next page)

Figure 2.9 (Continued). Loss of Merlin prevents centrosome clustering. **(A)** Loss of Merlin yields multipolar spindles. Caco2 cells grown in 3D (top) or 2D (bottom) were stained for α-tubulin (green), Pericentrin (red) or DNA (blue). Dotted line marks the cyst apical surface. **(B)** Loss of Merlin yields multipolar spindles in BT-549 mammary tumor cells. BT-549 cells grown in 2D were stained for α-tubulin (green), Centrin-2 (red) and DNA (blue). Bars, 10μm.

Similar results were observed in U2OS osteosarcoma cells (Figure 2.10). These data suggest that Merlin promotes centrosome clustering and silences multipolar spindle formation by restricting the distribution of the cortical force-generator Ezrin in many cell types; they also suggest that defective centrosome clustering may contribute to the tumorigenic consequences of NF2-loss.

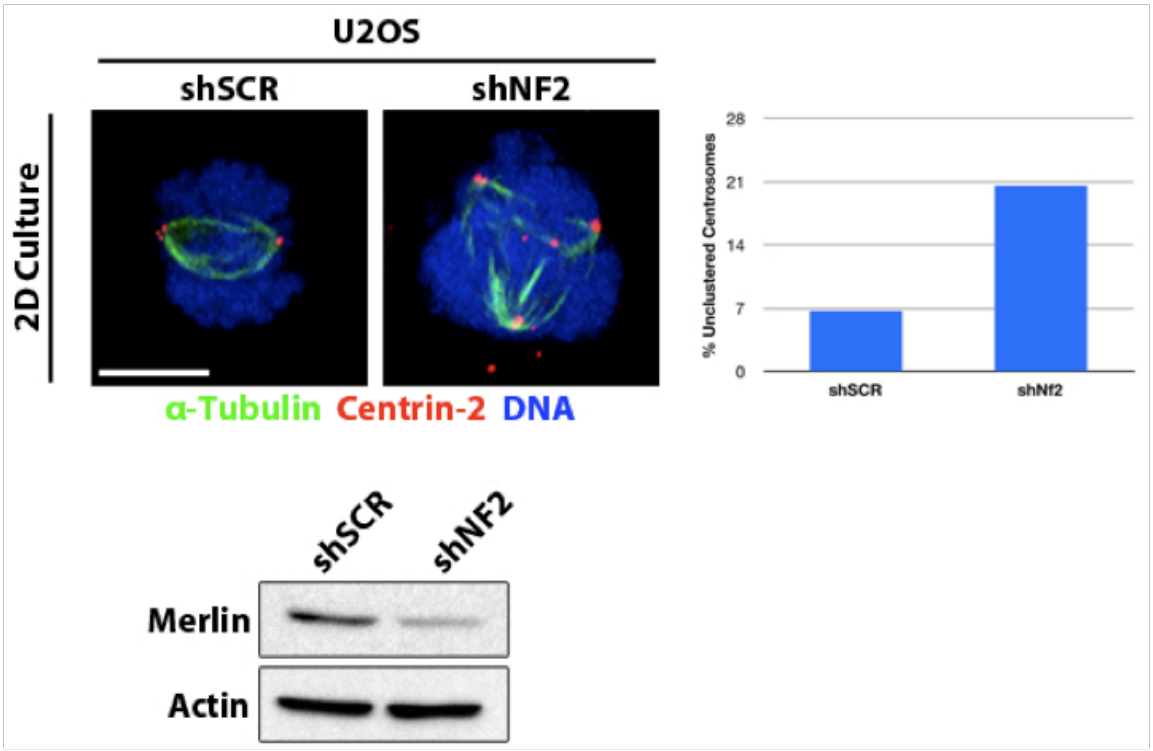

Figure 2.10 Loss of Merlin prevents centrosome clustering. U2OS cells grown in 2D were stained for α-tubulin (green), Centrin-2 (red) and DNA (blue). Loss of Merlin yields multipolar spindles (top left) and prevents centrosome clustering (top right). Bar 10μm.

Concomitant loss of Merlin and ERM function is detrimental

We have shown that Merlin and the ERM proteins function to organize the cortex of single cells, which, in turn, is critical for proper centrosome positioning, mitotic spindle orientation and tissue morphogenesis. A number of studies suggest that Merlin and the ERMs functionally interact but the nature of their interaction is unknown. Our work suggests that Merlin and the ERMs cooperate to organize the cell cortex to maintain proper tissue organization. To begin to understand the nature of potential cooperativity between Merlin and the ERM proteins we perturbed Merlin and ERM function together by concomitant expression of *shNf2* and $Ezr^{\Delta act}$ in CaCo2 cells. We note that cells fail to form caps and arrest as single cells upon loss of both Merlin and ERM function (Figure 2.11). This suggests strong cooperativity for Merlin/ERMs in organizing the cell cortex and prompted an investigation of their functional interaction *in vivo* using our available $Nf2^{lox/lox}$ and $Ezr^{lox/lox}$;Vil-Cre-ER^{T2} mice to generate mice that conditionally delete both *Nf2* and *Ezr* in the intestinal epithelium. Therefore, we describe their functional interaction *in vivo* using the highly dynamic mouse intestinal epithelium as a model (Chapter 3).

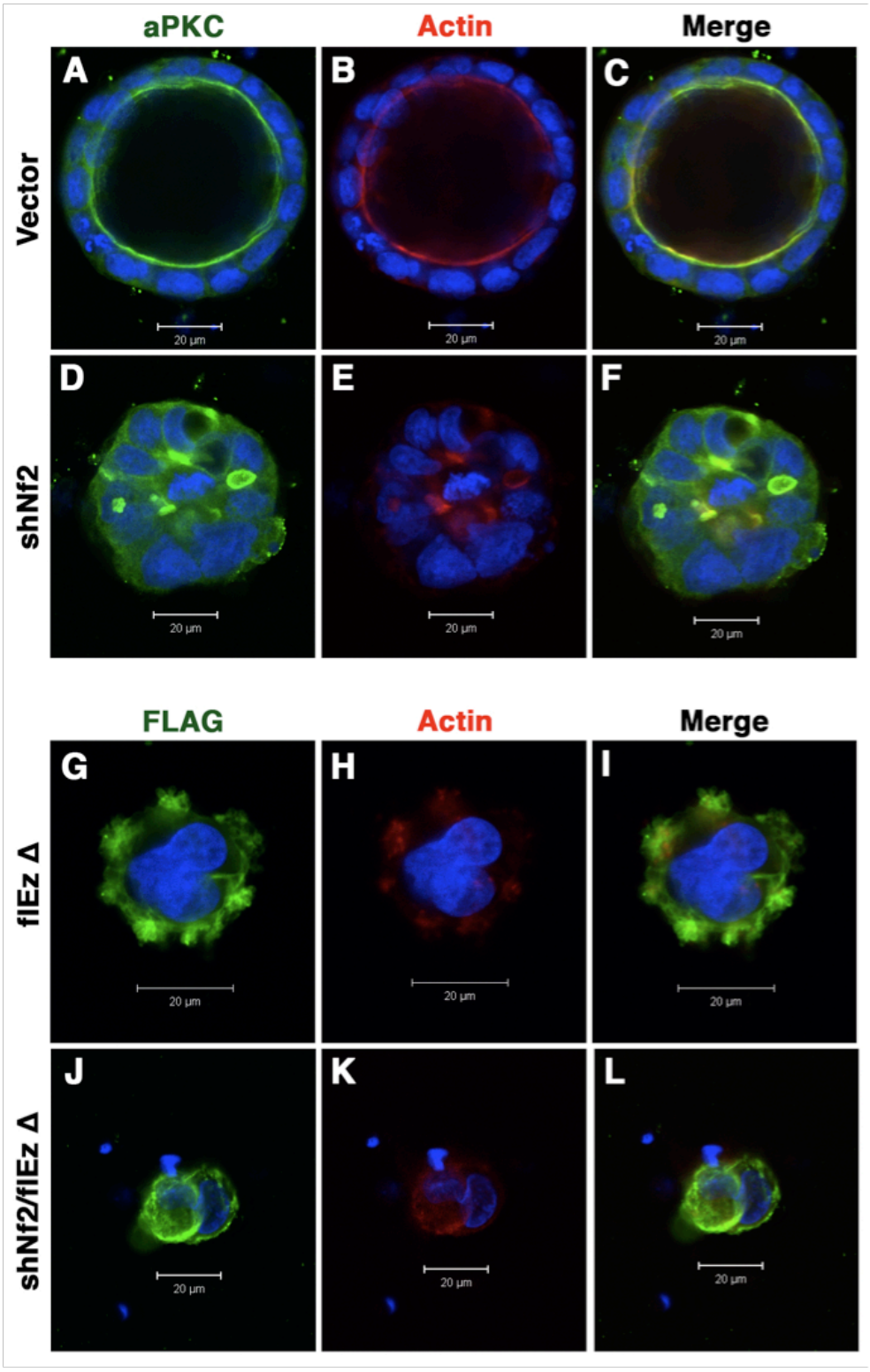

Figure 2.11 (Continued on next page)

Figure 2.11 (Continued). Merlin and ERMs are required together function Cyst formation of CaCo2 cells infected with empty vector, shNf2, EzΔ, or both shNf2 and EzΔ together. Infected cells were trypsinized into single cell suspension, embedded into matrigel, and allowed to develop into cysts for 7 days. **(A-C)** Cells infected with empty vector develop into cysts with a single lumen where actin and aPKC concentrate at the apical surface of the cell facing the lumen. **(D-F)** shNf2 expressing cells develop multiple-lumens within the cyst structure as indicated by concentration of actin and aPKC (white arrows). **(G-I)** Cells infected with EzΔ fail to form lumens and concentrate EzΔ and actin around the outer edge of the cyst that contacts the ECM indicating a reversal of polarity. **(J-L)** The vast majority of cells infected with both shNf2 and EzΔ fail to develop past the 2-cell stage into cyst structures indicating a cooperative interaction between Merlin and ERMs.

Discussion

Our studies identify Merlin/ERM proteins as critical organizers of the cell cortex and advance our understanding of several fundamental cellular processes. For example, although studies in several model organisms have delineated diverse mechanisms whereby external cues initiate cortical asymmetry, our discovery of cell-cycle mediated redistribution of cortical Ezrin in single cells demonstrates that cortical asymmetry can be intrinsically achieved in the absence of external cues. Our data suggest that a key consequence of symmetry-breaking is to organize cortical mechanical forces. Mounting evidence indicates that ERM proteins alter the mechanical properties of the cell cortex; thus ERM proteins stiffen the cortex during mitotic cell rounding and provide cortical force-generating elements for retraction fiber placement and cytokinetic furrow ingression (Thery et al. 2005; Kunda et al. 2008; Rosenblatt 2008; Luxenburg et al. 2011). Our discovery that single spherical epithelial cells actively restrict cortical Ezrin distribution prior to centrosome duplication suggests that the mechanical properties of the cortex are asymmetrically organized long before mitosis.

Importantly, the cortical Ezrin cap that forms in single cells does not contain other polarity or adhesion proteins; these proteins, along with Ezrin are subsequently recruited to the nascent junction and apical lumen during or after cleavage furrow formation (Fig. 1C; (Jaffe et al. 2008). Interestingly, forced activation of the LKB1 kinase can induce the formation of a domain containing apical polarity, junctional and brush border proteins in single Caco2 cells (Baas et al. 2004); in fact, Mst4-induced Ezrin activation was implicated in brush border formation but not polarity in these studies (ten Klooster et al. 2009). However, knockdown of Mst4 had no effect on Ezrin capping or cyst formation

(Fig. 2C; not shown). Thus activation of LKB1 and Mst4 may cooperate with the mechanism of Ezrin cap formation described here to further activate Ezrin and other targets, converting the Ezrin cap into a differentiated apical brush border.

Our data suggest that the proximal function of the Ezrin cap is to position the interphase centrosome. In fact, the centrosome remains positioned beneath Ezrin-decorated cortex during the progressive, cell-cycle correlated restriction of Ezrin (Fig. 4A). Astral microtubules connect centrosomes to the cell cortex and apply pulling forces to the cortical cytoskeleton during mitosis (Manneville and Etienne-Manneville 2006; Kunda and Baum 2009; Vaughan and Dawe 2010). Cortical actin patches may localize anchoring and/or microtubule motor proteins such as dynein to counteract such forces (Sandquist et al 2011). Our studies are consistent with a model wherein the cell-cycle-dependent restriction of Ezrin locally stabilizes actin, providing a force-generating platform for astral microtubule-mediated centrosome positioning *prior* to spindle formation. The mechanism by which cortical Ezrin is progressively restricted is not yet clear, but it is not halted by inhibitors of myosin, suggesting that it is not equivalent to the cortical flow that follows fertilization of the *C. elegans* oocyte (Munro et al. 2004). Although nocodazole disrupts the tight correlation between the mature cortical Ezrin cap and centrosome, it remains possible that the process is initiated by the astral microtubule-mediated delivery of a key factor that modifies the activity of Ezrin, Merlin or both.

During cytokinesis active Ezrin is redistributed to the cleavage furrow, which becomes the junction between two equal daughter cells. This occurs even in the absence of Cdk5, suggesting that other Ezrin regulators drive this redistribution. Ezrin is then restricted to the nascent apical lumen that forms within the first cell junction and remains

apical thereafter as cells divide symmetrically around the central lumen (Fig. 1A). From the two-cell stage on, the interphase centrosome localizes beneath the Ezrin-positive apical surface in these cysts as it does in many epithelial tissues. Thus while the cell cycle-dependent Ezrin cap that forms in single cells does not contain other markers of polarity, Ezrin is central to the integration of cell cycle and polarity cues during tissue building. Indeed, Ezrin is essential for apical integrity in intestinal epithelial cells *in vivo* (Saotome et al. 2004). Notably, as in single cells, the mitotic spindle initiates perpendicular to the Ezrin-positive apical surface; however, from the two-cell stage on the spindle rotates 90 degrees to effect symmetric division. This rotation may involve transient inactivation of Ezrin at the apical pole, and/or the more dominant cortical force-generating activity of lateral AJs. The latter would fit well with studies of *Drosophila* neuroblast or germ cell division during which the AJ dominates over other cues to direct division orientation (Lu et al. 2001; Yamashita et al. 2010). Importantly, in the absence of Merlin, Ezrin is not restricted to the apical surface and interphase centrosomes localize near ectopic cortical Ezrin, leading to random spindle orientation and the formation of multiple lumens. Thus Merlin plays a key role in restricting the force generating activity of Ezrin in both single cells and multicellular cysts.

The discovery that Merlin actively restricts the cortical activity of Ezrin suggests that the physical properties of the Ezrin- versus Merlin-decorated cortex are distinct. While ERM proteins interact directly with actin filaments via a conserved C-terminal actin-binding domain, Merlin lacks this domain. Instead, we recently found that Merlin can directly associate with α-catenin, a core AJ component that can bind actin and modify actin remodeling (Gladden et al. 2010). Here we found that α-catenin is critical for the

stable localization of Merlin to the cortical cytoskeleton in single Caco2 cells. Moreover, loss of α-catenin phenocopies Merlin-deficiency in single cells and cysts, yielding ectopic cortical Ezrin and multiple lumens. Since α-catenin can regulate actin cytoskeleton dynamics (Drees et al. 2005; Yamada et al. 2005; Benjamin et al. 2010), it is tempting to speculate that Merlin uses α-catenin to modify cortical actin in a way that is distinct from that of Ezrin. Our data therefore uncover a novel junction-independent function for α-catenin in organizing the physical properties of the cell cortex and establishing cortical polarity. Notably, E-cadherin is uniformly localized around the cortex of single Caco2 cells (Figure 2.2B), so this function may not be cadherin-independent.

Finally, our studies reveal that the ability to restrict the cortical distribution of Ezrin is a fundamental property of Merlin that may contribute to the tumorigenic consequences of NF2 loss in several ways. Defects in centrosome positioning and spindle orientation can cause defective epithelial morphogenesis and altered stem cell homeostasis, processes that have been linked to tumorigenesis. Indeed, loss of Merlin yields defective spindle orientation and multilayering of basal cells in the mouse skin and a dramatic overproliferation of progenitor cells that precedes tumorigenesis in the mouse liver (Benhamouche et al. 2010; Gladden et al. 2010). Alternatively, in cells with supernumerary centrosomes, aberrant centrosome clustering could affect genome stability (Kwon et al. 2008). For example, transient defects in centrosome clustering can promote chromosome missegregation and aneuploidy (Ganem et al. 2009). *NF2* inactivation is found in an increasing number of sporadic malignant human cancers, including mesothelioma and renal adenocarcinoma, both of which are often aneuploid (Musti et al. 2006; Dalgliesh et al.). Alternatively, loss of spindle pole clustering can also decrease cell

viability due to mitotic catastrophe (Ganem et al. 2009). Thus in some contexts loss of Merlin could actually favor tumor genome stability, as displayed by the benign schwannomas that NF2 patients predominantly develop. Finally, the local restriction of cortical Ezrin could contribute to the established functions of Merlin in controlling membrane receptor distribution and/or cell-cell junctions (Lallemand et al. 2003; Maitra et al. 2006; Curto et al. 2007; Gladden et al. 2010). For example, the ability of Merlin to control the internalization of the Epidermal Growth Factor Receptor (EGFR) in a α-catenin- and cortical cytoskeleton-dependent manner (Curto et al. 2007; Cole et al. 2008; Morris and McClatchey 2009) could involve receptor-proximal restriction of the cortical force-generating properties of Ezrin. Similarly, Merlin-mediated restriction of Ezrin to the apical domain could drive junctional maturation (Gladden et al. 2010). Key future goals will be to determine how these activities are coordinated and whether certain cell types or cellular contexts are differentially sensitive to the loss of specific Merlin activities.

Materials and Methods

Cell Culture

Human Caco2 cells (the $Caco2_{BBe}$ subclone was used throughout; a gift from Wayne Lencer, Children's Hospital, Boston) were cultured in 2D in DMEM/10% fetal bovine serum (FBS). For 3D cultures cells were rinsed 2X in PBS, trypsinized, resuspended in culture medium and passed through a 40μ filter to remove cell aggregates. Single cell suspensions were spun at 4,000 RPM for 1 min at 4°C before resuspending in ice cold collagen/Matrigel (1mg/ml collagen I, 0.02M HEPES/40% Matrigel, BD Biosciences) to a concentration of $6x10^4$ cells/ml. 100 μl of embedded cells were plated in each well of an 8-well chamber slide, allowed to set at 37°C for 30 min and overlayed with 400 μl of media. BT-549 cells (a gift from Cyril Benes, MGH, Boston) were cultured in RPMI/5% FBS.

The following pharmacological inhibitors were added directly to the medium of 3D cultures: Calbiochem (blebbistatin 100 μM; jasplakinolide 1 μM; Y27632 20 μM), Sigma (cytochalasin D 5 μM; nocodazole 20 μM) Biomol (roscovitine 25 μM) and Cayman (latrunculin A 2 μM). The Click-iT® EdU cell proliferation assay (Invitrogen) was used to detect newly synthesized DNA.

Immunofluorescence and Microscopy

Caco2 cells in 3D culture were fixed in 3.7% formaldehyde in cytoskeletal buffer [CB; 10 mM 2-(*N*-morpholino)-ethanesulfonic acid sodium salt (MES), pH 6.1, 138 mM KCl, 3 mM $MgCl_2$ and 2 mM EGTA] for 20 min at RT, washed 3X in PBS and

permeabilized for 20 min in 0.5% Triton X-100 in PBS. For Centrin-2 staining cells were fixed in cold methanol instead of CB for 20 min. Cells were rinsed 3X in PBS then PBS/100mM glycine for 15 min each and blocked for 1 hr in PBST/0.2% Triton X-100/0.1% BSA/10% goat serum. Primary antibodies were diluted in block buffer and incubated overnight at RT. Cells were then rinsed 3X with PBST for 30 min, incubated with secondary antibodies, DAPI, and/or rhodamine-phalloidin for 1 hr and rinsed 3X with PBST. Labeled cells were visualized using a Nikon 90i fluorescence microscope or a Zeiss LSM510 laser scanning confocal microscope; images were processed using Elements (Nikon) or Zen (Zeiss) software.

Plasmids

C-terminal myc epitope tags on $hNF2^{wt}$ and $hNF2^{myr}$ (gifts from Helen Morrison, Leibniz Institute, Germany) were removed by PCR and a silent mutation in $hNF2^{wt}$ and $hNF2^{myr}$ was introduced by site directed mutagenesis to render these constructs resistant to shNF2 (details in Extended Experimental Procedures). N-terminal FLAG epitope tags were added onto $mNf2^{wt}$ and $mNf2^{18\text{-}595}$ by cloning into the pFLEX vector. Dominant negative ERM ($Ezr^{\Delta act}$) was a gift from Rick Fehon (U. of Chicago). Venus-tagged Par3 was a gift from Ian Macara (U. of Virginia). All constructs were subcloned into the pCSC-SP-PW (pBOB) mammalian lentiviral expression vector.

shRNA

Fourteen lentiviral short hairpin RNA (shRNA) constructs targeting human *Mst4*, α-*catenin* and *Slk* were purchased from Open Biosystems. Specificity was determined by

WB and constructs that most efficiently targeted protein expression were utilized (details in Extended Experimental Procedures). The short hairpins targeting *Cdk5* were gifts from Phil Hinds (Tufts U.). Scrambled control (shSCR) and *NF2*-targeting shRNA constructs were gifts from Marianne James (MGH).

Ten lentiviral short hairpin RNA (shRNA) constructs targeting human *Erin* and *Radixin* were purchased from Open Biosystems. Specificity was determined by WB and constructs that most efficiently targeted protein expression were utilized. The following short hairpin clones were used throughout our experiments: Ezrin (TRCN0000062458), Radixin (TRCN0000062435), Mst4 (TRCN0000003191) and α-E-catenin (TRCN0000002653). The short hairpins targeting *p35* were gifts from Phil Hinds (Tufts U.)

Lentivirus production

Lentiviruses expressing shRNAs were generated by co-transfecting 293T cells with shRNA constructs together with the packaging vectors ΔVPR and VSVG (Fugene). Lentiviruses derived from pBOB constructs were generated similarly using the packaging vectors psPAX and pMD2.G (Fugene). Lentiviral supernatants were collected 5X over a period of 48 hr, filtered (0.22 μm), aliquotted and frozen at -80°C. For infection, cells were trypsinized, resuspended in 6 ml of lentiviral supernatant and cultured for 24 hr. Cells were then transferred to fresh medium containing 7μg/ml puromycin for 48 hr and plated in 2D or 3D culture. Stable Caco2 cell lines expressing shSCR and shNF2 were subject to WB analysis to monitor NF2 levels in each experiment.

Measurement of spindle angles

Confocal images spanning both spindle poles of metaphase cells were taken. In single cells the angle between the spindle axis and a line connecting the center of the Ezrin cap to the center of the spindle was measured (Fig. 4B). In structures with 2 or more cells the angle between the spindle axis and a line connecting the center of the apical surface to the center of the spindle was measured (Fig. 5B). Axes were drawn and spindle angles measured using Zen software.

Antibodies

Primary antibodies for immunofluorescence (IF) and/or western blotting (WB) were from: Santa Cruz Biotechnology (NF2 sc332 1:100 for IF and 1:1000 for WB; aPKC sc-216 1:200 for IF; Cdk5 sc6247 1:1000 for WB; p35 sc820 1:1000 for WB), Cell Signaling Technology (ERM 3142 1:1000 for WB; phospho-ERM 3141 1:100 for IF; phospho-histone H3 9701 1:200 for IF), Zymed (α-catenin 7A4 1:1000 for WB), Sigma (Actin A3853 1:2000 for WB; FLAG M2 F1804 1:100 for IF and 1:1000 for WB; FLAG F7425 1:100 for IF and 1:1000 for WB), Epitomics (Mst4 2049-1 1:1000 for WB), Abcam (Pericentrin ab4448 1:1000 for IF), Bethyl Laboratories (Slk BL1917 1:500 for WB) and BD Transduction Laboratories (E-cadherin 610182 at 1:100 for IF). For IF the following secondary antibodies were used at 1:200: anti-rabbit or anti-mouse Alexa Fluor 488 (Invitrogen); anti-rabbit or anti mouse Cy3 or Cy5 (Jackson ImmunoResearch). Filamentous actin was labelled with rhodamine phalloidin (Invitrogen) and nuclei with 4’6’-diamidino-2-phenylindole (DAPI).

Western blotting

Cells were lysed using RIPA lysis buffer (50 mM Tris [pH 7.4], 1% Triton X-100, 1% SDS, 0.5% sodium deoxycholate, 150 mM NaCl, 1 mM EDTA, 1 mM EGTA, 1 mM PMSF, 1 mM Na_3VO_4, 10 mM sodium fluoride, 10 mM β-glycerophosphate, 1 mg/ml aprotinin and 1 mg/ml leupeptin) followed by brief sonication. Cell debris was cleared by centrifugation (14,000 rpm, 10 min, 4°C) and lysates were quantitated by DC protein assay (Bio-Rad), separated by SDS-PAGE, transferred to PVDF. Membranes were blocked in 5% milk, incubated with primary antibody for 1hr at RT or overnight at 4°C in 1% milk and then with anti-mouse or anti-rabbit horseradish peroxidase-conjugated secondary antibodies (1:5000; Amersham).

Merlin cortical localization

Caco2 cells expressing short hairpins targeting α-catenin (shα-cat) or scrambled control (shSCR) were infected with $hNF2^{wt}$ and plated in 3D culture for 16 hr at 37°C and 5% CO_2. Cells were washed in 1% Triton X-100 lysis buffer for 10 min, washed 1X with PBS and fixed for 20 min in 3.7% formaldehyde in CB. Cells were then stained for Merlin (NF2 sc332) and Ezrin then visualized using a Zeiss LSM510 laser scanning confocal microscope to assess Merlin localization to the cell cortex.

Cloning and mutagenesis

C-terminal myc epitope tags on $hNF2^{wt}$ and $hNF2^{myr}$ (gifts from Helen Morrison, Leibniz Institute, Germany) were removed by PCR and an Apa1 restriction site was

added to the 3' end of each construct for cloning into the pBob lentiviral vector using primers Fwd 5'-CGCTGTTTTGACCTCCATAGAAGACAC-3' and Rev 5'-AAGAATATGGGCCCTAGAGCTCTTCAAAGAAGGCCACTCGGGAC-3'. Aditionally, two silent mutations (G51A and A54G) in $hNF2^{wt}$ and $hNF2^{myr}$ were introduced using the Quick Chante® Site-Directed Mutagenesis Kit (Stratagene) to render these constructs resistant to shNF2 by using the mutagenesis primers Fwd 5'-CAGCTCTCTCAAGAGGAAACAGCCCAAGACGTTCACCGTG-3' and Rev 5'-CACGGTGAACGTCTTGGGCTGTTTCCTCTTGAGAGAGCTG-3'.

Centrosome clustering

U2OS cells, like with Caco2 and BT-549 cells (Figure 6A,B), were infected with lentiviruses expressing scrambled control (shSCR) or *NF2*-targeting (shNF2) short hairpins. Cells were then transferred to fresh medium containing 7μg/ml puromycin for 48 hr and plated on glass coverslips for 16 hr before fixing in 3.7% formaldehyde in CB. Cells were stained for α-tubulin (green), Centrin-2 (red) and DNA (blue). Mitotic cells were scored for normal vs. supernumerary centrosomes, clustered vs. unclustered centrosomes and bipolar vs. multipolar spindles using a Zeiss LSM510 laser scanning confocal microscope. U2OS cells (a gift from Cyril Benes, MGH, Boston) were cultured in RPMI/5% FBS.

Statistics

Throughout, data from at least three independent experiments were pooled and expressed as mean ± SEM. Values were compared by 2-tailed Student's *t*-test, with statistical significance of *$p<0.05$ or **$p<0.01$ indicated.

References

Algrain, M., Turunen, O., Vaheri, A., Louvard, D., and Arpin, M. 1993. Ezrin contains cytoskeleton and membrane binding domains accounting for its proposed role as a membrane-cytoskeletal linker. *J Cell Biol* **120**(1): 129-139.

Baas, A.F., Kuipers, J., van der Wel, N.N., Batlle, E., Koerten, H.K., Peters, P.J., and Clevers, H.C. 2004. Complete polarization of single intestinal epithelial cells upon activation of LKB1 by STRAD. *Cell* **116**(3): 457-466.

Benhamouche, S., Curto, M., Saotome, I., Gladden, A.B., Liu, C.H., Giovannini, M., and McClatchey, A.I. 2010. Nf2/Merlin controls progenitor homeostasis and tumorigenesis in the liver. *Genes Dev* **24**(16): 1718-1730.

Benjamin, J.M., Kwiatkowski, A.V., Yang, C., Korobova, F., Pokutta, S., Svitkina, T., Weis, W.I., and Nelson, W.J. 2010. AlphaE-catenin regulates actin dynamics independently of cadherin-mediated cell-cell adhesion. *J Cell Biol* **189**(2): 339-352.

Bettencourt-Dias, M., Hildebrandt, F., Pellman, D., Woods, G., and Godinho, S.A. 2011. Centrosomes and cilia in human disease. *Trends Genet* **27**(8): 307-315.

Bray, K., Brakebusch, C., and Vargo-Gogola, T. 2012. The Rho GTPase Cdc42 is required for primary mammary epithelial cell morphogenesis in vitro. *Small Gtpases* **2**(5): 247-258.

Carreno, S., Kouranti, I., Glusman, E.S., Fuller, M.T., Echard, A., and Payre, F. 2008. Moesin and its activating kinase Slik are required for cortical stability and microtubule organization in mitotic cells. *J Cell Biol* **180**(4): 739-746.

Charras, G.T., Hu, C.K., Coughlin, M., and Mitchison, T.J. 2006. Reassembly of contractile actin cortex in cell blebs. *J Cell Biol* **175**(3): 477-490.

Cole, B.K., Curto, M., Chan, A.W., and McClatchey, A.I. 2008. Localization to the cortical cytoskeleton is necessary for Nf2/merlin-dependent epidermal growth factor receptor silencing. *Mol Cell Biol* **28**(4): 1274-1284.

Curto, M., Cole, B.K., Lallemand, D., Liu, C.H., and McClatchey, A.I. 2007. Contact-dependent inhibition of EGFR signaling by Nf2/Merlin. *J Cell Biol* **177**(5): 893-903.

Dalgliesh, G.L., Furge, K., Greenman, C., Chen, L., Bignell, G., Butler, A., Davies, H., Edkins, S., Hardy, C., Latimer, C. et al. 2010. Systematic sequencing of renal carcinoma reveals inactivation of histone modifying genes. *Nature* **463**(7279): 360-363.

Drees, F., Pokutta, S., Yamada, S., Nelson, W.J., and Weis, W.I. 2005. Alpha-catenin is a molecular switch that binds E-cadherin-beta-catenin and regulates actin-filament assembly. *Cell* **123**(5): 903-915.

Durgan, J., Kaji, N., Jin, D., and Hall, A. 2011. Par6B and atypical PKC regulate mitotic spindle orientation during epithelial morphogenesis. *J Biol Chem* **286**(14): 12461-12474.

Fehon, R.G., McClatchey, A.I., and Bretscher, A. 2010. Organizing the cell cortex: the role of ERM proteins. *Nat Rev Mol Cell Biol* **11**(4): 276-287.

Ganem, N.J., Godinho, S.A., and Pellman, D. 2009. A mechanism linking extra centrosomes to chromosomal instability. *Nature* **460**(7252): 278-282.

Gladden, A.B., Hebert, A.M., Schneeberger, E.E., and McClatchey, A.I. 2010. The NF2 tumor suppressor, Merlin, regulates epidermal development through the establishment of a junctional polarity complex. *Dev Cell* **19**(5): 727-739.

Gobel, V., Barrett, P.L., Hall, D.H., and Fleming, J.T. 2004. Lumen morphogenesis in C. elegans requires the membrane-cytoskeleton linker erm-1. *Dev Cell* **6**(6): 865-873.

Godinho, S.A., Kwon, M., and Pellman, D. 2009. Centrosomes and cancer: how cancer cells divide with too many centrosomes. *Cancer Metastasis Rev* **28**(1-2): 85-98.

Hipfner, D.R., Keller, N., and Cohen, S.M. 2004. Slik Sterile-20 kinase regulates Moesin activity to promote epithelial integrity during tissue growth. *Genes Dev* **18**(18): 2243-2248.

Jaffe, A.B., Kaji, N., Durgan, J., and Hall, A. 2008. Cdc42 controls spindle orientation to position the apical surface during epithelial morphogenesis. *J Cell Biol* **183**(4): 625-633.

Kunda, P. and Baum, B. 2009. The actin cytoskeleton in spindle assembly and positioning. *Trends Cell Biol* **19**(4): 174-179.

Kunda, P., Pelling, A.E., Liu, T., and Baum, B. 2008. Moesin controls cortical rigidity, cell rounding, and spindle morphogenesis during mitosis. *Curr Biol* **18**(2): 91-101.

Kwon, M., Godinho, S.A., Chandhok, N.S., Ganem, N.J., Azioune, A., Thery, M., and Pellman, D. 2008. Mechanisms to suppress multipolar divisions in cancer cells with extra centrosomes. *Genes Dev* **22**(16): 2189-2203.

LaJeunesse, D.R., McCartney, B.M., and Fehon, R.G. 1998. Structural analysis of Drosophila merlin reveals functional domains important for growth control and subcellular localization. *J Cell Biol* **141**(7): 1589-1599.

Lallemand, D., Curto, M., Saotome, I., Giovannini, M., and McClatchey, A.I. 2003. NF2 deficiency promotes tumorigenesis and metastasis by destabilizing adherens junctions. *Genes Dev* **17**(9): 1090-1100.

Lallemand, D., Manent, J., Couvelard, A., Watilliaux, A., Siena, M., Chareyre, F., Lampin, A., Niwa-Kawakita, M., Kalamarides, M., and Giovannini, M. 2009. Merlin regulates transmembrane receptor accumulation and signaling at the plasma membrane in primary mouse Schwann cells and in human schwannomas. *Oncogene* **28**(6): 854-865.

Lu, B., Roegiers, F., Jan, L.Y., and Jan, Y.N. 2001. Adherens junctions inhibit asymmetric division in the Drosophila epithelium. *Nature* **409**(6819): 522-525.

Luxenburg, C., Pasolli, H.A., Williams, S.E., and Fuchs, E. 2011. Developmental roles for Srf, cortical cytoskeleton and cell shape in epidermal spindle orientation. *Nat Cell Biol* **13**(3): 203-214.

Macara, I.G. and Mili, S. 2008. Polarity and differential inheritance--universal attributes of life? *Cell* **135**(5): 801-812.

Maitra, S., Kulikauskas, R.M., Gavilan, H., and Fehon, R.G. 2006. The tumor suppressors Merlin and Expanded function cooperatively to modulate receptor endocytosis and signaling. *Curr Biol* **16**(7): 702-709.

Manneville, J.B. and Etienne-Manneville, S. 2006. Positioning centrosomes and spindle poles: looking at the periphery to find the centre. *Biol Cell* **98**(9): 557-565.

McClatchey, A.I. and Fehon, R.G. 2009. Merlin and the ERM proteins--regulators of receptor distribution and signaling at the cell cortex. *Trends Cell Biol* **19**(5): 198-206.

McClatchey, A.I., Saotome, I., Mercer, K., Crowley, D., Gusella, J.F., Bronson, R.T., and Jacks, T. 1998. Mice heterozygous for a mutation at the Nf2 tumor suppressor locus develop a range of highly metastatic tumors. *Genes Dev* **12**(8): 1121-1133.

Morin, X. and Bellaiche, Y. 2011. Mitotic spindle orientation in asymmetric and symmetric cell divisions during animal development. *Dev Cell* **21**(1): 102-119.

Morris, Z.S. and McClatchey, A.I. 2009. Aberrant epithelial morphology and persistent epidermal growth factor receptor signaling in a mouse model of renal carcinoma. *Proc Natl Acad Sci U S A* **106**(24): 9767-9772.

Munro, E., Nance, J., and Priess, J.R. 2004. Cortical flows powered by asymmetrical contraction transport PAR proteins to establish and maintain anterior-posterior polarity in the early C. elegans embryo. *Dev Cell* **7**(3): 413-424.

Musti, M., Kettunen, E., Dragonieri, S., Lindholm, P., Cavone, D., Serio, G., and Knuutila, S. 2006. Cytogenetic and molecular genetic changes in malignant mesothelioma. *Cancer Genet Cytogenet* **170**(1): 9-15.

Nigg, E.A. 2007. Centrosome duplication: of rules and licenses. *Trends Cell Biol* **17**(5): 215-221.

Pearson, M.A., Reczek, D., Bretscher, A., and Karplus, P.A. 2000. Structure of the ERM protein moesin reveals the FERM domain fold masked by an extended actin binding tail domain. *Cell* **101**(3): 259-270.

Pereira, G. and Yamashita, Y.M. 2011. Fly meets yeast: checking the correct orientation of cell division. *Trends Cell Biol* **21**(9): 526-533.

Pilot, F., Philippe, J.M., Lemmers, C., and Lecuit, T. 2006. Spatial control of actin organization at adherens junctions by a synaptotagmin-like protein Btsz. *Nature* **442**(7102): 580-584.

Rauzi, M. and Lenne, P.F. 2011. Cortical forces in cell shape changes and tissue morphogenesis. *Curr Top Dev Biol* **95**: 93-144.

Rilla, K., Pasonen-Seppanen, S., Karna, R., Karjalainen, H.M., Torronen, K., Koistinen, V., Tammi, M.I., Tammi, R.H., Teravainen, T., and Manninen, A. 2011. HAS3-induced accumulation of hyaluronan in 3D MDCK cultures results in mitotic spindle misorientation and disturbed organization of epithelium. *Histochem Cell Biol* **137**(2): 153-164.

Rodriguez-Fraticelli, A.E., Vergarajauregui, S., Eastburn, D.J., Datta, A., Alonso, M.A., Mostov, K., and Martin-Belmonte, F. 2010. The Cdc42 GEF Intersectin 2 controls mitotic spindle orientation to form the lumen during epithelial morphogenesis. *J Cell Biol* **189**(4): 725-738.

Rosenblatt, J. 2008. Mitosis: moesin and the importance of being round. *Curr Biol* **18**(7): R292-293.

Rouleau, G.A., Merel, P., Lutchman, M., Sanson, M., Zucman, J., Marineau, C., Hoang-Xuan, K., Demczuk, S., Desmaze, C., Plougastel, B. et al. 1993. Alteration in a

new gene encoding a putative membrane-organizing protein causes neuro-fibromatosis type 2. *Nature* **363**(6429): 515-521.

Sandquist, J.C., Kita, A.M., and Bement, W.M. 2011. And the dead shall rise: actin and myosin return to the spindle. *Dev Cell* **21**(3): 410-419.

Saotome, I., Curto, M., and McClatchey, A.I. 2004. Ezrin is essential for epithelial organization and villus morphogenesis in the developing intestine. *Dev Cell* **6**(6): 855-864.

Siller, K.H. and Doe, C.Q. 2009. Spindle orientation during asymmetric cell division. *Nat Cell Biol* **11**(4): 365-374.

St Johnston, D. and Ahringer, J. 2010. Cell polarity in eggs and epithelia: parallels and diversity. *Cell* **141**(5): 757-774.

ten Klooster, J.P., Jansen, M., Yuan, J., Oorschot, V., Begthel, H., Di Giacomo, V., Colland, F., de Koning, J., Maurice, M.M., Hornbeck, P. et al. 2009. Mst4 and Ezrin induce brush borders downstream of the Lkb1/Strad/Mo25 polarization complex. *Dev Cell* **16**(4): 551-562.

Thery, M., Racine, V., Pepin, A., Piel, M., Chen, Y., Sibarita, J.B., and Bornens, M. 2005. The extracellular matrix guides the orientation of the cell division axis. *Nat Cell Biol* **7**(10): 947-953.

Trofatter, J.A., MacCollin, M.M., Rutter, J.L., Murrell, J.R., Duyao, M.P., Parry, D.M., Eldridge, R., Kley, N., Menon, A.G., Pulaski, K. et al. 1993. A novel moesin-, ezrin-, radixin-like gene is a candidate for the neurofibromatosis 2 tumor suppressor. *Cell* **75**(4): 826.

Turunen, O., Wahlstrom, T., and Vaheri, A. 1994. Ezrin has a COOH-terminal actin-binding site that is conserved in the ezrin protein family. *J Cell Biol* **126**(6): 1445-1453.

Van Furden, D., Johnson, K., Segbert, C., and Bossinger, O. 2004. The C. elegans ezrin-radixin-moesin protein ERM-1 is necessary for apical junction remodelling and tubulogenesis in the intestine. *Dev Biol* **272**(1): 262-276.

Vaughan, S. and Dawe, H.R. 2010. Common themes in centriole and centrosome movements. *Trends Cell Biol* **21**(1): 57-66.

Yamada, S., Pokutta, S., Drees, F., Weis, W.I., and Nelson, W.J. 2005. Deconstructing the cadherin-catenin-actin complex. *Cell* **123**(5): 889-901.

Yamashita, Y.M., Yuan, H., Cheng, J., and Hunt, A.J. 2010. Polarity in stem cell division: asymmetric stem cell division in tissue homeostasis. *Cold Spring Harb Perspect Biol* **2**(1): a001313.

Yang, H.S. and Hinds, P.W. 2003. Increased ezrin expression and activation by CDK5 coincident with acquisition of the senescent phenotype. *Mol Cell* **11**(5): 1163-1176.

Yi, C., Troutman, S., Fera, D., Stemmer-Rachamimov, A., Avila, J.L., Christian, N., Persson, N.L., Shimono, A., Speicher, D.W., Marmorstein, R. et al. 2011. A tight junction-associated Merlin-angiomotin complex mediates Merlin's regulation of mitogenic signaling and tumor suppressive functions. *Cancer Cell* **19**(4): 527-540.

Chapter 3

Merlin and Ezrin cooperate to organize tissue architecture *in vivo*

Alan M. Hebert[1] and Andrea I. McClatchey[1]

[1]Massachusetts General Hospital Center for Cancer Research and
Harvard Medical School Department of Pathology
149 13th St. Charlestown, MA 02129

Publications and Contributions: All figures in this chapter were contributed by A. M. Hebert. Tissue samples of mice deficient for *Nf2* following tamoxifen induction at time points 2 weeks and greater in the mouse intestinal epithelium (*Nf2$^{lox/lox}$;Vil-Cre-ER^{T2}*) were generated by Zachary S. Morris.

Abstract

Merlin and the ERM proteins build, organize and regulate specialized membrane domains to control cellular activity during tissue development and homeostasis. Several lines of evidence, including similar modes of regulation, co-expression in most cell types, multiple common binding partners and the ability to physically interact suggest a functional relationship between Merlin and the ERM proteins. Additionally, my *in vitro* results (Chapter 2) demonstrate a cooperative effect upon concomitant loss of both Merlin and ERM function, which may reflect their complementary roles in membrane organization. Defining the relationship between Merlin and the ERMs will be critical for appreciating their respective roles in membrane organization and tumorigenesis. To determine whether Merlin and the ERM proteins cooperate to control tissue organization and proliferation *in vivo,* I compared the phenotypic consequence of deleting *Ezrin* or *Nf2* alone to compound deletion of both *Ezrin* and *Nf2* in the mouse intestinal epithelium using a tamoxifen inducible system. Ezrin is the sole ERM protein expressed in the mouse intestinal epithelium, eliminating potential compensation by Radixin and Moesin; this is therefore the only context where the interaction between Merlin and the ERMs can be studied *in vivo* via the genetic manipulation of only two genes. I have identified multiple defects that are unique to compound *Nf2;Ezr* deficient tissue compared to either single mutant, illustrating strong genetic interaction.

Introduction

Three-dimensional (3D) cell culture models aid to span the gap between two-dimensional *in vitro* cell cultures and *in vivo* animal models. By emulating features of the *in vivo* setting and exploiting the same tools used to study cells in traditional cell culture, 3D models provide unique perspectives on stem cell behavior, developing tissues and organs, and tumors. These models have already provided key insight into understanding how cortical organization impacts epithelial morphogenesis. However, 3D culture models do not perfectly reflect *in vivo* biology and fall short in a number of ways. For example, the 3D CaCo2 model that we describe in Chapter 2 does not mimic the highly organized crypt/villus structure where proliferation is restricted to the crypts that harbor the stem cells (Barker et al. 2007; Sato et al. 2009). Furthermore, there are a number of differentiated cell types including enterocytes, goblet cells, enteroendocrine cells and paneth cells whose abundance and localization is highly regulated throughout the intestine. Finally, 3D cultures are in many cases not able to account for complex *in vivo* interactions including vascularization, host immune responses and exposure to nutrients and the normal gut flora. Therefore, it is important to also experimentally delineate the functional relationship between Merlin and Ezrin *in vivo.*

Defining the relationship between Merlin and the ERM proteins in mammals has been hampered in part because redundancy among the ERMs could conceal a role for these proteins in tumor development. Importantly, *Ezrin* is the only ERM protein expressed in the mouse intestinal epithelium making this a valuable setting for studying the genetic interaction between Merlin and the ERMs without the

caveat of redundancy. Work from our lab has demonstrated that Ezrin is essential for epithelial organization and villus morphogenesis in the developing mouse intestine (Saotome et al. 2004). Here, Ezrin is not required for formation of brush border microvilli or for the establishment of epithelial polarity. Instead, Ezrin organizes the terminal web, which is critical for formation and expansion of *de novo* lumens as the stratified embryonic intestinal epithelium transforms into a polarized columnar epithelial monolayer surrounding each villus. Indeed, Ezrin deficiency results in incomplete villus morphogenesis (villus fusion) and neonatal death. Consistent with Ezrin's ability to associate with and control the distribution of various membrane proteins Ezrin also seems to be required for the localization and/or function of certain apical membrane proteins that support intestinal function (Saotome et al., 2004).

Surprisingly, deletion of *Ezrin* after villus morphogenesis has taken place yields the same villus fusion phenotype, revealing a previously unrecognized role for Ezrin in intestinal homeostasis (Casaletto et al. 2011). Individual studies of the ERMs have demonstrated an array of functions including control of membrane receptors, stabilization of the membrane:cytoskeleton interface and regulation of the small GTPase Rho. Casaletto *et al* showed that Ezrin carries out all of these functions in the same tissue *in vivo* supporting the hypothesis that ERMs can simultaneously coordinate multiple cellular activities. Indeed, *in vivo* studies of ERMs in other organisms confirm this.

Similar to what we observed in mice, loss of the sole ERM ortholog, Moesin, in *D. melanogaster* leads to defective apical morphogenesis, increased Rho1

activation, and loss of epithelial integrity/morphology (Speck et al. 2003). Here, F-actin accumulates in ectopic sites within Moesin deficient cells of the wing imaginal epithelium and many of these cells lose polarity and extrude basally from the epithelial monolayer. Ultrastructural analysis by EM demonstrates that large abnormal protrusions replace the microvillar projections seen in wild-type cells. Additionally, loss of the single ERM ortholog (*ERM-1)* in *C. elegans* yields similar defects in apical integrity throughout the developing intestinal epithelium (Gobel et al. 2004; Van Furden et al. 2004). Intestinal lumen morphogenesis in *C. elegans* is thought to be accompanied by the migration of adherens junction components from the apical to apicolateral position yielding a free apical surface (Bossinger et al. 2001). One group suggests that this process is incomplete in the absence of ERM-1 yielding intestinal obstructions caused by aberrant points of adhesion along the gut lumen (Van Furden et al. 2004). Another group suggests that these obstructions result from twisting of the intestinal segments that arise later during the repositioning of cells around the already formed lumen (Gobel et al. 2004). Either way, these studies support that ERM-1 function is critical at the apical:junctional interface during lumen morphogenesis *in vivo*.

Like the ERMs, Merlin organizes membrane complexes and associates with the cytoskeleton. However, overproliferation is often a consequence of Merlin deficiency and *in vivo* studies have begun to provide clues as to why this might be. Like the ERM proteins, Merlin's effect on proliferation is likely a reflection of its fundamental ability to organize membrane complexes. Indeed, mouse models have highlighted a role for Merlin in establishing adherens junctions, spindle orientation,

tumorigenesis and metastasis (McClatchey et al. 1998; Morris and McClatchey 2009; Benhamouche et al. 2010; Gladden et al. 2010). *Nf2* null embryos fail at gastrulation but the study of either mosaic *Nf2* $^{-/-}$:*WT* embryos or targeted deletion of *Nf2* in specific tissues, reveals broad roles for Merlin in many developing tissues. For example, early studies revealed roles for Merlin in the developing neural tube (McLaughlin et al. 2007). Targeted deletion of *Nf2* in the basal layer of the mouse skin leads to mitotic spindle orientation defects where tight control of symmetric and asymmetric cell division is completely lost (Gladden et al. 2010). In multicellular organisms aberrant spindle orientation can cause defective tissue architecture and stem cell gain/loss, which is known to contribute to tumorigenesis (Morin and Bellaiche 2011). Indeed, targeted *Nf2* deficiency in the mouse liver leads to an expansion of progenitor cells and tumorigenesis (Benhamouche et al. 2010). Additionally, targeted *Nf2* deficiency in the proximal convoluted epithelium of the kidney yields multifocal tumor development featuring lumen-filling neoplasia that progress to invasive carcinoma (Morris and McClatchey 2009). Independent *in vivo* models of Merlin and ERM function suggest that they function similarly by organizing the cell cortex while distinct phenotypic consequences suggest unique functions.

To complement our studies of 3D organotypic cyst formation by intestinal epithelial cells, we sought to examine the functional relationship between Merlin and Ezrin in the intestinal epithelium *in vivo*. The consequences of loss of *Nf2* in the mouse intestinal epithelium have not been examined. Surprisingly, we found that conditional deletion of *Nf2* in the mouse intestinal epithelium leads to no obvious

proliferative or morphological defect unless the epithelium is compromised by chemical damage. Moreover, we demonstrate a strong genetic interaction between *Nf2* and *Ezrin* in this tissue and observe defects in proliferation and tissue architecture that are not observed in either single mutant. Notably, in contrast to the deletion of either *Nf2* or *Ezrin* alone, deletion of both *Nf2* and *Ezrin* lead to severe wasting and death. This Chapter presents an examination of this phenotype in the context of the studies of Merlin/ERM function that we uncovered in 3D organotypic cultures in Chapter 2.

Results

Inducible deletion of *Nf2* and/or *Ezr* in the mouse intestinal epithelium

To examine the functional relationship between Merlin and Ezrin *in vivo* we set up crosses (Figure 3.1) to generate mice in which *Nf2* or *Ezr* or both *Nf2* and *Ezrin* can be inducibly deleted in the mouse intestinal epithelium upon tamoxifen treatment. Comparing single *Nf2* and *Ezr* deficient tissue to compound *Nf2; Ezr* deficient tissue will allow us to define their functional relationship *in vivo*. In short, $Ez^{lox/lox}$;*Vil-Cre-ER*^{T2} mice (*Vil-Cre-ER*^{T2} mice kindly provided by Silvie Robine, Curie Institute) (Casaletto et al. 2011) were crossed with $Nf2^{lox/lox}$ mice (Giovannini et al. 2000) to generate $Nf2^{lox/+}$;$Ez^{lox/+}$;*Vil-Cre-ER*^{T2} mice. The progeny were then inter-crossed to generate control ($Nf2^{lox/+}$;$Ez^{lox/+}$;*Vil-Cre-ER*^{T2}), or mice in which conditional deletion of *Nf2* ($Nf2^{lox/lox}$;$Ez^{lox/+}$;*Vil-Cre-ER*^{T2}), *Ezr* ($Nf2^{lox/+}$;$Ez^{lox/lox}$;*Vil-Cre-ER*^{T2}) or both (*(*$Nf2^{lox/lox}$;$Ez^{lox/lox}$;*Vil-Cre-ER*^{T2}) in the mouse intestinal epithelium can be achieved. Notably, this is the only known setting where Ezrin is the sole expressed ERM protein and therefore the only setting where we can examine the relationship between Merlin and the ERMs without the possibility of compensation by other ERM proteins.

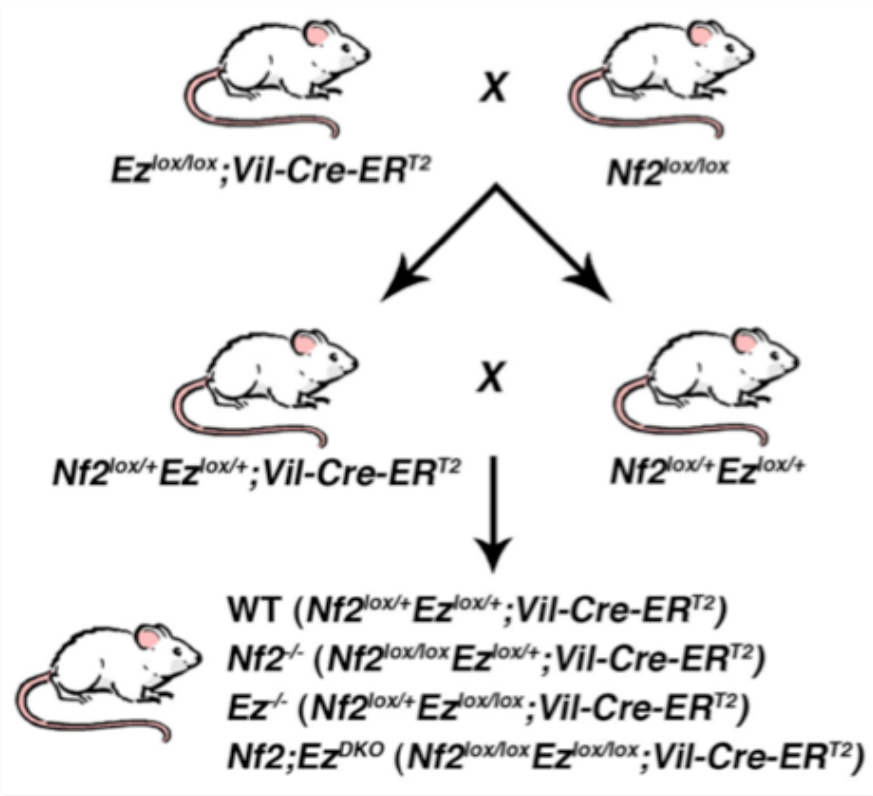

Figure 3.1 Schematic of breeding strategy for generation of tamoxifen inducible mice. Using this strategy we are able to generate mice to induce single *Nf2*, *Ezrin* and double *Nf2;Ezrin* deficiency in the mouse intestinal epithelium upon tamoxifen treatment.

Nf2 is required for tissue remodeling and Ezrin distribution in the mouse intestinal epithelium

To establish the basis of comparison to our compound tamoxifen induced *Nf2;Ezr* mutant (which will be referred to herein as *Nf2;Ezr*^{DKO}), we examined the consequences of *Nf2* deletion alone in the mouse intestinal epithelium. Our lab has previously demonstrated that tissue-specific loss of *Nf2* leads to an expansion of

progenitor cells in the mouse liver (Benhamouche et al. 2010) and to the development of multifocal tumors that exhibit ectopic Ezrin localization in the mouse kidney (Morris and McClatchey 2009). Additionally, targeted deletion of *Nf2* in the mouse skin yields defects in tissue architecture, barrier function and basal cell polarity (Gladden et al. 2010). In the following studies, we deleted *Nf2* in the mature intestinal epithelium - an already established, fully polarized and differentiated epithelial structure - and therefore might not observe proliferative defects upon *Nf2* deletion. Indeed, six week old tamoxifen treated $Nf2^{lox/lox}$;$Vil\text{-}Cre\text{-}ER^{T2}$ mice demonstrated no obvious morphological or proliferative defects after two (Figure 3.2) or twelve weeks (provided by Zachary S. Morris; not shown) as evidenced by H&E staining and quantitation of BrdU-positive nuclei per crypt compared to control (tamoxifen treated $Nf2^{lox/lox}$) mice.

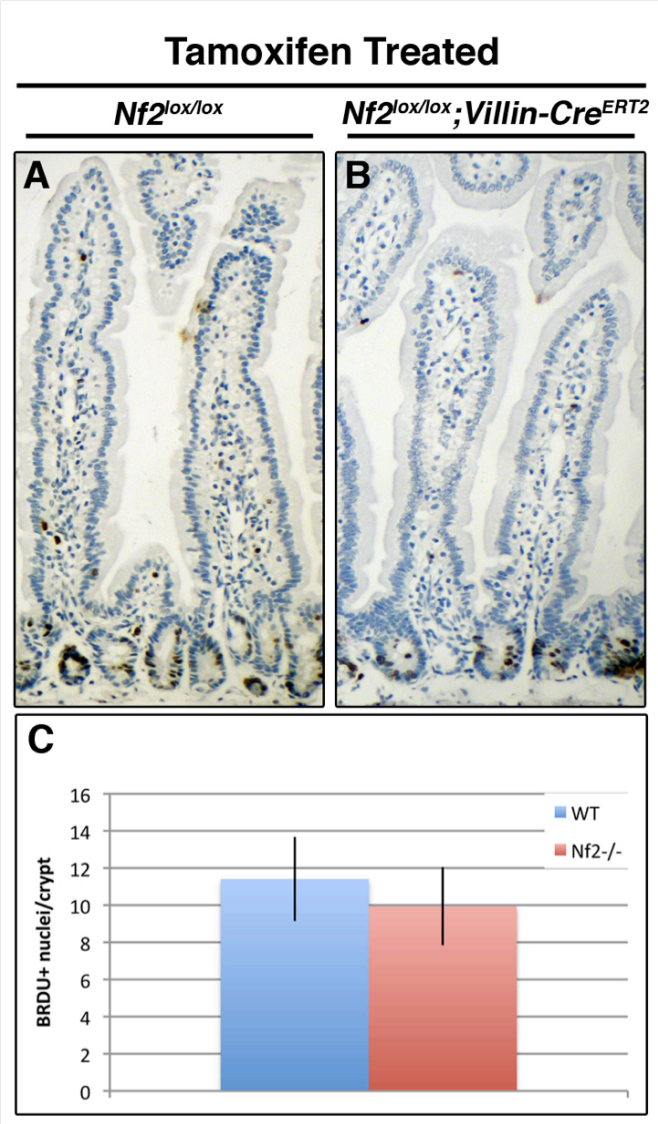

Figure 3.2 (Continued on next page)

Figure 3.2 (Continued). Loss of *Nf2* alone does not yield morphological or proliferative defects in the intestinal epithelium. Two week old *Nf2*$^{lox/lox}$ or *Nf2*$^{lox/lox}$*;Villin-Cre-ER*^{T2} were treated with tamoxifen and sacrificed 30 days post treatment. BrdU staining of wild type **(A)** or *Nf2* deficient **(B)** intestinal epithelial sections reveals comparable rates of proliferation, quantified in **(C)**, and normal crypt/villus morphology when *Nf2* is deleted in the epithelium. **(D)** Western blot of intestinal epithelial lysates confirming the absence of Merlin.

The localization of junctional markers (α-catenin and E-cadherin) and apical markers (crumbs-3, aPKC and NHE-RF1) were also unaffected in the *Nf2* deficient mouse intestinal epithelium (not shown). Additionally, we did not observe activation of EGFR, its preferred dimerization partner ErbB2 or their downstream effectors Akt, MAPK, or STAT3 by Western blot using phospho-specific antibodies (not shown) which is observed upon tissue specific deletion of *Nf2* in mouse renal adenomas (Morris and McClatchey 2009).

In vitro and *in vivo* studies from our lab demonstrate that Merlin is critical for epidermal development through the establishment of a junctional polarity complex in the mouse skin (Gladden et al. 2010). As mentioned, the mouse intestinal and colonic epithelium is already fully polarized and differentiated prior to tamoxifen-induced deletion, which may preclude the manifestation of an *Nf2* deficient phenotype. To address whether *Nf2* is required for the proper establishment of cellular and tissue architecture, we chemically-induced damage to the colonic epithelium by treatment with DSS and asked whether Merlin is required for the re-establishment of the epithelial monolayer.

Based on the role of Merlin in restricting the distribution of Ezrin in single CaCo2 cells (Figure 2.5), in adherens junction maturation (Lallemand et al. 2003), and in orienting the mitotic spindle (Gladden et al. 2010), we hypothesized that the *Nf2* deficient epithelium would fail to properly remodel compared to control. In support of this, we found that induced $Nf2^{lox/lox}$;$Vil\text{-}CreER^{T2}$ mice are more sensitive to DSS treatment and lose weight more quickly than control (Figure 3.3G). Following 6 days of DSS treatment both the wild-type and *Nf2*-deficient colonic epithelia are visibly damaged. However, by day 10 (4 days after DSS withdrawal) the wild-type tissue re-forms a normal monolayer, while the *Nf2*-deficient tissue fails to properly reorganize (Figure 3.3A-F). Notably, in strong agreement with what we observe in single CaCo2 cells described in Chapter 2, Ezrin is ectopically localized in intestinal epithelial cells 2 days after DSS withdrawal and fails to reposition even after 4 days post DSS treatment in *Nf2* deficient tissue (Figure 3.4). The areas of tissue that exhibit ectopic Ezrin distribution, can be mono- or multi-layered, suggesting that the failure to restrict cortical Ezrin may eventually lead to multi-layering (see below).

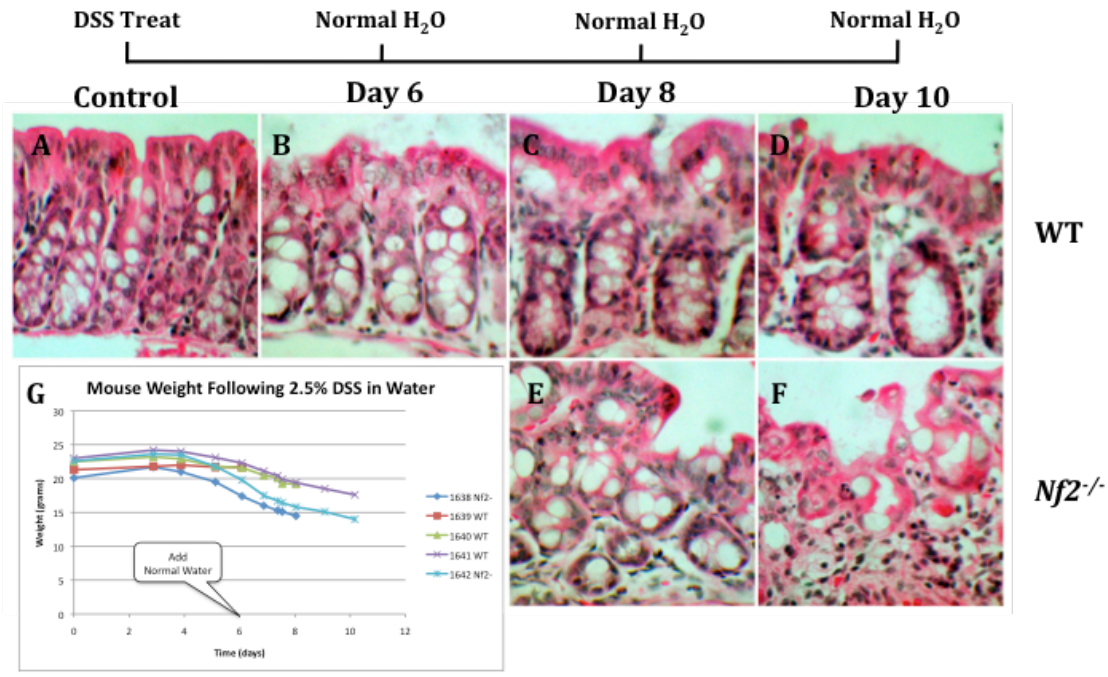

Figure 3.3 The *Nf2* deficient mouse colonic epithelium fails to properly organize following DSS induced chemical damage. **(A)** The colonic epithelium of control mice prior to DSS treatment is morphologically normal. **(B)** Following 5 days of DSS treatment the colonic epithelium of control and *Nf2* deficient tissue are visibly damaged on day 6. **(C-F)** By day 8 and 10 the colonic epithelium of control mice recovers and appears morphologically normal while the *Nf2* deficient tissue fails to properly reorganize and recover. **(G)** Notably, all mice lose weight following DSS treatment, however, mice deficient for *Nf2* in the intestinal and colonic epithelium are more sensitive as they lose weight more quickly.

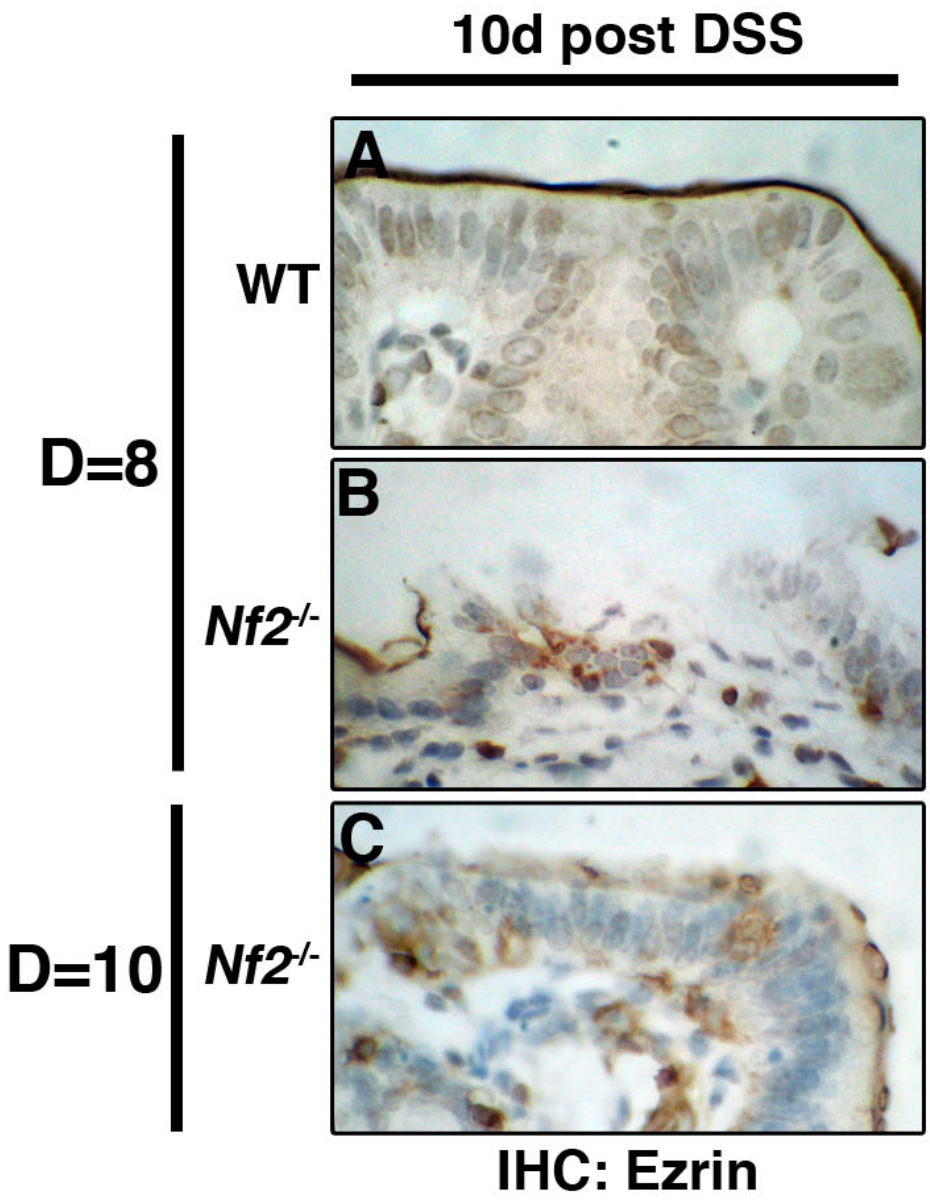

Figure 3.4 The *Nf2* deficient mouse colonic epithelium fails to properly position Ezrin following DSS induced chemical damage. **(A)** The colonic epithelium of control mice position Ezrin normally at the apical surface 2 days following DSS withdrawal (8 days following DSS treatment). **(B)** *Nf2* deficient tissue fails to organize properly 2 days following DSS withdrawal and Ezrin is disorganized in these cells. **(C)** By day 10, *Nf2* deficient tissue still fails to properly localize Ezrin and parts of the epithelium display multilayering.

Strong cooperativity upon compound deletion of *Nf2* and *Ezr* in the mouse intestinal epithelium

Our studies of Merlin and ERM deficiency using CaCo2 cells in 3D culture highlight both distinct and overlapping functions. Here, Merlin is required for restricting the cortical distribution of Ezrin, which is critical for orienting the interphase centrosome and mitotic spindle (Chapter 2). Conversely, upon loss of ERM function, cysts are unable to form lumens and exhibit aberrant localization of polarity proteins, centrosomes and spindles (Figure 2.7). Notably, loss of both Merlin and ERM function in these cells yields a catastrophic inability to form structures at all, indicating a functional overlap (Figure 2.11).

To date, a functional interaction between Merlin and the ERMs has not been defined in an *in vivo* setting. We found that upon tamoxifen induction, *Nf2;Ez*^{DKO} mice quickly lost weight (Figure 3.5A) and were visibly sick within four days following the start of tamoxifen treatment compared to control or single mutant mice. Notably, these mice had severe diarrhea and blood in the stool, indicating a severe functional barrier defect, which led to death between 4 and 9 days following tamoxifen induction (Figure 3.5B). The requirement for both Merlin and Ezrin in the intestinal epithelium indicates a functional overlap, which is in agreement with our *in vitro* data (Figure 2.11).

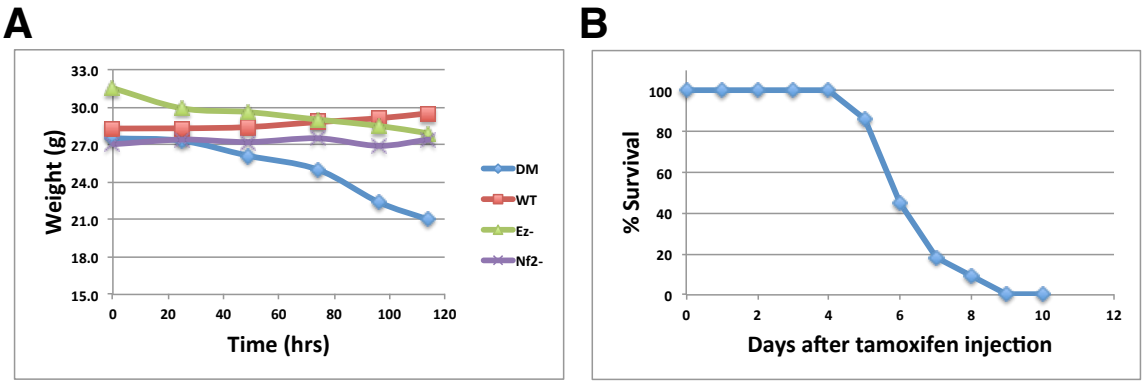

Figure 3.5 Targeted deletion of both *Nf2* and *Ezrin* in the mouse intestinal epithelium leads to severe wasting and death. **(A)** Plot of mouse weight over time following tamoxifen induction at time = 0. Notably, compound *Nf2;Ezr* mutant mice lose weight quickly compared to control or single *Nf2* or *Ezrin* deficiency in the mouse intestinal epithelium. **(B)** Survival curve of $Nf2^{lox/lox};Ez^{lox/lox};Vil\text{-}Cre\text{-}ER^{T2}$ following tamoxifen induction at day = 0.

Junctional remodeling (Lallemand et al. 2003; Saotome et al. 2004; Gladden et al. 2010; Casaletto et al. 2011) is one point where Merlin and ERM function could intersect and in a dynamic tissue, such as the intestinal epithelium, we might expect severe morphological defects that could, in turn affect tightly regulated processes such as proliferation and apoptosis. Since most tamoxifen induced $Nf2;Ez^{DKO}$ mice do not survive past day 7 following tamoxifen induction we sacrificed mice on day 6 to observe gross tissue architecture by H&E staining and quantified proliferation by BrdU staining. $Nf2;Ez^{DKO}$ mice exhibit severe tissue architecture defects not seen in either single mutant or control mice (Figure 3.6A,D; not shown). Most prominently,

instead of a single monolayer, the *Nf2;Ez*^{DKO} intestinal epithelium becomes multi-layered.

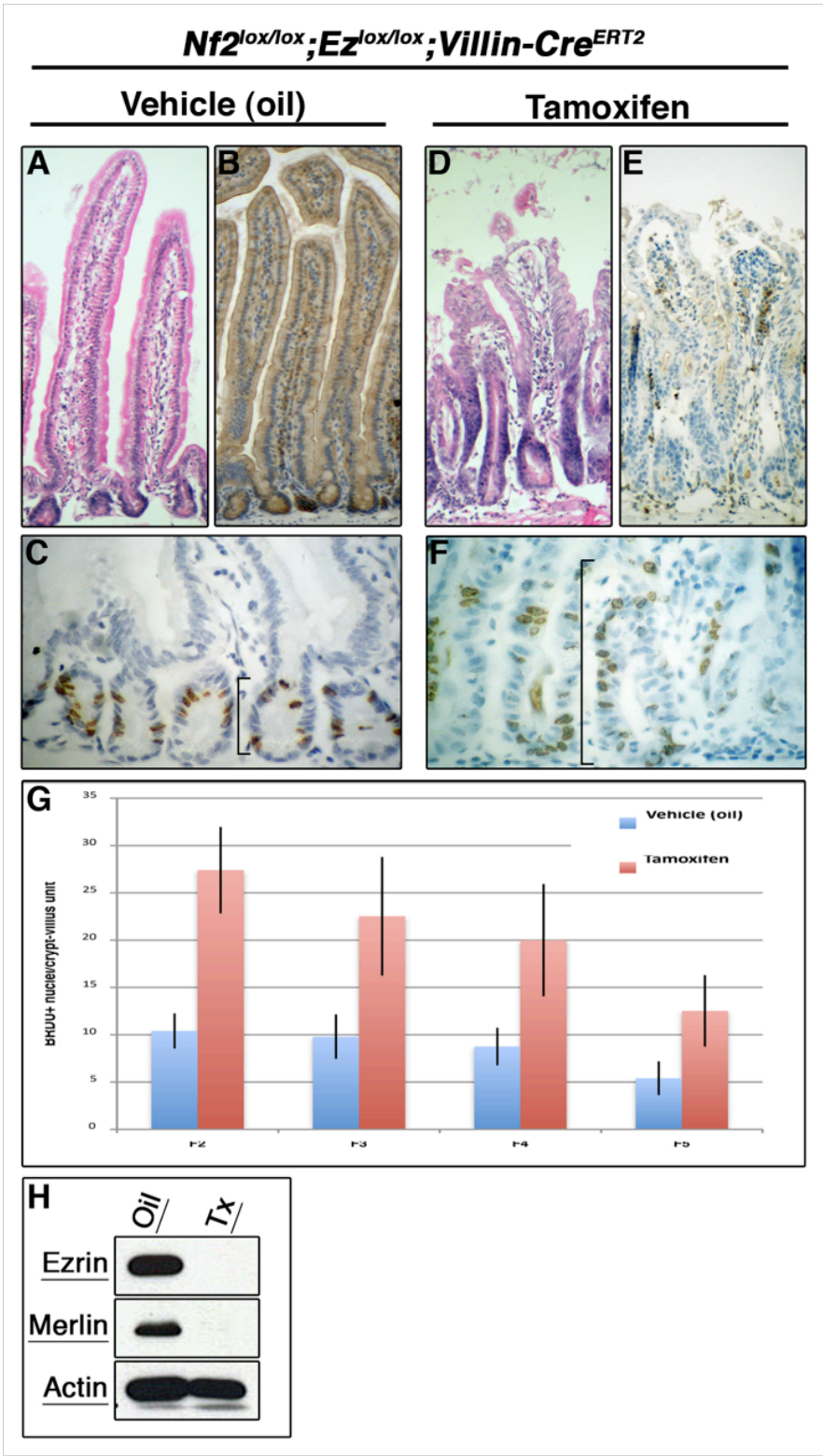

Figure 3.6 (Continued on next page)

Figure 3.6 (Continued). Loss of both *Nf2* and *Ezrin* in the mouse intestinal epithelium leads to an expansion of the proliferative compartment. **(A-C)** Vehicle-treated *Nf2$^{lox/lox}$;Ez$^{lox/lox}$;Villin-Cre-ER^{T2}* mouse intestinal epithelia exhibit normal crypt/villus morphology as indicated by H&E staining **(A)** and express Ezrin protein **(B)**. BrdU positive nuclei are restricted to the proliferative compartment in the crypt (C, bracket). **(D-F)** When the mice are treated with tamoxifen to delete *Nf2* and *Ezrin*, Ezrin is not detected in the epithelium, as expected **(E)**, and crypt/villus architecture is compromised **(D)**. BrdU staining reveals that the proliferative compartment in the *Nf2;Ez^{DKO}* intestinal epithelium is expanded (F, bracket). **(G)** Quantification of BrdU positive nuclei per crypt-villus unit in five sections of the small intestine (F2-duodenum, F3-jejunum, F4-proximal ileum, F5-distal ileum) confirms an overall increase in the number of proliferating cells following concomitant loss of Merlin and Ezrin. **(H)** Western blot of intestinal epithelial lysates demonstrates that both Merlin and Ezrin are lost following tamoxifen treatment.

We also observed that the proliferative zone in the crypt was expanded (Figure 3.6C,F) and the overall number of BrdU positive cells per crypt increased more than two fold across the entire length of the intestine (Figure 3.6G). While the increase in proliferation in *Nf2;Ez^{DKO}* tissue is almost entirely due to an expansion of the proliferative compartment, we also noted rare cells within the villus that stain positive for BrdU (not shown). Notably we observe similar defects in tissue architecture and proliferation in the *Nf2;Ez^{DKO}* colonic epithelium (Figure 3.7) indicating that although Merlin and Ezrin have unique functions they demonstrate strong cooperativity in organizing tissue structure, and regulating proliferation.

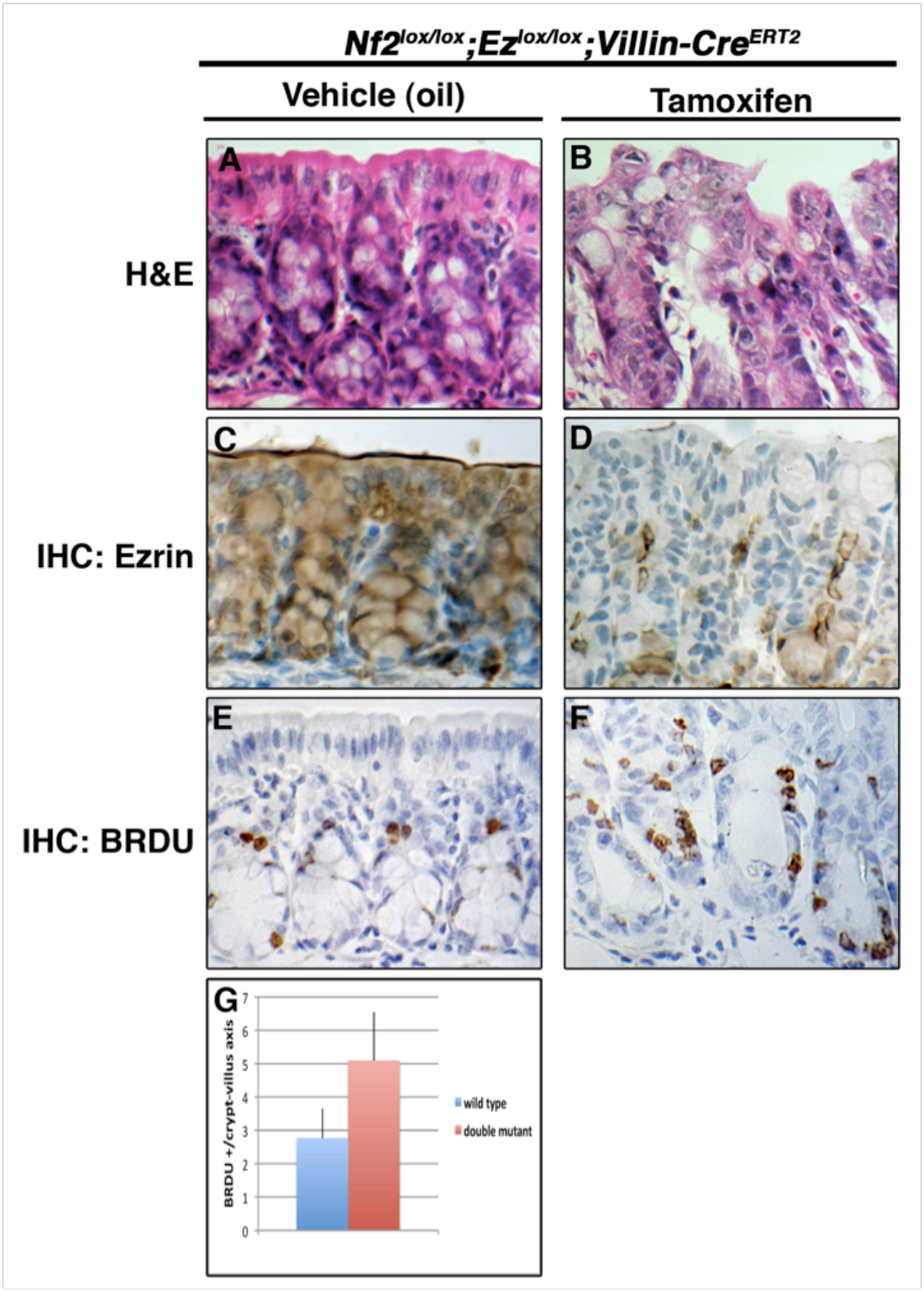

Figure 3.7 (Continued on next page)

Figure 3.7 (Continued). Loss of both *Nf2* and *Ezrin* in the colonic epithelium leads to disorganization of epithelial architecture and an increase in proliferation. **(A,C,E)** Wild-type mouse colonic epithelia from vehicle treated *Nf2$^{lox/lox}$;Ez$^{lox/lox}$;Villin-Cre-ER^{T2}* mice displays normal morphology **(A)** by H&E staining, Ezrin localization **(C)** by IHC and proliferation **(E)** by BrdU incorporation. After tamoxifen treatment **(B,D,F)** Ezrin is no longer detected by IHC **(D)** the colonic epithelium loses monolayer architecture **(B)** and there is an increase in the number of BrdU positive nuclei per crypt. Panel **(G)** confirms an increase in proliferation in the absence of Merlin and Ezrin.

In Chapter 2 we showed that loss of both Merlin and ERM function together leads to a catastrophic inability to organize the cell cortex and cell death, even in the presence of a strong ECM cue. To test whether *Nf2* and *Ezr* are required for cell survival we monitored apoptotisis in *Nf2;Ez^{DKO}* tissue by staining for cleaved-caspase 3 (Figure 3.8). Indeed, we observe a dramatic increase in apoptotic cells within the multilayered areas that either retain or lose attachment to the ECM indicating that apoptosis is not simply the result of ECM detachment (anoikis).

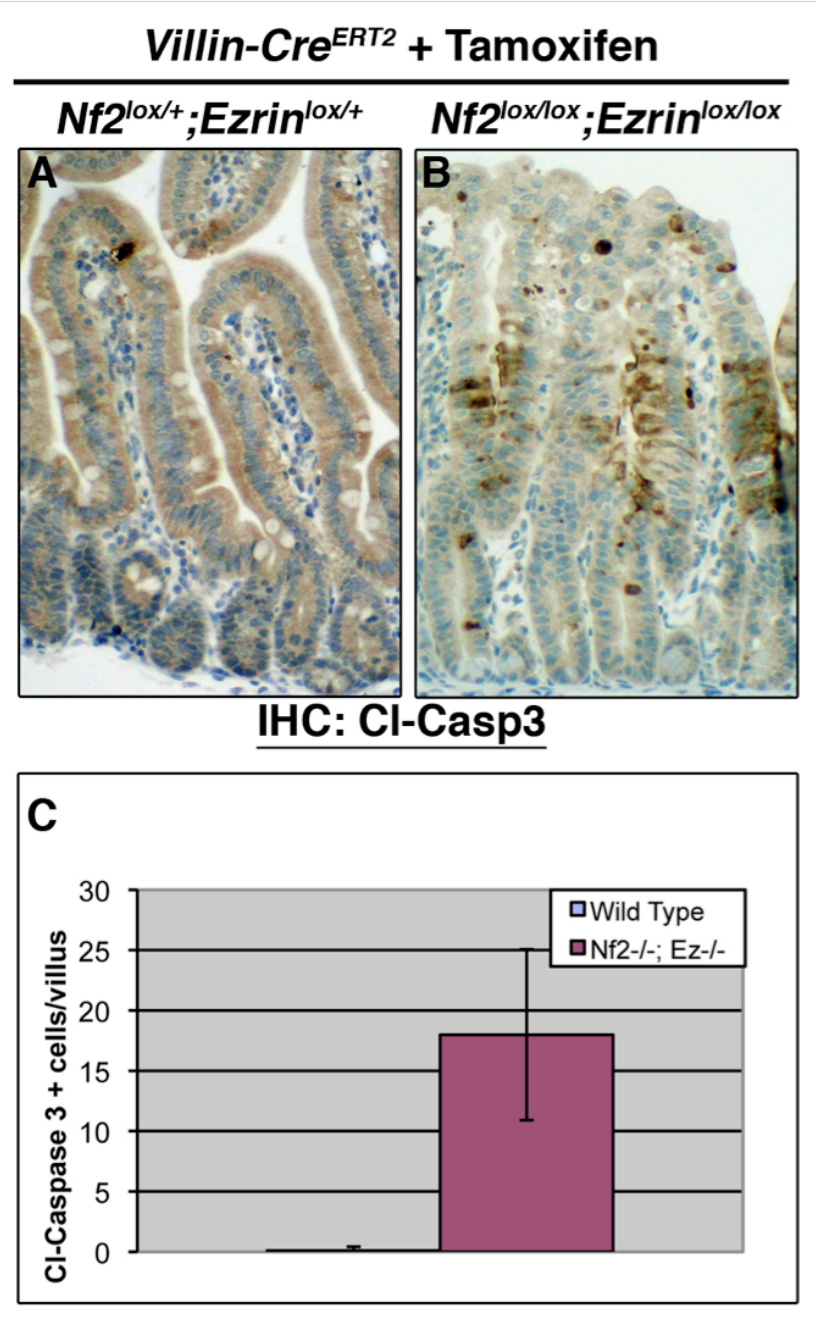

Figure 3.8 Concomitant loss of *Nf2* and *Ezrin* leads to an increase of apoptosis in the intestine. **(A-C)** Eight-week-old *Nf2$^{lox/+}$;Ez$^{lox/+}$;Villin-Cre-ER^{T2}* and *Nf2$^{lox/lox}$;Ez$^{lox/lox}$;Villin-Cre-ER^{T2}* mice were treated with tamoxifen and sacrificed 8 days post treatment. **(A,B)** Cleaved-caspase 3 staining of intestinal epithelial sections demonstrates a low frequency of apoptotic cleaved-caspase 3 positive cells in wild-type tissue **(A)** and an increase of apoptosis in double *Nf2;Ezrin* deficient tissue **(B)**. Quantification of cleaved-caspase 3 positive cells per villus indicates an almost 15 fold increase of apoptosis in the intestinal epithelium following loss of *Nf2 and Ezrin* **(C)**.

Deletion of *Nf2* and *Ezr* yields cell autonomous defects in epithelial integrity, proliferation and apoptosis

To distinguish cell autonomous from non-cell autonomous defects we injected *Nf2$^{lox/lox}$;Ez$^{lox/lox}$;Vil-Cre-ER^{T2}* mice with a low dose of tamoxifen and sacrificed the mice over varying periods of time such that we can compare wild-type cells to compound mutant *Nf2;Ezrin* cells within a single villus in the mouse intestinal epithelium (Figure 3.9A). Tissue samples were stained for Ezrin by immunohistochemistry to identify a tamoxifen injection protocol that yielded approximately 50% wild type versus *Nf2;Ezrin* mutant mosaic tissue (Figure 3.9B). We observed that within a single villus, wild-type tissue (marked by the presence of Ezrin) remained a single monolayer while double *Nf2;Ezrin* deficient tissue (marked by the absence of Ezrin) was disorganized and multilayered indicating a cell autonomous effect on tissue organization/epithelial integrity. Notably, cells begin multilayering at the site of ectopic proliferation as cells migrate out of the crypt and up the villus. This is a critical transition point where some cells must remodel their junctions to segregate and ascend two different villi. This process is defective in *Ezrin* deficient mice leading to the fusion of villi (Casaletto et al. 2011). We know Merlin is also critical for remodeling adherens junctions and orienting the mitotic spindle (Lallemand et al. 2003; Gladden et al. 2010) (Chapter 2). Perhaps Merlin cooperates with Ezrin at this transition to maintain stable adherens junctions leading to the formation of a multilayered epithelium when function of both Merlin and Ezrin is lost. In that regard, it will be important to determine whether defective

spindle orientation might play a causative role in multilayering or may be a secondary effect of unstable adherens junctions.

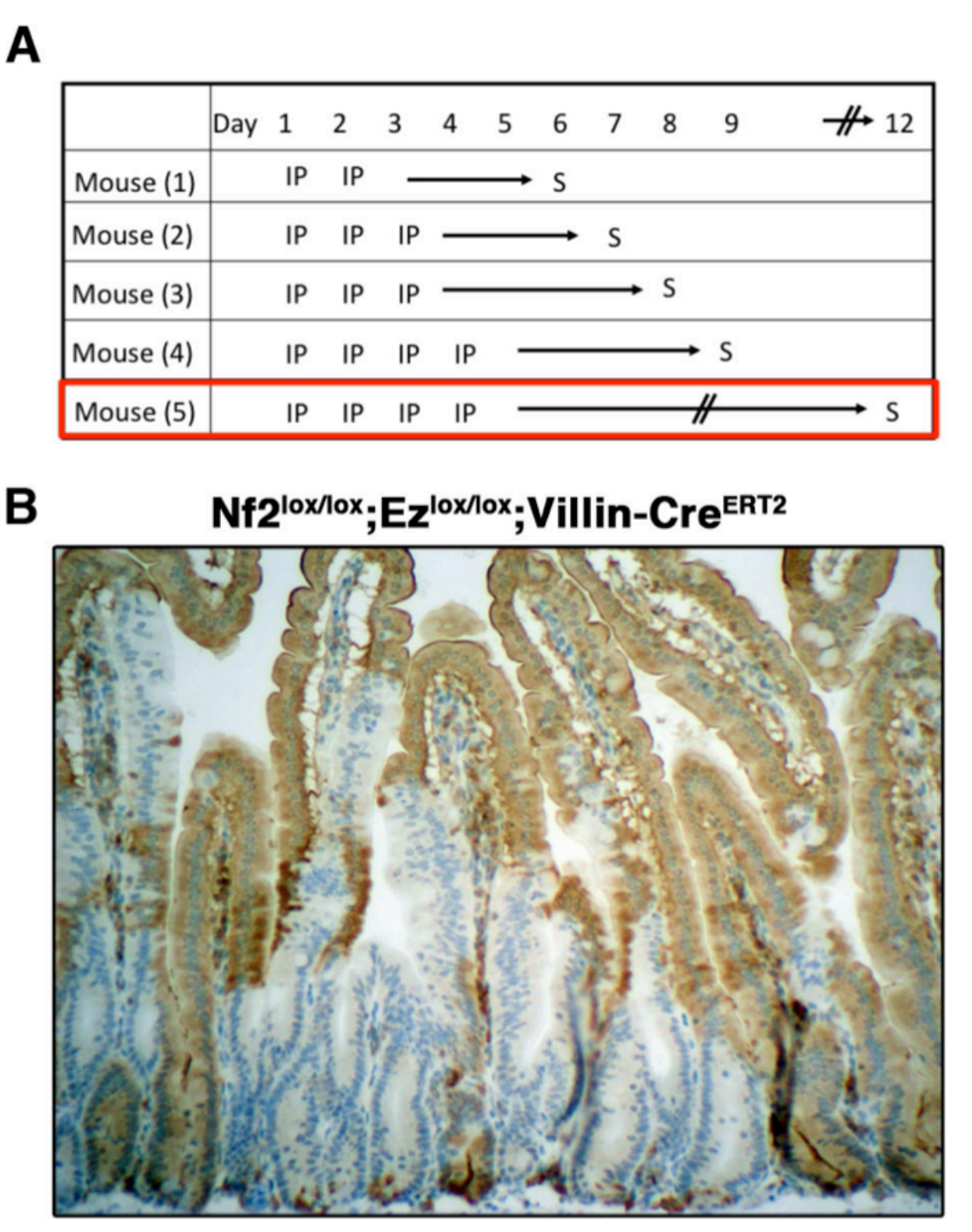

Figure 3.9 (Continued on next page)

Figure 3.9 (Continued). Generation of mice with mosaic loss of both *Nf2* and *Ezrin* in the mouse intestinal epithelium demonstrates cell autonomous phenotype. **(A)** Schematic of tamoxifen induction conditions used to generate mosaic deficiency of *Nf2;Ezrin* in the intestinal epithelium. The tamoxifen injection protocol used for mouse 5 (boxed in red) generated mice with approximately 50% mosaicism, as demonstrated by IHC detection of Ezrin in **(B)**.

Deletion of *Nf2* and *Ezrin* in the mouse intestinal epithelium leads to an expansion of the proliferative compartment, loss of epithelial integrity and multilayering of the epithelium. However, disruption of overall tissue architecture could lead to inflammation and secondary effects on proliferation. To determine whether ectopic proliferation in the *Nf2;Ez*^{DKO} intestine is cell autonomous, we compared adjacent wild-type and *Nf2;Ez*^{DKO} crypts in mosaic animals (Figure 3.10). By staining serial sections we demonstrate that *Nf2;Ez*^{DKO} tissue on one side of a single villus displays an expanded proliferative zone when directly compared to the wild type tissue on the opposing side of the villus (Figure 3.10), indicating that the proliferative defect is cell autonomous.

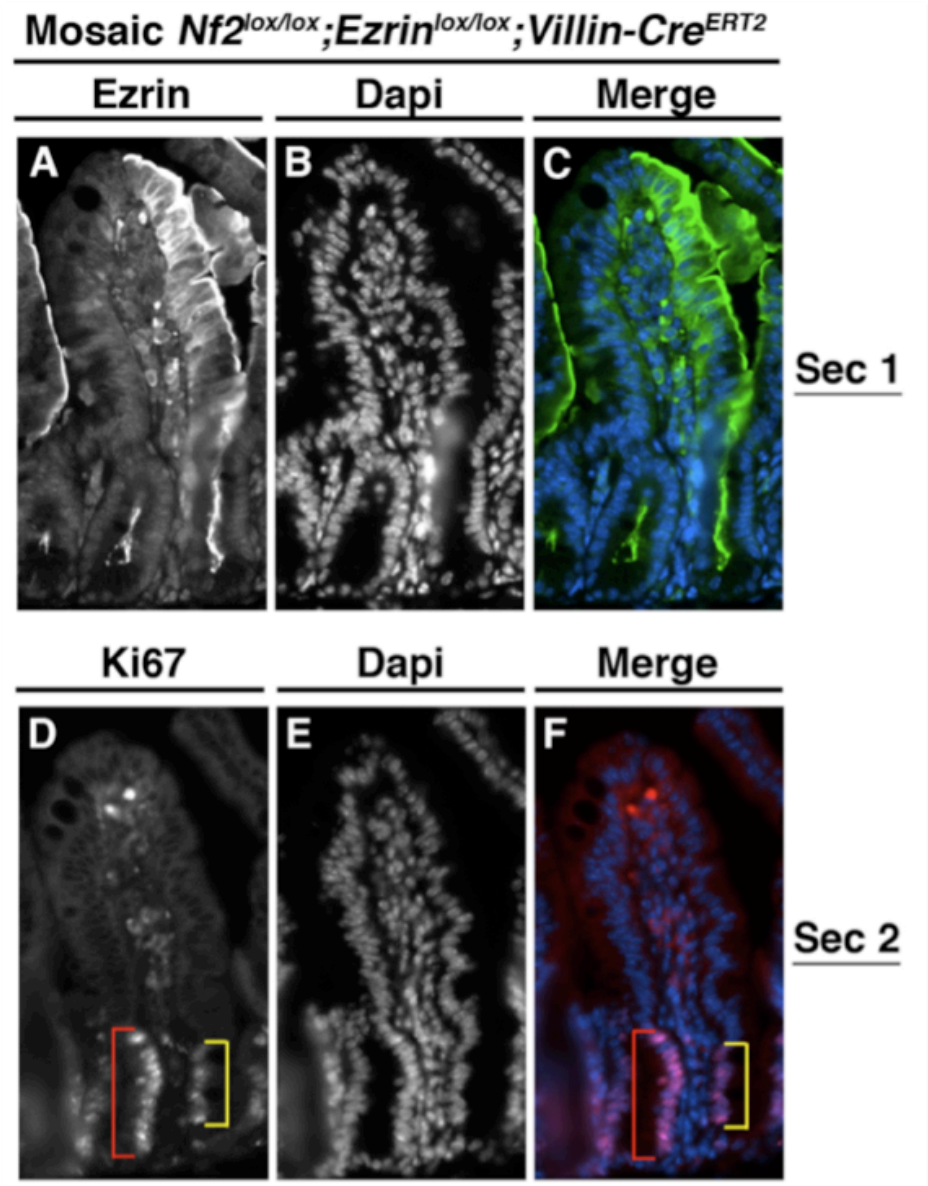

Figure 3.10 Cell autonomous increase in proliferation in double *Nf2;Ezrin* deficient tissue. **(A-F)** Serial sections (Sec1 and Sec2) of mosaic *Nf2*$^{lox/lox}$*;Ezrin*$^{lox/lox}$*;Villin-Cre-ER*^{T2} mice (Figure 3.9). Adjacent sections were cut (Sec1 & Sec2) and stained for either Ezrin **(A-C)** or the marker of proliferation Ki67 **(D-F)**. On the right side of the villus shown in **(A)**, ezrin expression denotes wild-type *Nf2* and *Ezrin* expressing tissue while on the left side ezrin is not detected indicating that *Nf2* and *Ezrin* are lost in this section of the villus. **(B,E)** Dapi staining reveals the disorganized epithelia on the left side of the villus where *Nf2* and *Ezrin* are lost. **(D-F)** Ki67 staining shows that the proliferative compartment in *Nf2* and *Ezrin* deficient tissue (red brackets D,F) becomes expanded compared to the adjacent wild-type tissue (yellow brackets D,F).

In agreement with our studies of CaCo2 cells, which do not tolerate loss of both Merlin and ERM function, we observe a dramatic increase in apoptotic cells in *Nf2;Ez*^{DKO} animals (Figure 3.8). However, the presence of lymphocytes in *Nf2;Ez*^{DKO} mice by H&E staining (not shown) indicates a robust immune response, which could induce apoptosis non-cell autonomously. To test this we assayed for apoptotic cells in the mosaic *Nf2;Ez*^{DKO} mice. In agreement with the 3D CaCo2 system (Chapter 2), we found that apoptotic cells were restricted to patches of *Nf2*/*Ezr* deficient tissue, as indicated by the absence of Ezrin staining (Figure 3.11), demonstrating a cell autonomous effect on apoptosis.

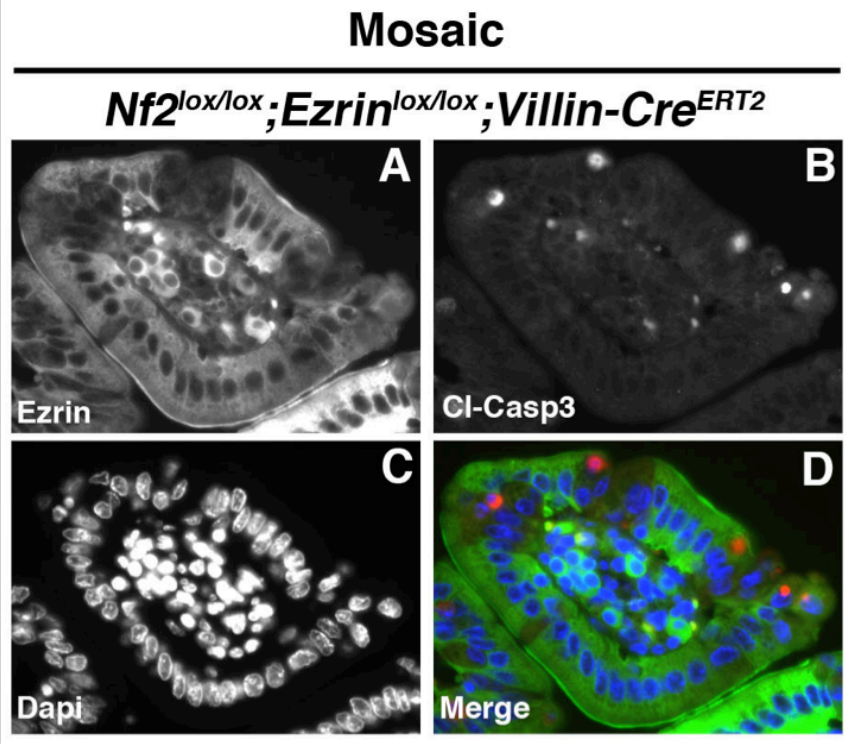

Figure 3.11 Concomitant loss of *Nf2* and *Ezrin* leads to a cell autonomous increase of apoptosis in the intestine **(A-D).** Cross-section of an individual villus exhibiting mosaic loss of *Nf2* and *Ezrin.* Tissue stained with **(A)**Ezrin, **(B)** Cleaved-caspase 3, and **(C)** DAPI. Ezrin staining **(D)** reveals patches of *Ezrin* deficient (presumably *Nf2*$^{-/-}$) tissue among wild type tissue. Cleaved-caspase3 staining demonstrates that only mutant tissue has increased levels of apoptosis, indicating that the apoptotic defect is cell autonomous.

Compound *Nf2*:*Ezr* deletion yields polarity defects

Many studies have demonstrated a role for Merlin and the ERM proteins in controlling polarity (Jankovics et al. 2002; Miller 2003; Speck et al. 2003; Gladden et al. 2010; Wiley et al. 2010). Additionally, our studies described in Chapter 2 demonstrate that Merlin and the ERMs are critical for establishing cortical asymmetry. To test whether Merlin and Ezrin cooperate to maintain polarity we tested whether the localization of apical and basolateral cell markers were perturbed in *Nf2;Ezrin* deficient tissue using both mosaic and fully induced *Nf2;Ez^{DKO}* tissue. We found that cells exposed to the lumen maintain localization of apical and basolateral markers including Crumbs-3 (Figure 3.12A,B), aPKC (not shown), E-cadherin (not shown) and β-catenin (Figure 3.12C,D). However, cells within multi-layered areas that are not lumen-exposed completely lose polarity (Figure 3.12A-D), reminiscent of what is observed in *D. melanogaster* upon deletion of the single ERM ortholog Moesin where cells within the developing wing epithelium extrude basally and lose polarity (Speck et al. 2003).

Our observation that *Nf2;Ez^{DKO}* cells opposing the lumen maintain apicobasal polarity indicates that *Nf2* and *Ezrin* are not absolutely required for polarity. However, our studies in CaCo2 cells in 3D demonstrate that Merlin and Ezrin are critical for proper centrosome and mitotic spindle orientation. We note that multilayering within the villus in *Nf2;Ez^{DKO}* mice occurs at the site of ectopic proliferation at the top of crypts (not shown), strongly suggesting that multilayering and subsequent loss of polarity are likely the result of misoriented mitotic spindles and failure to divide symmetrically.

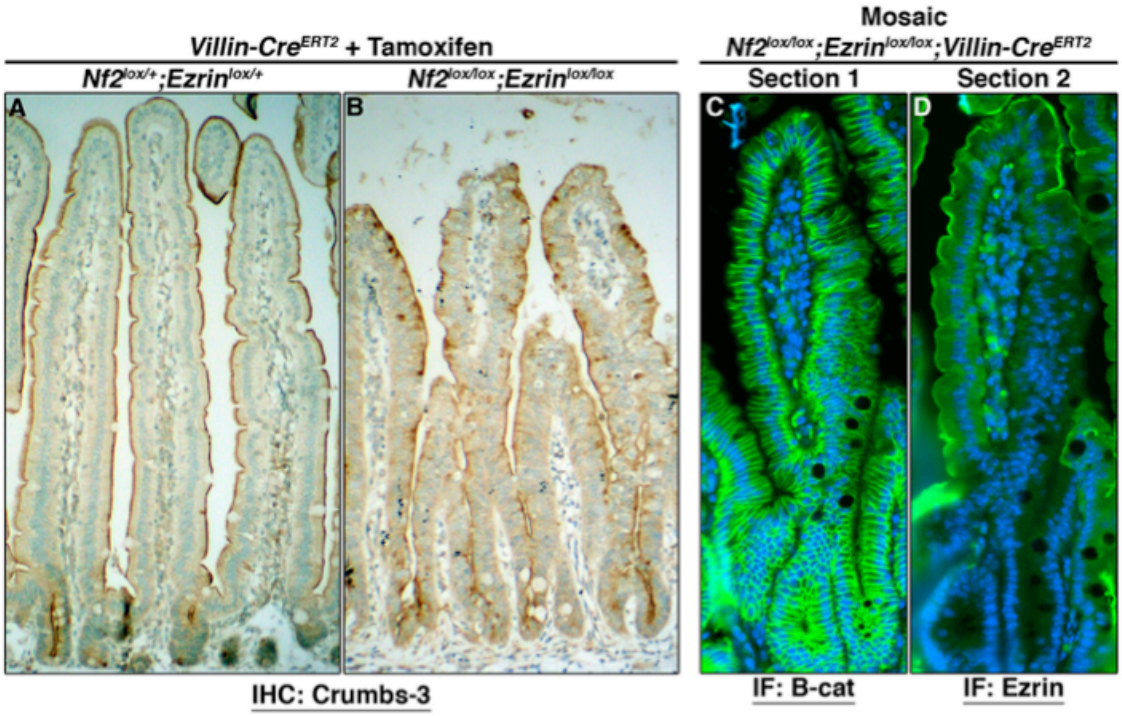

Figure 3.12. Both *Nf2* and *Ezrin* together are not absolutely required for the maintenance of apical-basal polarity. **(A,B)** IHC detection of the apical marker Crumbs3 in wild-type tissue **(A)** exhibits uniform apical localization. When *Nf2* and *Ezrin* are deleted **(B)** apical localization of Crumbs3 remains indicating that *Nf2* and *Ezrin* are not required for the maintenance of polarity. Notably, however, Crumbs3 staining is not uniform throughout the villus hinting at a subtle polarity defect when *Nf2* and *Ezrin* are lost. **(C,D)** Adjacent sections of villi (Sec1 & Sec2) from mice that are mosaic for loss of *Nf2* and *Ezrin* were stained for either Ezrin **(D)** or ß-catenin **(C)** to determine whether junctional localization of ß-catenin is perturbed when *Nf2 and Ezrin* are lost. On the right side of the villus where Ezrin staining is absent cells pile up on top of each other while on the left side where *Nf2* and *Ezrin* are expressed cells remain in a monolayer. **(C)** ß-catenin stains the lateral cell contacts in the wild-type tissue on the left side of the villus. However, when *Nf2* and *Ezrin* are lost, as seen on the right side of the villus, the epithelial cells become stratified and lose polarity as indicated by ß-catenin staining throughout the membrane.

Compound deletion of Nf2:Ezr leads to an increase in total EGFR and activation of downstream signaling

Work from our lab has demonstrated that Merlin-deficient cells in culture bypass contact dependent inhibition of proliferation, which can be restored upon expression of exogenous Merlin (Lallemand et al. 2003). Our follow up studies suggest that Merlin coordinates the establishment of stable adherens junctions (AJs) with inhibition of EGFR internalization and mitogenic signaling providing a molecular explanation for contact inhibition of cell proliferation (Curto et al. 2007; Cole et al. 2008). We have demonstrated that in the intact intestinal epithelium loss of *Nf2* or *Ezrin* alone does not lead to a defect in proliferation (Figure 3.2)(Saotome et al. 2004). However, we do observe an expansion of the proliferative compartment and loss of polarity upon deletion of *Nf2* and *Ezrin* together (Figures 3.4C,F,G and 3.12). While no evidence has implicated Ezrin in regulating EGFR or mitogenic signaling, there is abundant evidence that both Merlin and the ERMs control receptor distribution within cells (Saotome et al. 2004; Lamprecht and Seidler 2006; Maitra et al. 2006; Curto et al. 2007). Indeed, EGFR is basolaterally restricted in the rat intestine (Scheving et al. 1989). Therefore, we might expect that the failure to properly distribute EGFR at the membrane could affect receptor levels and/or activation.

Indeed, we observe a marked increase in the levels of total EGFR in mouse intestinal epithelial tissue following loss of both Merlin and Ezrin but not in either single mutant suggesting that Merlin and Ezrin could cooperate to control EGFR distribution within the cell (Figure 3.13). This would be consistent with our

observation that many cells within the multilayered epithelium ubiquitously localize basolateral markers, and likely EGFR, all around the cell membrane. Notably, the increase in total EGFR is associated with activation of its downstream effectors (Figure 3.13, not shown). These data suggest that defects in mitogenic signaling upon deletion of *Nf2* and *Ezrin* are the result of defective membrane and tissue organization rather than direct control of receptor activation, which has been suggested for Merlin (Curto et al. 2007).

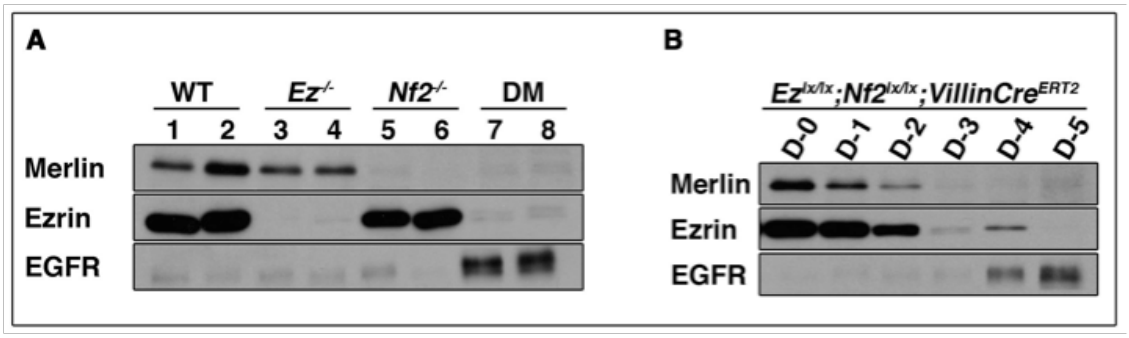

Figure 3.13 Western Blots of mouse intestinal epithelial cell lysates. **(A)** Conditional *Nf2$^{lox/+}$; Ez$^{lox/+}$; Villin-Cre-ER^{T2}* (WT,1-2), *Nf2$^{+/+}$; Ez$^{lox/lox}$; Villin-CreER^{T2}* (*Ez$^{-/-}$*, 3-4), *Nf2$^{lox/lox}$; Ez$^{+/+}$; Villin-Cre-ER^{T2}* (*Nf2$^{-/-}$*, 5-6) and *Nf2$^{lox/lox}$; Ez$^{lox/lox}$; Villin-Cre-ER^{T2}* (DM, 7-8) mutant mice were induced with 2μg of tamoxifen each day for 5 days and sacrificed 10 days following the first injection. DM mice 7 and 8 were sacrificed on day 6 and 6.5 respectively as they became too sick to continue. Epithelial cell lysates were probed with anti Merlin and Ezrin antibodies to confirm the loss of protein and epidermal growth factor receptor (EGFR). **(B)** Conditional *Nf2$^{lox/lox}$; Ez$^{lox/lox}$; Villin-Cre-ER^{T2}* mice were induced with 2μg of tamoxifen each day. One mouse was sacrificed each day for 5 days (D0-5) to determine when Merlin and Ezrin protein were absent and when EGFR levels increased.

Intestinal Defects	*Ez*$^{-/-}$	*Nf2*$^{-/-}$	*Nf2*$^{-/-}$;*Ez*$^{-/-}$
Fused villi	Y	N	Y
Expansion of terminal web	Y	N	?
Disorganized brush border	Y	N	?
Altered crypt architecture	Y	N	Y
Loss of EBP50 localization	Y	N	Y
Expansion of proliferative compartment	N	N	Y
Aberrant proliferative foci	N	N	Y
Paneth cell migration	N	N	Y
Paneth cell expansion	N	N	Y
Multi-layered epithelium	N	N	Y
Loss of polarity (extruded cells)	N	N	Y
Increased apoptosis	N	N	Y

Table 3.1 List of intestinal defects observed in single *Nf2* or *Ezrin* mutant and *Nf2;Ezrin* double mutant. Defects shaded in gray are unique to the *Nf2;Ezrin* double mutant.

Physiological Defects	*Ez*$^{-/-}$	*Nf2*$^{-/-}$	*Nf2*$^{-/-}$;*Ez*$^{-/-}$
Diarrhea	Y	N	Y
Weight loss	marginal	N	Y
Severe wasting	N	N	Y
Death	N	N	Y
Steatosis	N	N	Y
Fecal occult blood	N	N	Y

Table 3.2 List of physiological defects observed in single *Nf2* or *Ezrin* mutant and *Nf2;Ezrin* double mutant**.** Defects shaded in gray are unique to the *Nf2;Ezrin* double mutant. The green (marginal) indicates that the defect is subtle.

Discussion

Our studies using CaCo2 cells in Chapter 2 have demonstrated severe morphological defects upon loss of either Merlin or ERM function as single cells develop into cyst structures in 3D culture. However, deletion of *Nf2* in the highly dynamic yet fully polarized, intestinal epithelial monolayer yields no obvious proliferative or morphological defects (Figure 3.2). Deletion of *Ezrin* in this setting leads to defective apical morphogenesis and villus fusion, but the intestinal epithelial cells retain polarity and form a monolayer without ectopic proliferation (Casaletto et al. 2011). The ability of either single mutant to form a polarized monolayer is likely due to the strong positional cues (apicobasal polarity, cell:cell and cell:ECM contacts) that already exist when *Nf2* or *Ezrin* are deleted in this tissue. In support of this, chemical damage of the *Nf2* deficient mouse intestinal epithelium yields defects in cortical and tissue organization that feature the improper localization of Ezrin and multilayering of the epithelium (Figure 3.4)

Co-deletion of *Nf2* and *Ezrin* in the adult mouse intestinal epithelium yields severe morphological and proliferative defects identifying a strong functional interaction between Merlin and Ezrin for the first time *in vivo*. Since these phenotypes manifest without chemically disrupting the existing epithelial architecture, loss of both *Nf2* and *Ezrin* together may render these cells unable to sense or respond to the existing positional cues. While studies have suggested that Merlin and the ERMs have similar, distinct, or antagonistic functions our results indicate that they have both unique and overlapping functions. In support of this the *Nf2* and *Ezrin* deficient phenotypes are not identical and loss of both *Nf2* and

Ezrin together yield phenotypes that are not observed in either single mutant (Tables 3.1, 3.2), indicating they can compensate for one another for certain functions. So, what might be the basis for their functional overlap?

Individual studies have demonstrated that both Merlin and the ERMs have critical roles in establishing and remodeling cell:cell junctions (Lallemand et al. 2003; Speck et al. 2003; Saotome et al. 2004; Gladden et al. 2010; Casaletto et al. 2011). In the mouse intestinal epithelium, each crypt contributes to several of the surrounding villi. Therefore, as cells continuously migrate out of the crypt to repopulate the villi they must segregate and reform contacts with other cells. Studies from Casaletto *et al.* support the notion that in the *Ezrin* deficient intestinal epithelium, adjacent cells are unable to segregate and instead remain in contact as they emerge from an individual crypt and ascend two different villi, resulting in villus fusion. It is interesting to note that in *Nf2;Ezr*^{DKO} tissue multilayering, apoptosis, and expansion of the proliferative compartment occur approximately at this location. and crypt architecture is itself perturbed. This suggests that Merlin and Ezrin function may be critical for and cooperate to remodel cell junctions at the dynamic crypt-villus junction.

Recent studies in *D. melanogaster* have provided insight into the dynamic control of cell junctions in the context of epithelial remodeling that may explain how Merlin and Ezrin could cooperate to remodel junctions (Cavey et al. 2008). In the *D. melanogaster* embryo Cavey *et al.* found that E-cadherin complexes partition into hyper-stable microdomains that represent adhesive foci. They show that the stability and mobility of these microdomains depend on two actin populations: 1)

small, stable actin patches that concentrate at homophilic E-cadherin clusters and 2) a rapidly turning over, contractile network that constrains their lateral movement by an α-catenin dependent tethering mechanism. Considering that Merlin and Ezrin can directly bind α-catenin (Gladden et al. 2010) and actin (Turunen et al. 1994; Reczek and Bretscher 1998) respectively, it is interesting to speculate that Merlin and Ezrin could control distinct pools of actin to cooperatively stabilize and localize E-cadherin complexes at cell:cell contacts to remodel junctions.

We have shown that Merlin deficient CaCo2 cells fail to properly position Ezrin, which leads to aberrant mitotic spindle orientation (Chapter 2). Therefore, in *Nf2;Ezr^{DKO}* mice, defective spindle orientation could contribute to the epithelial mutilayering that occurs as cells migrate out of the crypt and ectopic proliferation occurs (Figure 3.6). To this end it will be important to assess whether orientation of the mitotic spindle is perturbed in the *Nf2;Ezr^{DKO}* intestine. Notably, our CaCo2 studies support the notion that ectopically localized Ezrin, which occurs in the absence of Merlin function, actively mislocalizes centrosomes to perturb mitotic spindle orientation. However, *Nf2;Ezr^{DKO}* mice do not express Ezrin and therefore cannot actively mislocalize centrosomes in this situation. If we find that misoriented mitotic spindles do play a role in epithelial mulatilayering it may be that *Nf2;Ezr^{DKO}* cells fail to sense or generate cortical forces at the lateral adherens junctions which can dominate over other cues to direct division orientation (Lu et al. 2001; Yamashita et al. 2010).

Our data suggest for the first time that Merlin and Ezrin may also cooperate to control mitogenic receptor abundance and signaling (Figure 3.12). Previous

work from our lab has demonstrated that Merlin NHE-RF1 dependent manner (Curto et al. 2007). Notably, Merlin seems to regulate EGFR signaling rather than total levels. While Ezrin has not previously been implicated in controlling EGFR signaling, there is abundant evidence that both Merlin and the ERMs control receptor distribution within cells (Saotome et al. 2004; Lamprecht and Seidler 2006; Maitra et al. 2006; Curto et al. 2007). In our studies we note that many *Nf2;Ezr*^{DKO} cells lose polarity upon multilayering of the intestinal epithelium indicating that proper EGFR receptor distribution is likely perturbed. Therefore, the failure to properly distribute EGFR at the membrane could affect receptor levels and/or activation. Since Merlin can also control EGFR internalization and signaling in non-polarized cells, this cooperativity may not simply reflect the apical mislocalization of EGFR and exposure to apically provided ligands; instead this cooperativity could reflect a more fundamental (and complex) relationship between receptor trafficking and polarity establishment. Indeed, the intestinal epithelium may prove to be a valuable setting in which to study this.

Studies in *D. melanogaster* provide evidence that the sole ERM ortholog Moesin and Merlin functionally interact through competition for Slik kinase activity, (Hughes and Fehon 2006) although previous studies have shown that Merlin and the ERMs physically interact (Gonzalez-Agosti et al. 1999; Gronholm et al. 1999; Meng et al. 2000). If Merlin and Ezrin were functionally interacting by simply competing for kinase activity of the mammalian homolog of Slik (SLK) then we would expect to see an increase in Ezrin phosphorylation in *Nf2* deficient tissue, which we do not observe by Western blot of total epithelial cell lysates (not shown).

Alternatively, competition for SLK activity might occur within a specific compartment within the intestinal epithelium, such as the crypts where proliferation takes place, and elevated levels of ERM phosphorylation within the villus may mask changes in Ezrin phosphorylation upon deletion of *Nf2*. Therefore, we will address potential coordinate regulation of Merlin and Ezrin by the Ste20-like kinase SLK in the following chapter (Chapter 4).

Here we have been able to demonstrate a clear functional relationship between *Nf2* and *Ezrin in vivo.* The complexity of our phenotype makes it difficult to determine the precise molecular basis of their functional interaction. However, our data provide important clues to guide future molecular studies. Defects in epithelial integrity suggest that they cooperate to remodel cell:cell junctions. Additionally, Merlin and Ezrin cooperativity could lie in competition for SLK activity, EGFR turnover or a combination of them.

Materials and Methods

Animals and Animal Procedures

Tamoxifen inducible *Ez$^{lox/lox}$;Vil-Cre-ER^{T2}* mice (Casaletto et al. 2011) were crossed with homozygous *Nf2$^{lox/lox}$* provided by M. Giovaninni (Giovannini et al. 2000) to produce *Ez$^{lox/+}$; Nf2$^{lox/+}$; Vil-Cre-ER^{T2}* mice. These progeny were self-crossed to generate inducible control (*Ez$^{lox/+}$; Nf2$^{lox/+}$; Vil-Cre-ER^{T2})*, single *Nf2* deficient (*Ez$^{lox/+}$; Nf2$^{lox/lox}$; Vil-Cre-ER^{T2}*), single *Ezrin* deficient (*Ez$^{lox/lox}$; Nf2$^{lox/+}$; Vil-Cre-ER^{T2}*) or double *Ezrin;Nf2* deficient (*Ez$^{lox/lox}$; Nf2$^{lox/lox}$; Vil-Cre-ER^{T2}*) mouse intestinal epithelial tissue. Tamoxifen (MP Biomedicals) was solubilized (50 mg/mL in ethanol) and diluted to 10 mg/mL in corn oil. Mice (12–18 wk of age) were injected i.p. with 200 µL tamoxifen (2mg) or vehicle/day for 5 d and sacrificed 4–5 d after cessation of treatment unless otherwise specified. Animal procedures were performed according to federal and institutional guidelines and approved by the Massachusetts General Hospital Subcommittee on Research Animal Care.

DSS Induced Damage of the Colonic Epithelium

Nf2$^{lox/lox}$;Villin-Cre-ER^{T2} mice were treated with 2mg tamoxifen or vehicle only for 5 days to generate mice with *Nf2* deficiency in the mouse intestinal/colonic epithelium and control mice. 18 days following tamoxifen or vehicle treatment mice were treated with 2.5% dextran sulfate sodium (DSS) in the drinking water, ad libitum, for 5 days to induce damage to the colonic epithelium. Mice were sacrificed

at day 0, 6, 8 and 10 to confirm DSS induced damage and determine if and when the epithelial monolayer reorganized.

Epithelial Cell Isolation

Intestinal and Colonic tissue sections were cut lengthwise, rinsed with PBS and incubated in 1.5 ml cold chelating buffer (96mM NaCl, 8mM KH_2PO_4, 5.6mM Na_2HPO_4, 1.5mM KCl and 10mM EDTA pH 6.8) for 10 minutes on ice. Tissues were agitated by gentle shaking and epithelial cells were spun at 4,000 RPM for 2 min and either lysed or snap frozen in liquid N_2 for future use. This procedure was repeated a second time for isolation of additional material.

Histochemistry, Immunohistochemistry and BrdU Labeling

Dissected tissues were fixed in 10% neutral buffered-formalin, processed and paraffin-embedded. Sections were stained with hematoxylin and eosin or subject to immunohistochemistry using the following antibodies: anti-Ezrin (1:200; NeoMarkers #3C12), anti-Crumbs3 (1:200, a kind gift from Ben Margolis (Makarova et al. 2003)), anti-cleaved caspase-3 (1:200; Cell Signaling 9661), anti-lysozyme (1:500, DAKO), anti-BrdU (1:200; Becton Dickinson), and anti-ZO-1 (1:60, Zymed). Antigen retrieval was achieved by boiling in 10mM citrate buffer (20min) for all antibodies except anti-BrdU and anti-ZO-1, which utilized treatment with 0.1% trypsin (20min, 37˚C) and 2mg/ml protease (10min, 37˚C Sigma), respectively. HRP-conjugated secondary antibodies were detected using the DAB peroxidase substrate kit (Vector Laboraties). For BrdU labeling, mice were injected with 100 μg

of BrdU (Sigma) per gram of body weight and sacrificed after 2 h. Histochemical identification of goblet cells was performed by Alcian Blue.

Electron Microscopy

Tissues were fixed in 2.5% glutaraldehyde/2.5% paraformaldehyde in 0.1 M sodium cacodylate buffer (Electron Microscopy Sciences) and embedded in epoxy resin (Harvard University EM Core Facility). 1μm sections were prepared and stained with toluidine blue. Representative areas were chosen, thin-sectioned, stained with lead citrate (Susumu Ito) and examined on a Philips 301 electron microscope. Images were captured by an Advanced Microscopy Techniques imaging system.

Immunofluorescence

Single or serial paraffin sections were processed the same as for immunohistochemistry (described above) and incubated overnight with the following primary antibodies: BD Biosciences (anti-β-catenin, 1:500, #610154), Novocastra (anti-Ki67, 1:200), Cell Signaling (cleaved caspase-3, 1:500 #9661), Abcam (anti-EBP-50/NHE-RF, 1:2000, #3452) and BD Transduction Laboratories (E-cadherin 1:100, #610182). Cells were then rinsed 3X with PBST for 30 min, incubated with secondary antibodies, DAPI, and/or rhodamine-phalloidin for 1 hr and rinsed 3X with PBST. Labeled cells were visualized using a Nikon 90i fluorescence microscope or a Zeiss LSM510 laser scanning confocal microscope; images were processed using Elements (Nikon) or Zen (Zeiss) software.

Western Blot Analysis

Tissue extracts were lysed using RIPA lysis buffer (50 mM Tris [pH 7.4], 1% Triton X-100, 1% SDS, 0.5% sodium deoxycholate, 150 mM NaCl, 1 mM EDTA, 1 mM EGTA, 1 mM PMSF, 1 mM Na_3VO_4, 10 mM sodium fluoride, 10 mM β-glycerophosphate, 1 mg/ml aprotinin and 1 mg/ml leupeptin) followed by brief sonication. Cell debris was cleared by centrifugation (14,000 rpm, 10 min, 4°C) and lysates were quantitated by DC protein assay (Bio-Rad), separated by SDS-PAGE (30-40μg) and transferred to PVDF. Membranes were blocked in 5% milk, probed with anti-Ezrin (1:1000, NeoMarkers #3C12), anti-Nf2 (1:1000, Santa Cruz sc332), anti-actin (1:2000, Sigma A3853), anti-activated-beta-catenin (1:1000, Millapore 8E7) or from Cell Signaling (anti-pEGFR, #2235; EGFR, #03; pSTAT-3, #9145; STAT-3 #4904; pAkt, #4060; Akt, #4685; pMAPK #4370; MAPK #4696 all at 1:1000) for 1hr at RT or overnight at 4°C in 1% milk. Anti-mouse or anti-rabbit horseradish peroxidase-conjugated secondary antibodies (1:5000; Amersham) were detected by chemiluminesence.

References

Barker, N., van Es, J.H., Kuipers, J., Kujala, P., van den Born, M., Cozijnsen, M., Haegebarth, A., Korving, J., Begthel, H., Peters, P.J. et al. 2007. Identification of stem cells in small intestine and colon by marker gene Lgr5. *Nature* **449**(7165): 1003-1007.

Benhamouche, S., Curto, M., Saotome, I., Gladden, A.B., Liu, C.H., Giovannini, M., and McClatchey, A.I. 2010. Nf2/Merlin controls progenitor homeostasis and tumorigenesis in the liver. *Genes Dev* **24**(16): 1718-1730.

Bossinger, O., Klebes, A., Segbert, C., Theres, C., and Knust, E. 2001. Zonula adherens formation in Caenorhabditis elegans requires dlg-1, the homologue of the Drosophila gene discs large. *Dev Biol* **230**(1): 29-42.

Casaletto, J.B., Saotome, I., Curto, M., and McClatchey, A.I. 2011. Ezrin-mediated apical integrity is required for intestinal homeostasis. *Proc Natl Acad Sci U S A* **108**(29): 11924-11929.

Cavey, M., Rauzi, M., Lenne, P.F., and Lecuit, T. 2008. A two-tiered mechanism for stabilization and immobilization of E-cadherin. *Nature* **453**(7196): 751-756.

Cole, B.K., Curto, M., Chan, A.W., and McClatchey, A.I. 2008. Localization to the cortical cytoskeleton is necessary for Nf2/merlin-dependent epidermal growth factor receptor silencing. *Mol Cell Biol* **28**(4): 1274-1284.

Curto, M., Cole, B.K., Lallemand, D., Liu, C.H., and McClatchey, A.I. 2007. Contact-dependent inhibition of EGFR signaling by Nf2/Merlin. *J Cell Biol* **177**(5): 893-903.

Giovannini, M., Robanus-Maandag, E., van der Valk, M., Niwa-Kawakita, M., Abramowski, V., Goutebroze, L., Woodruff, J.M., Berns, A., and Thomas, G. 2000. Conditional biallelic Nf2 mutation in the mouse promotes manifestations of human neurofibromatosis type 2. *Genes Dev* **14**(13): 1617-1630.

Gladden, A.B., Hebert, A.M., Schneeberger, E.E., and McClatchey, A.I. 2010. The NF2 tumor suppressor, Merlin, regulates epidermal development through the establishment of a junctional polarity complex. *Dev Cell* **19**(5): 727-739.

Gobel, V., Barrett, P.L., Hall, D.H., and Fleming, J.T. 2004. Lumen morphogenesis in C. elegans requires the membrane-cytoskeleton linker erm-1. *Dev Cell* **6**(6): 865-873.

Gonzalez-Agosti, C., Wiederhold, T., Herndon, M.E., Gusella, J., and Ramesh, V. 1999. Interdomain interaction of merlin isoforms and its influence on intermolecular binding to NHE-RF. *J Biol Chem* **274**(48): 34438-34442.

Gronholm, M., Sainio, M., Zhao, F., Heiska, L., Vaheri, A., and Carpen, O. 1999. Homotypic and heterotypic interaction of the neurofibromatosis 2 tumor suppressor protein merlin and the ERM protein ezrin. *J Cell Sci* **112 (Pt 6)**: 895-904.

Hughes, S.C. and Fehon, R.G. 2006. Phosphorylation and activity of the tumor suppressor Merlin and the ERM protein Moesin are coordinately regulated by the Slik kinase. *J Cell Biol* **175**(2): 305-313.

Jankovics, F., Sinka, R., Lukacsovich, T., and Erdelyi, M. 2002. MOESIN crosslinks actin and cell membrane in Drosophila oocytes and is required for OSKAR anchoring. *Curr Biol* **12**(23): 2060-2065.

Lallemand, D., Curto, M., Saotome, I., Giovannini, M., and McClatchey, A.I. 2003. NF2 deficiency promotes tumorigenesis and metastasis by destabilizing adherens junctions. *Genes Dev* **17**(9): 1090-1100.

Lamprecht, G. and Seidler, U. 2006. The emerging role of PDZ adapter proteins for regulation of intestinal ion transport. *Am J Physiol Gastrointest Liver Physiol* **291**(5): G766-777.

Lu, B., Roegiers, F., Jan, L.Y., and Jan, Y.N. 2001. Adherens junctions inhibit asymmetric division in the Drosophila epithelium. *Nature* **409**(6819): 522-525.

Maitra, S., Kulikauskas, R.M., Gavilan, H., and Fehon, R.G. 2006. The tumor suppressors Merlin and Expanded function cooperatively to modulate receptor endocytosis and signaling. *Curr Biol* **16**(7): 702-709.

Makarova, O., Roh, M.H., Liu, C.J., Laurinec, S., and Margolis, B. 2003. Mammalian Crumbs3 is a small transmembrane protein linked to protein associated with Lin-7 (Pals1). *Gene* **302**(1-2): 21-29.

McClatchey, A.I., Saotome, I., Mercer, K., Crowley, D., Gusella, J.F., Bronson, R.T., and Jacks, T. 1998. Mice heterozygous for a mutation at the Nf2 tumor suppressor locus develop a range of highly metastatic tumors. *Genes Dev* **12**(8): 1121-1133.

McLaughlin, M.E., Kruger, G.M., Slocum, K.L., Crowley, D., Michaud, N.A., Huang, J., Magendantz, M., and Jacks, T. 2007. The Nf2 tumor suppressor regulates cell-cell adhesion during tissue fusion. *Proc Natl Acad Sci U S A* **104**(9): 3261-3266.

Meng, J.J., Lowrie, D.J., Sun, H., Dorsey, E., Pelton, P.D., Bashour, A.M., Groden, J., Ratner, N., and Ip, W. 2000. Interaction between two isoforms of the NF2 tumor suppressor protein, merlin, and between merlin and ezrin, suggests modulation of ERM proteins by merlin. *J Neurosci Res* **62**(4): 491-502.

Miller, K.G. 2003. A role for moesin in polarity. *Trends Cell Biol* **13**(4): 165-168.

Morin, X. and Bellaiche, Y. 2011. Mitotic spindle orientation in asymmetric and symmetric cell divisions during animal development. *Dev Cell* **21**(1): 102-119.

Morris, Z.S. and McClatchey, A.I. 2009. Aberrant epithelial morphology and persistent epidermal growth factor receptor signaling in a mouse model of renal carcinoma. *Proc Natl Acad Sci U S A* **106**(24): 9767-9772.

Reczek, D. and Bretscher, A. 1998. The carboxyl-terminal region of EBP50 binds to a site in the amino-terminal domain of ezrin that is masked in the dormant molecule. *J Biol Chem* **273**(29): 18452-18458.

Saotome, I., Curto, M., and McClatchey, A.I. 2004. Ezrin is essential for epithelial organization and villus morphogenesis in the developing intestine. *Dev Cell* **6**(6): 855-864.

Sato, T., Vries, R.G., Snippert, H.J., van de Wetering, M., Barker, N., Stange, D.E., van Es, J.H., Abo, A., Kujala, P., Peters, P.J. et al. 2009. Single Lgr5 stem cells build crypt-villus structures in vitro without a mesenchymal niche. *Nature* **459**(7244): 262-265.

Scheving, L.A., Shiurba, R.A., Nguyen, T.D., and Gray, G.M. 1989. Epidermal growth factor receptor of the intestinal enterocyte. Localization to laterobasal but not brush border membrane. *J Biol Chem* **264**(3): 1735-1741.

Speck, O., Hughes, S.C., Noren, N.K., Kulikauskas, R.M., and Fehon, R.G. 2003. Moesin functions antagonistically to the Rho pathway to maintain epithelial integrity. *Nature* **421**(6918): 83-87.

Turunen, O., Wahlstrom, T., and Vaheri, A. 1994. Ezrin has a COOH-terminal actin-binding site that is conserved in the ezrin protein family. *J Cell Biol* **126**(6): 1445-1453.

Van Furden, D., Johnson, K., Segbert, C., and Bossinger, O. 2004. The C. elegans ezrin-radixin-moesin protein ERM-1 is necessary for apical junction remodelling and tubulogenesis in the intestine. *Dev Biol* **272**(1): 262-276.

Wiley, L.A., Dattilo, L.K., Kang, K.B., Giovannini, M., and Beebe, D.C. 2010. The tumor suppressor merlin is required for cell cycle exit, terminal differentiation, and cell polarity in the developing murine lens. *Invest Ophthalmol Vis Sci* **51**(7): 3611-3618.

Yamashita, Y.M., Yuan, H., Cheng, J., and Hunt, A.J. 2010. Polarity in stem cell division: asymmetric stem cell division in tissue homeostasis. *Cold Spring Harb Perspect Biol* **2**(1): a001313.

Chapter 4

Coordinating Merlin and ERM function at the membrane

Alan M. Hebert[1] and Andrea I. McClatchey[1]

[1]Massachusetts General Hospital Center for Cancer Research and
Harvard Medical School Department of Pathology
149 13th St. Charlestown, MA 02129

Publications and Contributions: All figures in this chapter were contributed by A. M. Hebert.

Abstract

Our studies of CaCo2 cells in Chapter 2 highlight the dynamic and interdependent localization of Merlin and the ERMs across the cell cycle. Recent evidence in *Drosophila* suggests that Merlin and the ERM proteins may be coordinately regulated by the Ste20-like kinase Slik (SLK in the mouse), suggesting a mechanism by which Merlin and ERM activities could be coordinated to organize the membrane. To date, it is not known whether Merlin and the ERMs are coordinately regulated in mammalian cells or whether mammalian SLK has any role in regulating their activity. Here, we show for the first time that SLK can induce phosphorylation of all three ERM proteins in mammalian cells; however, in the cells/conditions that we examined, SLK was sufficient but not necessary for ERM phosphorylation. It is less clear if or how SLK might control Merlin activity and the most important challenge will be to identify a context where SLK, or another kinase, might be required for coordinating Merlin and ERM activity.

Introduction

As dynamic organizers of the cell cortex, Merlin and the ERM proteins must be highly regulated. Numerous studies highlight phosphorylation as a critical modification for controlling Merlin and the ERM activity. In mammals, phosphorylation of the ERM proteins at the C-terminus (EzT567, RadT564, MoeT558) weakens self-association and leads to translocation to the membrane:cytoskeleton interface (Bretscher et al. 2002; Fehon et al. 2010). This phosphorylated, presumably open, conformation is often referred to as the 'active' ERM form. Indeed, a number of kinases in vertebrate cells can phosphorylate the ERMs on this regulatory threonine, including Rho Kinase, PKCα, PKCΘ, NIK, Mst4 and LOK (Matsui et al. 1998; Simons et al. 1998; Ng et al. 2001; Belkina et al. 2009; ten Klooster et al. 2009). Phosphorylation of other sites can also contribute to ERM activation. For example, CDK5 can phosphorylate Ezrin on threonine 235, which lies on the interface between the FERM domain and C-ERMAD interface directly apposed to T567 (Pearson et al. 2000; Yang and Hinds 2003). Ezrin can also be phosphorylated on tyrosine residues 145 and 353 by various tyrosine kinases, including EGFR (Krieg and Hunter 1992), but it is unclear how these modifications might tune Ezrin conformation or function.

For Merlin, studies in mammalian cells indicate that the hypo-phosphorylated version is active in terms of inhibiting proliferation (Sherman et al. 1997; Shaw et al. 1998; Gutmann et al. 1999; Morrison et al. 2001). In mammals, serine 518 of Merlin is phosphorylated downstream of Rac activity (Shaw et al. 2001) by the p21-activated kinase (PAK) (Kissil et al. 2002; Xiao et al. 2002).

Although Merlin is phosphorylated on multiple residues, phosphorylation of S518 causes a mobility shift and has therefore been the best studied. However, the C-terminal threonine residue that is analogous to the major ERM regulatory residue (T567) is conserved in both mammalian and fly Merlin. Therefore, the consequences of phosphorylating this residue, which have not been examined, may be critical for Merlin's function.

It is clear that phosphorylation-mediated regulation of Merlin and the ERMs is complex and studies in flies have helped us to better understand this process. Recent evidence indicates that *D. melanogaster* Slik can regulate both Merlin and the ERM proteins thereby potentially providing coordinate control (Hughes and Fehon 2006). Slik is necessary for the C-terminal phosphorylation of the sole ERM protein Moesin, although it is unclear whether Slik phosphorylates Moesin directly or via an intermediate kinase (Hipfner et al. 2004). Phosphorylation of this residue in Merlin has not been directly shown; however, a recent study demonstrated that Slik controls the subcellular localization and overall phosphorylation of Merlin, suggesting that phosphorylation of this residue could be important in regulating Merlin activity (Hughes and Fehon 2006).

The discovery of coordinate regulation of Merlin and ERM activity is particularly interesting given our discovery that Merlin is necessary for positioning cortical Ezrin in single cells and 3D organotypic cultures (Chapter 2). Coordinated phosphorylation of Merlin and Ezrin by a single upstream kinase could explain their dynamic cortical localization and activity in mammalian cells. In this regard, the suggestion that Merlin and Moesin compete for Slik activity in the fly (Hughes and

Fehon 2006) suggests a mechanism by which Merlin and Ezrin could be dynamically controlled across the membrane. To date little is known about how Slik functions in flies or mammals (SLK). Studies indicate that Slik promotes cell proliferation and controls survival. However, it is unknown whether mammalian SLK can regulate Merlin and/or the ERM proteins. Determining whether a single protein can coordinate Merlin and ERM protein function in a mammalian system would be an important step for understanding their complex relationship and provide clues for understanding how dysregulation of these proteins contribute to cancer and tumor progression in humans. Therefore, we set out to determine whether SLK coordinately regulates Merlin and the ERM proteins in mammalian cells.

Results

Cloning the Ste20-like kinase SLK

Murine SLK (SLK) was previously cloned by two separate laboratories that identified the two known isoforms of SLK (Pytowski et al. 1998; Sabourin and Rudnicki 1999). The long isoform (isoform 1) is 1233aa in length while the short isoform (isoform 2) lacks a 31aa stretch near the C-terminus and is 1202aa in length (Figure 4.1A). We initially cloned SLK from an osteoblast cDNA pool (generated by Jennifer Gervais). Sequence analysis indicated that this clone represents a unique isoform (referred to here as isoform 3), which is identical to isoform 2 with an additional stretch of 24aa missing near the C-terminus (Figure 4.1A). However, we did not detect this expression of this isoform in any of our adult mouse tissues indicating it may be specific to osteoblasts (Figure 4.1B)

It has been reported that SLK is ubiquitously expressed during all stages of murine development and in all examined adult tissues. However, it is not clear whether the known isoforms of SLK display any tissue specificity or if any are predominantly expressed. To address this we designed primers flanking the region of SLK that encompass the alternative splice sites (Figure 4.1A arrows). PCR analysis of tissue specific cDNA pools demonstrates that isoforms 1 and 2 were co-expressed in many tissues and demonstrated some tissue specificity where isoform 2 was more predominant (Figure 4.1B). In addition, the vast majority of the literature has focused on isoform 2. Therefore, we cloned isoform 2 of SLK from our mouse ovary cDNA pool and used it for the following experiments.

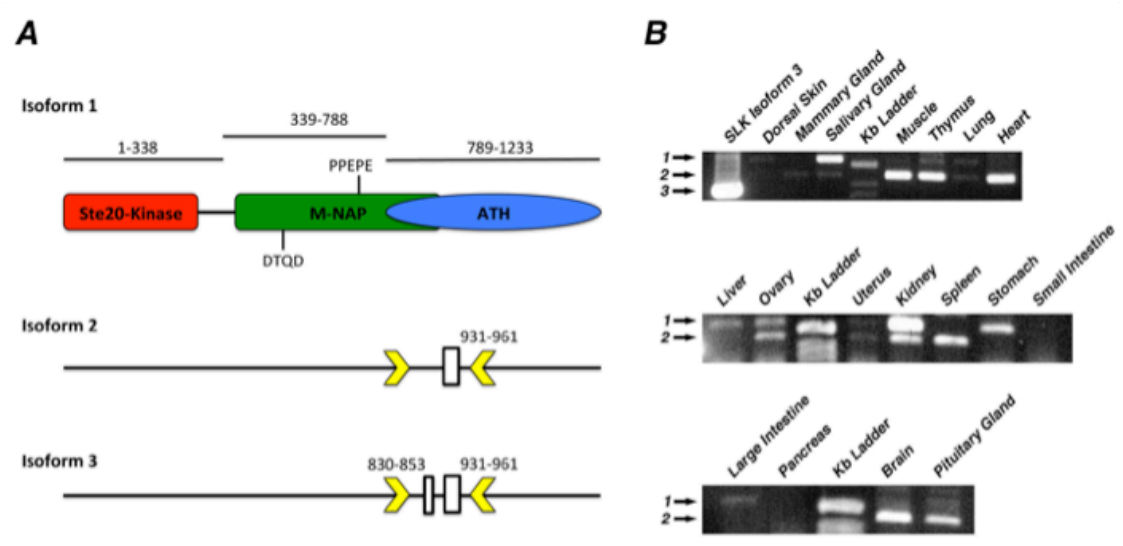

Figure 4.1 SLK isoforms and their tissue specific expression. **(A)** Schematic representation of SLK and homologous domains to other proteins (colored boxes and oval). The catalytic domain (red) is most similar to LOK and MST1/2, two Ste20-related kinases. SLK is highly homologous to the microtubule and nuclear associated protein, M-NAP (green) and to a protein of unknown function AT1-46 (blue oval) in the C-terminus. The SLK caspase 3 consensus cleavage site (DTQD), and a putative SH3 binding domain (PPEPE) are shown. Numbers above the different domains denote the amino acid residues representing the boundaries. White boxes in isoform 2 and 3 represent streatches of amino acids not present in the respective isoforms. Yellow arrows denote the location of primers designed to distinguish each isoform. **(B)** Detection of SLK isoforms form mouse specific cDNA pools. SLK isoform 3 was cloned from *p53* deficient osteoblasts and was not detected in any of our mouse tissues. Isoforms 1 and 2 display tissue specificity but are also co-expressed in many tissue types. PCR products were run on a 1.5% agarose gel and stained with ethidium bromide.

SLK is sufficient but not necessary to induce ERM phosphorylation

It has been shown in *D. melanogaster* that Slik (the fly homolog of SLK) associates with and induces phosphorylation of the sole ERM protein Moesin at residue T559 (Hipfner et al. 2004; Hughes and Fehon 2006). However, it is not known whether SLK regulates any or all of the ERM proteins in mammalian cells. To test this we over-expressed SLK in a variety of cell types and assayed for phosphorylation of the C-terminal threonine of ERM proteins by Western blot. We demonstrated that SLK overexpression leads to an increase in phosphorylation of all three ERMs in epithelial liver derived cells (LDCs), NIH3T3 cells and HEK293T cells indicating that SLK is sufficient to phosphorylate all three ERMs in different mammalian cell types (Figure 4.2A).

We observe a basal level of ERM phosphorylation (Figure 4.2A) in cells grown in 2D culture. Indeed, there are a number of kinases reported to phosphorylate this residue (Matsui et al. 1998; Simons et al. 1998; Ng et al. 2001; Belkina et al. 2009; ten Klooster et al. 2009) and it is not known which might be the principal kinase that maintains ERM phosphorylation in these cells. To determine whether SLK is required for ERM phosphorylation we eliminated SLK expression using two independent short hairpins. We observed no change in phosphorylation of the ERMs in LDCs (Figure 4.2B), NIH 3T3, or HEK293T cells in the presence or absence of serum (not shown) indicating that SLK is not required for activation of the ERMs in the context of 2D cell culture in these cell types.

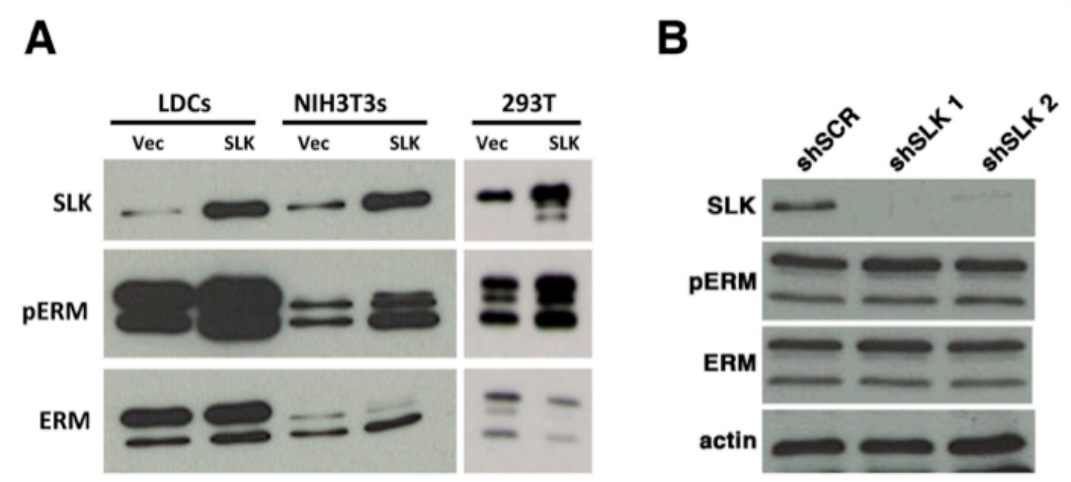

Figure 4.2 Mouse SLK is sufficient but not necessary to induce phosphorylation of the ERM proteins. **(A)** When SLK is overexpressed in three different cell types in 2D culture (LDCs, NIH3T3s and 293T cells) we observe an increase in phosphorylation of all three ERMs. **(B)** Upon targeting mouse SLK with two independent short hairpins we demonstrate a robust decrease in SLK expression but no change in ERM phosphorylation in LDCs.

A phosphomimetic (T577D) mutation alters Merlin localization to the insoluble membrane compartment

In contrast to ERMs, the majority of studies on Merlin regulation and activation have focused on the phosphorylation of serine 518, which is thought to modulate Merlin intramolecular association and binding to effectors (Shaw et al. 2001; Kissil et al. 2002; Rong et al. 2004; Jung et al. 2005). This is despite the fact that the best-studied phosphorylation site on the ERMs (T567) is conserved in Merlin. Indeed, SLK is predicted to phosphorylate mouse Merlin on its conserved C-terminal threonine (T577) residue.

In *D. melanogaster*, Merlin localization to the membrane is decreased upon deleting Slik and over-expressing Slik induces phosphorylation of the C-terminal threonine residue (T616) (Hughes and Fehon 2006). We were unable to detect changes in total Merlin localization by immunofluorescence upon loss of SLK expression (not shown). Since phospho-specific antibodies are not available for detecting Merlin T577, we expressed ectopic wild type, a phosphomimetic (T577D) and a nonphosphorylatable (T577A) version of Merlin in *Nf2* deficient LDCs and assayed Merlin localization by biochemical fractionation. We found that substantial pools of wild-type and T577D Merlin are present in both the soluble and insoluble membrane compartments. In contrast, although well represented in the soluble membrane, Nf2 T577A is greatly diminished from the Triton X-100-insoluble membrane compartment (Figure 4.3A). These data suggest that phosphorylation of this residue could alter Merlin localization. However, knockdown of SLK did not prevent Merlin from localizing to the Triton X-100-insoluble membrane

compartment (Figure 4.3B). This suggests that, as for the ERMs, SLK might not be required for basal levels of Merlin T577 phosphorylation. Notably, studies in the fly demonstrated that Slik over-expression induces phosphorylation of the C-terminal threonine on Merlin (T616) but did not report whether deleting Slik had any effect on Merlin phosphorylation (Hughes and Fehon 2006).

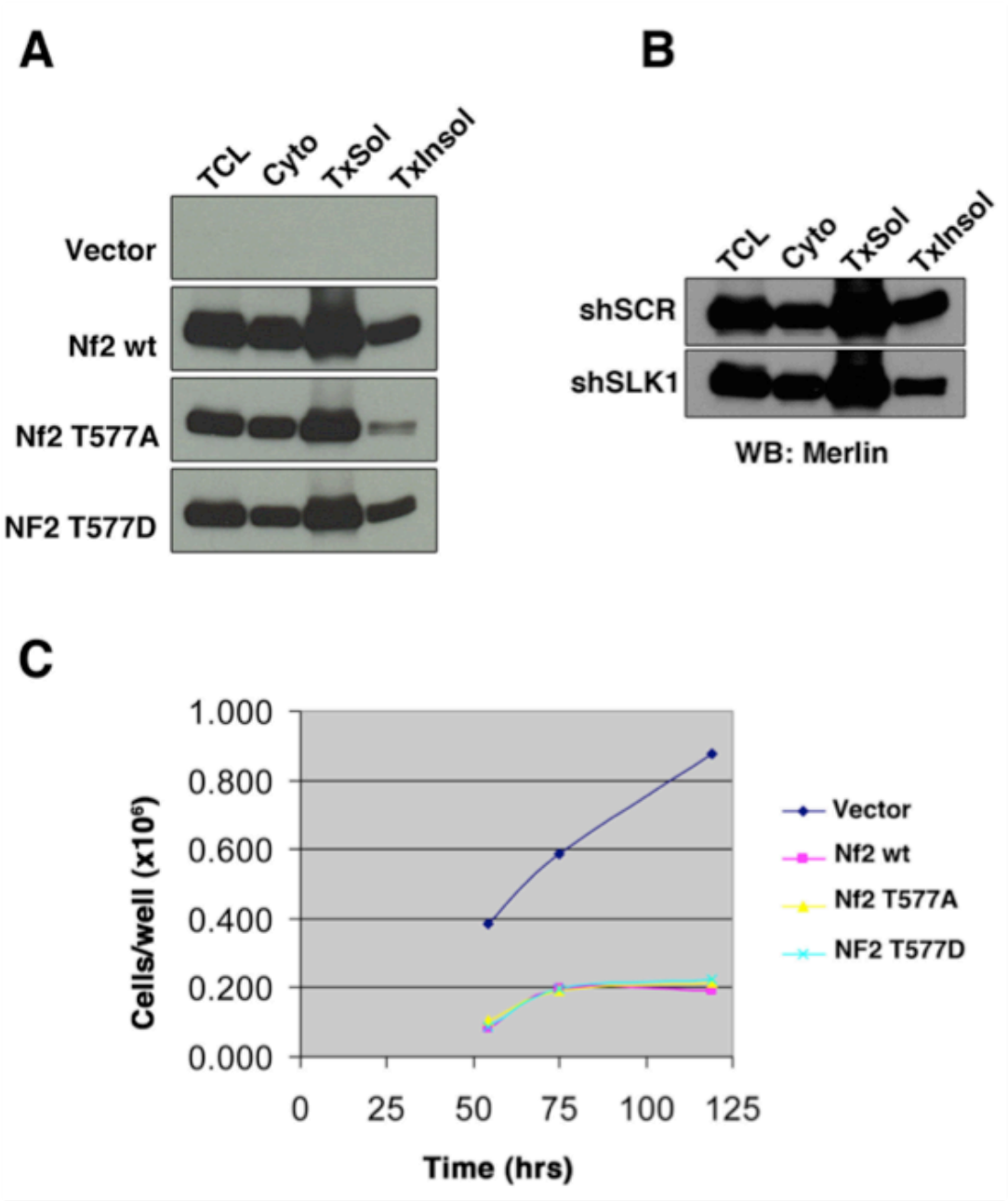

Figure 4.3 Phosphorylation of T577 on Merlin affects subcellular localization but not contact dependent inhibition of proliferation. **(A)** *Nf2* deficient LDCs were infected with vector control, *Nf2* wild type, *Nf2* T577A and *Nf2* T577D. After three days cells were biochemically fractionated revealing that the nonphosphorylatable Merlin T577A is less enriched in the Triton X-100-insoluble fraction. **(B)** Wild type *Nf2* was exogenously expressed in *Nf2* deficient LDCs. Targeted knockdown of SLK by expression of shSLK1 had no clear effect on Merlin solubility. **(C)** Expressing *Nf2* wild type, *Nf2* T577A or *Nf2* T577D in *Nf2* deficient LDCs was able to confer contact dependent inhibition of proliferation compared to control.

Next, we tested whether the T577A or T577D mutant versions of Merlin could alter the ability of Merlin to inhibit cell proliferation. Specifically, we tested whether wild type or T577A and T577D Merlin mutants could rescue contact dependent inhibition of proliferation in *Nf2* deficient LDCs. Growth curves indicate that T577 phosphorylation does not affect Merlin activity in this setting as both T577D and T577A confer contact dependent inhibition of proliferation, at least when overexpressed (Figure 4.3C). Indeed, we observed some Merlin T577A in the Triton X-100-insoluble membrane compartment (Figure 4.3A) indicating that expressing T577A Merlin above physiological levels may mask potential phenotypic consequences of Merlin T577 phosphorylation at physiological levels.

SLK is not necessary for cortical Merlin/ERM localization in developing CaCo2 cysts

We have shown in 2D cell culture that SLK expression is sufficient to induce phosphorylation of all three ERM proteins in mammalian cells; however, SLK is not required for ERM phosphorylation (or Merlin regulation) under basal conditions in these cell types. Interestingly, SLK seems to have an important role in developing tissues and perhaps in developing epithelia. For example, SLK is expressed throughout the developing mouse embryo (Sabourin and Rudnicki 1999), and its expression and activity are increased during kidney development (Cybulsky et al.). Therefore, we asked whether SLK was critical for the regulation of ERMs in the context of epithelial cyst development using CaCo2 cells in 3D culture (described in

Chapter 2). Upon loss of SLK expression in single CaCo2 cells Ezrin cap formation proceeded normally and single cells developed into normal cyst structures with a single lumen (Figure 4.4) suggesting that SLK is not required for ERM regulation in this context. Since Merlin itself is required for cap formation this also suggests that SLK does not have a significant impact on Merlin activity in these cells or in this assay.

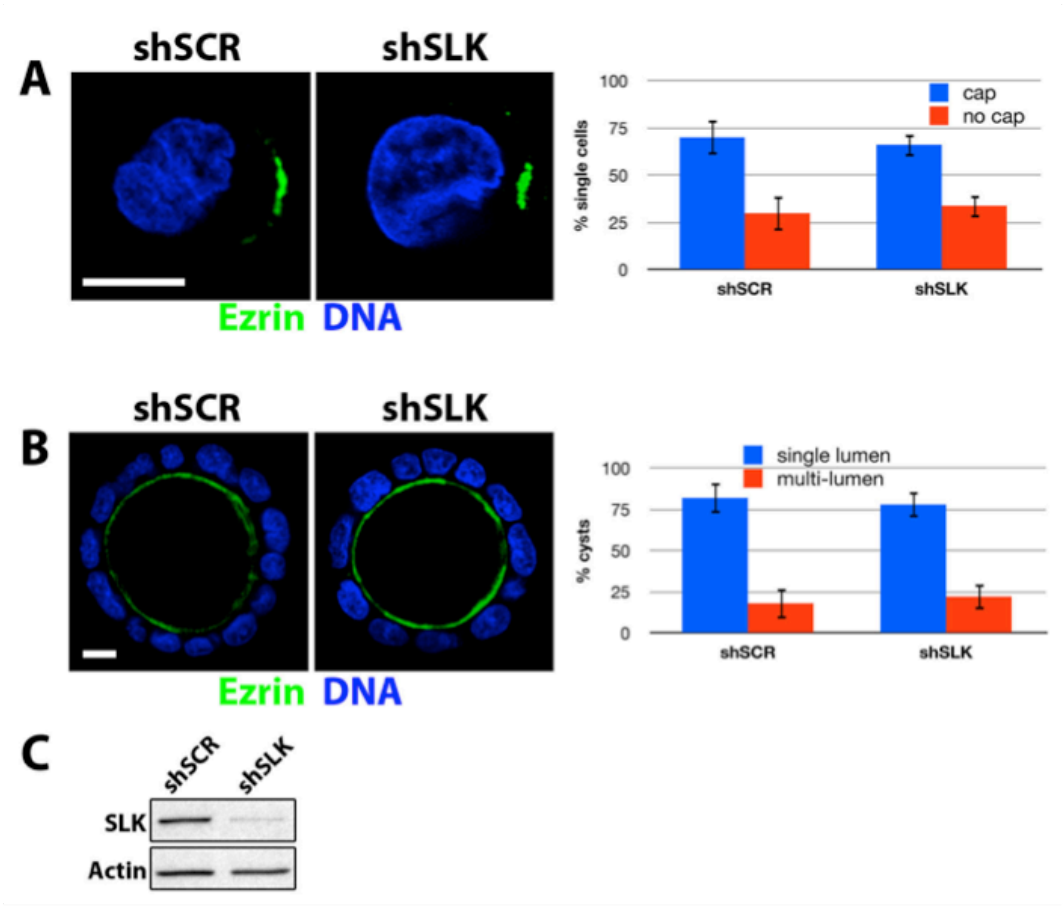

Figure 4.4 SLK is not required for Ezrin cap formation or cyst morphogenesis in 3D culture. **(A)** Single CaCo2 cells in 3D matrigel culture expressing shSLK form normal Ezrin caps (left) which are quantified (right). **(B)** Single CaCo2 cells in 3D matrigel culture expressing shSLK develop into normal cysts with a single lumen (left) which are quantified (right) **(C)** Western blot of SLK demonstrating robust knockdown in shSLK expressing CaCo2 cells. Bars 10μm.

Discussion

My studies of CaCo2 cells (Chapter 2) reveal the striking dynamic and interdependent localization of Merlin and the ERMs across the cell cycle. This raises the fascinating question of how these localization changes are coordinated. One interesting possibility is that the regulation of Merlin and the ERMs during this process is coordinated. Interestingly, in *D. melanogaster*, Slik has been reported to induce phosphorylation of Merlin and the sole ERM ortholog Moesin suggesting a mechanism by which they could be coordinately regulated (Hipfner and Cohen 2003; Speck et al. 2003; Hughes and Fehon 2006; Martin-Belmonte et al. 2008). In mammals, SLK is predicted to phosphorylate Merlin on residue T577 and little is known about how modification of this residue may regulate Merlin function.

Our studies show that SLK is not essential for regulating Merlin or the ERMs in the cell types and contexts we tested. However, SLK can induce phosphorylation of the ERM proteins, indicating that there are likely to be unidentified contexts where SLK activity is essential for ERM and perhaps Merlin activation. To this end we would first need to identify a context where SLK-mediated regulation of Merlin and ERMs is required. Contrary to the oversimplified model that hyperphosphorylated Merlin is thought to be inactive in terms of limiting proliferation, our studies support that phosphorylation of Merlin on T577 is not a critical regulator of proliferation. Therefore, a clearer understanding of the functional consequences of T577 phosphorylation will be beneficial for identifying a context where coordinate regulation of Merlin and the ERMs by SLK might be essential. Alternatively, a number of other kinases that are capable of

phosphorylating Merlin and the ERMs could be responsible for their coordinate regulation.

Studies in flies have shown that C-terminal phosphorylation of Merlin at T616 (analogous to T577 in mammalian Merlin) by SLK affects its sub-cellular localization (Hughes and Fehon 2006). Our biochemical fractionation studies also indicate that modification of this residue on mouse Merlin (T577) affects its distribution within the cell. However, modification of this residue does not seem to affect the ability of Merlin to mediate contact dependent inhibition of cell proliferation. Importantly, the CaCo2 studies described in Chapter 2 clearly show proliferation independent effects of Merlin deficient cells. The role of T577 phosphorylation is not yet clear but highlights the notion that Merlin is phosphorylated on multiple residues. Therefore, Merlin phosphorylation is clearly not a simple "active" vs. "inactive" regulatory step. Rather, there are likely to be multiple Merlin functions that may be regulated independently. In that regard, it will be interesting to determine whether T577A/D mutants can rescue the Ezrin cap formation in Merlin deficient CaCo2 cells in 3D.

While SLK is not required in CaCo2 cells for the dynamic localization of Ezrin throughout epithelial morphogenesis in 3D cultures (Figure 4.4), we have found that the cyclin dependent kinase CDK5 is (Figure 2.3E). It is interesting to note that residue T235 on Ezrin, which is directly phosphorylated by CDK5, is also conserved in Merlin (T251). In addition, the T251 residue in the N-terminal FERM domain is directly apposed to the T577 and not the S518 residue of Merlin and would be predicted to have the same effect on (to weaken) self-association (Pearson et al.

2000; Yang and Hinds 2003). This suggests that phosphorylation of T251 on Merlin by CDK5 may be equivalent to T577 phosphorylation, which we have shown is not critical for Merlin's role in controlling proliferation. Rather, phosphorylation of residue T251 could be important for Merlin's proliferation-independent function to position Ezrin and orient the centrosome and mitotic spindle. Therefore, we hypothesize that the dynamic localization of Ezrin in single CaCo2 cells relies on coordinate regulation of the Merlin and Ezrin FERM domains by CDK5. In this regard, it will be important to test whether CDK5 can directly regulate Merlin and to determine whether CDK5 mediated phosphorylation of Merlin is important for its ability to restrict cortical Ezrin. Finally, if we identify a context where CDK5 or SLK can coordinately regulate Merlin and the ERMs it will be equally important to elucidate how CDK5 or SLK are themselves regulated and how their activities may coordinate with the cell cycle.

Materials and Methods

Cell Culture

Mouse *Nf2* deficient liver derived epithelial cells (LDCs) generated as previously described (Lallemand et al. 2003; Curto et al. 2007), NIH3T3, HEK293T, and Human Caco2 cells (the $Caco2_{BBe}$ subclone was used throughout; a gift from Wayne Lencer, Children's Hospital, Boston) were cultured in DMEM 10% fetal bovine serum (FBS) with P/S. For serum starvation, cells were rinsed 1x with PBS before adding serum free DMEM with P/S.

All 3D cell culture experiments were performed as described in Chapter 2. Briefly, single CaCo2 control cells or SLK deficient cells were suspended in matrigel and cultured for 14 hours (single cell analysis) or 6 days (cyst analysis). Cells were stained for Ezrin and visualized using an LSM510 confocal microscope to assess Ezrin cap formation and cyst morphogenesis. Phenotypes were quantified and representative images for each condition were taken.

cDNA Pool Generation and PCR Detection of SLK Isoforms

Individual tissues from wild type FVB mice were isolated and snap frozen in liquid N_2 and homogenized in Trizol before adding chloroform (0.2 mL per 1mL Trizol). The aqueous phase was isolated by centrifugation at 12,000*g* and 0.5mL of isopropanol was added per 1mL trizol incubated for 10min at RT and stored at -80°C. To make cDNA, samples were thawed on ice and spun at 10k RPM in a microfuge for 10 min at 4°C. The supernatant was removed and washed with 1mL

cold 75% Ethanol and spun at 7k RPM for 5 min at 4°C. The remaining Ethanol was removed and pellet was resuspended in between 20µl and 100µl sterile ddH_2O. RNA concentration was determined by measuring OD_{260} and 5µg RNA was used for the reverse transcription M-MLV RT reaction (Promega). For PCR detection of different isoforms, 25µM of each the forward and reverse primer were used with 1µl of cDNA and 1µl Taq polymerase (Invitrogen) in a 20µl reaction volume. The PCR reaction was performed with a T_m of 60°C and an extension time of 1 minute for 30 cycles. GAPDH was used as a control for cDNA quality.

Biochemical Cell Fractionation

Cells were lysed by mechanical disruption in cold hypotonic buffer (10 mM HEPES at pH 7.4, 1 mM EDTA, and protease inhibitors). Nuclei were pelleted by centrifugation at 750*g* for 10 min. Further centrifugation of the resulting supernatant at $1\times10^5 g$ for 1 h led to recovery of the cytosolic fraction (Cyto). The pellet was extracted with membrane extraction buffer (MEB; 50 mM Tris at pH 7.4, 1% Triton X-100, 150 mM NaCl, 1 mM EDTA, 1 mM Na_3VO_4, and protease inhibitors) and centrifuged at $1\times10^5 g$ for 1 h. This supernatant corresponded to the Triton X-100 soluble membrane extract (TxSol). The final pellet was extracted with modified RIPA buffer and centrifuged at $1\times10^5 g$ for 5 min; this supernatant corresponded to the Triton X-100 insoluble fraction (TxInsol). Equal quantities of protein were separated by SDS-PAGE, transferred to nitrocellulose membrane, and probed at 4°C overnight in PBS, 0.05% Tween-20, and 5% nonfat dry milk or 1% BSA for phospho-specific antibodies.

Antibodies and Constructs

Primary antibodies for immunofluorescence (IF) and/or western blotting (WB) were from: Santa Cruz Biotechnology (NF2 sc332 1:1000 for WB), Cell Signaling Technology (phospho-ERM 3141 1:1000 for WB; ERM 3142 1:1000 for WB), Bethyl (SLK BL1917 1:500 for WB) and Sigma (Actin A3853 1:2000 for WB).

Full length SLK was cloned from our mouse ovary cDNA pool using the primers corresponding to the N and C-terminus of mouse SLK. Sequence analysis confirmed our construct was isoform 2 of SLK, which was subcloned into our lentiviral pBOB vector. Mouse Nf2 mutants (T577A and T577D) were generated using site directed mutagenesis (Invitrogen) and subcloned into our lentiviral pBOB vector.

Western blotting

Cells were lysed using RIPA lysis buffer (50 mM Tris [pH 7.4], 1% Triton X-100, 1% SDS, 0.5% sodium deoxycholate, 150 mM NaCl, 1 mM EDTA, 1 mM EGTA, 1 mM PMSF, 1 mM Na_3VO_4, 10 mM sodium fluoride, 10 mM β-glycerophosphate, 1 mg/ml aprotinin and 1 mg/ml leupeptin) followed by brief sonication. Cell debris was cleared by centrifugation (14,000 rpm, 10 min, 4°C) and lysates were quantitated by DC protein assay (Bio-Rad), separated by SDS-PAGE, transferred to PVDF. Membranes were blocked in 5% milk, incubated with primary antibody for 1hr at RT or overnight at 4°C in 1% milk and then with anti-mouse or anti-rabbit horseradish peroxidase-conjugated secondary antibodies (1:5000; Amersham).

Growth Curves

For cell growth curves, 4×10^4 *Nf2* deficient LDCs were infected with empty vector, Nf2 wild type, Nf2 T577A or Nf2 T577D and seeded in triplicate in 15-mm wells in DMEM + 10% FBS. Beginning day 2 (48 hrs post plating), cells were trypsinized and counted on day 3 and day 5. Experiments were repeated at least three times.

shRNA

Five lentiviral short hairpin RNA (shRNA) constructs targeting human *SLK* and five targeting mouse SLK were purchased from Open Biosystems. We determined knockdown efficiency by WB and constructs that most efficiently targeted protein expression were utilized. The following short hairpin clones were used throughout our experiments: hSLK (TRCN0000000895), mSLK1 (TRCN0000025271) and mSLK2 (TRCN0000025272).

Lentivirus production

Lentiviruses expressing shRNAs were generated by co-transfecting 293T cells with shRNA constructs together with the packaging vectors ΔVPR and VSVG (Fugene). Lentiviruses derived from pBOB constructs were generated similarly using the packaging vectors psPAX and pMD2.G (Fugene). Lentiviral supernatants were collected 5X over a period of 48 hr, filtered (0.22 μm), aliquotted and frozen at -80°C. For infection, cells were trypsinized, resuspended in 6 ml of lentiviral supernatant and cultured for 24 hr. Cells were then transferred to fresh medium containing 7μg/ml puromycin (but not for

pBOB infected cells) for 48 hr and plated. Cells expressing short hairpins targeting SLK, protein constructs or control vectors were subject to WB analysis to monitor protein levels in each experiment.

Statistics

For 3D culture experiments, data from at least three independent experiments were pooled and expressed as mean ± SEM. Values were compared by 2-tailed Student's *t*-test, with statistical significance of *$p<0.05$ or **$p<0.01$ indicated. For LDC growth curves representative data from three independent experiments is shown.

References

Belkina, N.V., Liu, Y., Hao, J.J., Karasuyama, H., and Shaw, S. 2009. LOK is a major ERM kinase in resting lymphocytes and regulates cytoskeletal rearrangement through ERM phosphorylation. *Proc Natl Acad Sci U S A* **106**(12): 4707-4712.

Bretscher, A., Edwards, K., and Fehon, R.G. 2002. ERM proteins and merlin: integrators at the cell cortex. *Nat Rev Mol Cell Biol* **3**(8): 586-599.

Curto, M., Cole, B.K., Lallemand, D., Liu, C.H., and McClatchey, A.I. 2007. Contact-dependent inhibition of EGFR signaling by Nf2/Merlin. *J Cell Biol* **177**(5): 893-903.

Cybulsky, A.V., Takano, T., Papillon, J., Guillemette, J., Herzenberg, A.M., and Kennedy, C.R. Podocyte injury and albuminuria in mice with podocyte-specific overexpression of the Ste20-like kinase, SLK. *Am J Pathol* **177**(5): 2290-2299.

Fehon, R.G., McClatchey, A.I., and Bretscher, A. 2010. Organizing the cell cortex: the role of ERM proteins. *Nat Rev Mol Cell Biol* **11**(4): 276-287.

Gutmann, D.H., Haipek, C.A., and Hoang Lu, K. 1999. Neurofibromatosis 2 tumor suppressor protein, merlin, forms two functionally important intramolecular associations. *J Neurosci Res* **58**(5): 706-716.

Hipfner, D.R. and Cohen, S.M. 2003. The Drosophila sterile-20 kinase slik controls cell proliferation and apoptosis during imaginal disc development. *PLoS Biol* **1**(2): E35.

Hipfner, D.R., Keller, N., and Cohen, S.M. 2004. Slik Sterile-20 kinase regulates Moesin activity to promote epithelial integrity during tissue growth. *Genes Dev* **18**(18): 2243-2248.

Hughes, S.C. and Fehon, R.G. 2006. Phosphorylation and activity of the tumor suppressor Merlin and the ERM protein Moesin are coordinately regulated by the Slik kinase. *J Cell Biol* **175**(2): 305-313.

Jung, J.R., Kim, H., Jeun, S.S., Lee, J.Y., Koh, E.J., and Ji, C. 2005. The Phosphorylation status of merlin is important for regulating the Ras-ERK pathway. *Mol Cells* **20**(2): 196-200.

Kissil, J.L., Johnson, K.C., Eckman, M.S., and Jacks, T. 2002. Merlin phosphorylation by p21-activated kinase 2 and effects of phosphorylation on merlin localization. *J Biol Chem* **277**(12): 10394-10399.

Krieg, J. and Hunter, T. 1992. Identification of the two major epidermal growth factor-induced tyrosine phosphorylation sites in the microvillar core protein ezrin. *J Biol Chem* **267**(27): 19258-19265.

Lallemand, D., Curto, M., Saotome, I., Giovannini, M., and McClatchey, A.I. 2003. NF2 deficiency promotes tumorigenesis and metastasis by destabilizing adherens junctions. *Genes Dev* **17**(9): 1090-1100.

Martin-Belmonte, F., Yu, W., Rodriguez-Fraticelli, A.E., Ewald, A.J., Werb, Z., Alonso, M.A., and Mostov, K. 2008. Cell-polarity dynamics controls the mechanism of lumen formation in epithelial morphogenesis. *Curr Biol* **18**(7): 507-513.

Matsui, T., Maeda, M., Doi, Y., Yonemura, S., Amano, M., Kaibuchi, K., and Tsukita, S. 1998. Rho-kinase phosphorylates COOH-terminal threonines of ezrin/radixin/moesin (ERM) proteins and regulates their head-to-tail association. *J Cell Biol* **140**(3): 647-657.

Morrison, H., Sherman, L.S., Legg, J., Banine, F., Isacke, C., Haipek, C.A., Gutmann, D.H., Ponta, H., and Herrlich, P. 2001. The NF2 tumor suppressor gene product, merlin, mediates contact inhibition of growth through interactions with CD44. *Genes Dev* **15**(8): 968-980.

Ng, T., Parsons, M., Hughes, W.E., Monypenny, J., Zicha, D., Gautreau, A., Arpin, M., Gschmeissner, S., Verveer, P.J., Bastiaens, P.I. et al. 2001. Ezrin is a downstream effector of trafficking PKC-integrin complexes involved in the control of cell motility. *EMBO J* **20**(11): 2723-2741.

Pearson, M.A., Reczek, D., Bretscher, A., and Karplus, P.A. 2000. Structure of the ERM protein moesin reveals the FERM domain fold masked by an extended actin binding tail domain. *Cell* **101**(3): 259-270.

Pytowski, B., Hicklin, D.J., Kornhaber, G., Dellaratta, D.V., and Witte, L. 1998. Identification and initial characterization of mSLK, a murine member of the STE20 family of kinases. *Arch Biochem Biophys* **359**(2): 310-319.

Rong, R., Surace, E.I., Haipek, C.A., Gutmann, D.H., and Ye, K. 2004. Serine 518 phosphorylation modulates merlin intramolecular association and binding to critical effectors important for NF2 growth suppression. *Oncogene* **23**(52): 8447-8454.

Sabourin, L.A. and Rudnicki, M.A. 1999. Induction of apoptosis by SLK, a Ste20-related kinase. *Oncogene* **18**(52): 7566-7575.

Shaw, R.J., Henry, M., Solomon, F., and Jacks, T. 1998. RhoA-dependent phosphorylation and relocalization of ERM proteins into apical membrane/actin protrusions in fibroblasts. *Mol Biol Cell* **9**(2): 403-419.

Shaw, R.J., Paez, J.G., Curto, M., Yaktine, A., Pruitt, W.M., Saotome, I., O'Bryan, J.P., Gupta, V., Ratner, N., Der, C.J. et al. 2001. The Nf2 tumor suppressor, merlin, functions in Rac-dependent signaling. *Dev Cell* **1**(1): 63-72.

Sherman, L., Xu, H.M., Geist, R.T., Saporito-Irwin, S., Howells, N., Ponta, H., Herrlich, P., and Gutmann, D.H. 1997. Interdomain binding mediates tumor growth suppression by the NF2 gene product. *Oncogene* **15**(20): 2505-2509.

Simons, P.C., Pietromonaco, S.F., Reczek, D., Bretscher, A., and Elias, L. 1998. C-terminal threonine phosphorylation activates ERM proteins to link the cell's cortical lipid bilayer to the cytoskeleton. *Biochem Biophys Res Commun* **253**(3): 561-565.

Speck, O., Hughes, S.C., Noren, N.K., Kulikauskas, R.M., and Fehon, R.G. 2003. Moesin functions antagonistically to the Rho pathway to maintain epithelial integrity. *Nature* **421**(6918): 83-87.

ten Klooster, J.P., Jansen, M., Yuan, J., Oorschot, V., Begthel, H., Di Giacomo, V., Colland, F., de Koning, J., Maurice, M.M., Hornbeck, P. et al. 2009. Mst4 and Ezrin induce brush borders downstream of the Lkb1/Strad/Mo25 polarization complex. *Dev Cell* **16**(4): 551-562.

Xiao, G.H., Beeser, A., Chernoff, J., and Testa, J.R. 2002. p21-activated kinase links Rac/Cdc42 signaling to merlin. *J Biol Chem* **277**(2): 883-886.

Yang, H.S. and Hinds, P.W. 2003. Increased ezrin expression and activation by CDK5 coincident with acquisition of the senescent phenotype. *Mol Cell* **11**(5): 1163-1176.

Chapter 5

Discussion

The cell cortex comprises the dynamic interactions between plasma membrane proteins and/or lipids and the underlying cortical cytoskeleton (Fehon et al. 2010; Rauzi and Lenne 2011). This is the precise nexus where the ERM proteins (Ezrin, Radixin and Moesin) and closely related neurofibromatosis type 2 (*NF2*) tumor suppressor, Merlin, have emerged as key scaffolds that can assemble protein complexes to orchestrate cortical organization (McClatchey and Fehon 2009). Here, the ERMs can physically stabilize the cell cortex during mitotic rounding, membrane bleb retraction and the establishment of the apical and junctional region of epithelial cells by linking plasma membrane proteins and/or lipids directly to cortical actin (Gobel et al. 2004; Saotome et al. 2004; Van Furden et al. 2004; Charras et al. 2006; Pilot et al. 2006; Kunda et al. 2008; Luxenburg et al. 2011). ERM proteins can also control the distribution and activity of a number of associated membrane receptors (McClatchey and Fehon 2009).

Similarly, studies reveal that cortical Merlin can both control the distribution of certain membrane receptors and regulate cortical features such as cell junctions, polarity and spindle orientation (Lallemand et al. 2003; Maitra et al. 2006; Curto et al. 2007; Cole et al. 2008; Lallemand et al. 2009). Merlin and the ERMs are evolutionarily conserved and are thought to be derived from a common ancestor. They share a number of common binding partners, are co-expressed in most cell types, hetero-oligomerize, display coordinated regulation, and exhibit both distinct and overlapping localizations within cells indicating a functional relationship (McClatchey 2003; McClatchey and Fehon 2009). Defining the relationship between Merlin and the ERMs is central to considering their roles in cancer development.

Therefore the goal of my work was to gain a fundamental understanding of how Merlin and the ERMs cooperate to organize the membrane. My work advances our understanding of several basic cellular processes that Merlin and the ERMs control. Notably, I show that Merlin and the ERM proteins interdependently organize the membrane of single cells to generate cortical asymmetry in the absence of external cues.

Novel role for merlin and the ERMs in organizing the cell cortex

The *NF2* tumor suppressor gene was cloned nearly two decades ago without knowledge of the molecular basis for its associated tumor syndrome neurofibromatosis type 2 (Rouleau et al. 1993; Trofatter et al. 1993). Surprisingly, it was discovered that the *NF2*-encoded protein Merlin is closely related to the membrane:cytoskeleton associated ERM (Ezrin, Radixin and Moesin) proteins. This finding provided the first clue as to how a membrane:cytoskeleton associated protein could control cell proliferation. Indeed, this was in contrast to our knowledge of the now classic tumor suppressors p53, Rb, and NF1 that directly control the cell cycle machinery in the nucleus, or in the case of Nf1, to directly negatively regulate mitogenic Ras signaling (Sherr 2004). Many studies of Merlin function have been modeled after work on other tumor suppressors and it has been shown that overexpression of Merlin can block both cell proliferation and oncogene-induced transformation (Tikoo et al. 1994; Lutchman and Rouleau 1995). More recently, Merlin has been implicated in regulating the Hippo signaling pathway (Hamaratoglu et al. 2006) and even the expression of pro-proliferative genes in the

nucleus (Tikoo et al. 1994). Our lab has demonstrated that Merlin can associate with EGFR via the membrane adaptor NHE-RF1 and prevent mitogenic signaling in contacting cells (Curto et al. 2007); however, we have also identified key functions for Merlin in controlling other cell behaviors that impact cell proliferation less directly, such as adherens junction assembly/maturation and spindle orientation. So, is there a more proximal function of Merlin that might explain its role in controlling these multiple proliferative and non-proliferative pathways and cell behaviors?

My data suggest that Merlin may be a molecular 'Achilles heel', such that loss of its function could set in motion a series of events leading to tumorigenesis. First, loss of *Nf2* in my studies and others (Gladden et al. 2010) leads to altered spindle orientation, which may affect tissue architecture, morphogenesis and asymmetric cell divisions that maintain stem cell populations. These defects could, in turn, lead to the loss of polarity, which is critical for tissue architecture as well as receptor distribution (Maitra et al. 2006). Indeed, altering the distribution of receptors can lead to aberrant activation (Maitra et al. 2006). Ultimately, these defects could lead to centrosome unclustering and potentially changes in genome stability (Kwon et al. 2008; Godinho et al. 2009). Ultimately, my data suggest that this array of defects could all stem from the fundamental ability of Merlin to organize the membrane and restrict cortical Ezrin.

Extending our molecular studies of Merlin and the ERMs

Merlin-mediated restriction of cortical Ezrin

Going forth, a major focus will be to determine the molecular details of how Merlin mediates the restriction of Ezrin at the cortex, and how cortical organization may be coordinated with the cell cycle. The mechanism by which Ezrin is progressively restricted in a cell-cycle correlated way in normal Caco2 cells is not yet clear. In the *C. elegans* oocyte, actomyosin mediated cortical flow is required for asymmetric localization of the PAR proteins in response to the sperm entry cue (Munro et al. 2004). However, we have shown that inhibitors of myosin do not halt Ezrin cap formation indicating that this is not an equivalent mechanism (Figure 2.3A). In line with this, Par3 remains ubiquitously localized around the cortex in cells with an Ezrin cap (Figure 2.1C). In *D. melanogaster* Merlin and Moesin act as competitive substrates for Slik activity (Hughes and Fehon 2006) suggesting that Merlin might restrict Ezrin by simply competing for membrane space. However, we show that overexpression of Merlin, which localizes ubiquitously around the membrane, does not prevent Ezrin membrane localization (Figure 2.5A), so what could the mechanism be?

Activation of ERM proteins involves both the binding of the FERM domain to phosphoinositol 4,5-bisphosphate ($PI(4,5)P_2$) and phosphorylation of a conserved threonine residue on the C-terminus. Though phosphorylation is central to ERM activation, interaction with $PI(4,5)P_2$ plays an important regulatory role (Coscoy et al. 2002; Hao et al. 2009; Roch et al. 2010). Recently, Roubinet *et al* have identified

two networks that are required for the tight spatiotemporal regulation of the sole ERM ortholog, Moesin, during mitosis in *Drosophila* S2 cells (Roubinet et al. 2011). Briefly, the Pp1-87B phosphatase counteracts Slik kinase activity to restrict Moesin activity to early mitosis. Then, the PI(4)P 5-kinase Skittles and PI $(3,4,5)P_3$ phosphatase Pten further refine the pattern of activated Moesin through the local production of $PI(4,5)P_2$ which is required for both Moesin cortical recruitment and phosphorylation.

In *Drosophila* S2 cells, Pp1-87B and Slik restrict activation of Moesin to mitosis. Notably, in CaCo2 cells, activated Ezrin concentrates into a cap during G1, prior to S phase (Figure 2.1D), a process for which SLK is dispensable. Instead, Cdk5 is required for ERM activation and membrane localization prior to S phase, indicating that other kinases could temporally activate ERMs at different points during the cell cycle. In the context of spatial restriction of Ezrin, we note that Merlin is required for Ezrin cap formation but not recruitment to the cleavage furrow. Therefore, we hypothesize that kinases or phosphatases that directly or indirectly control $PI(4,5)P_2$ metabolism, other than Skittles or Pten, could regulate cortical restriction of Ezrin during G1. If it is true that lipid metabolism mediates Ezrin cap formation in single cells it will be important to determine if Merlin's α-catenin dependent association with the cortical cytoskeleton is required for proper generation of $PI(4,5)P_2$ at the membrane or for Ezrin's association with it.

Coordinating cortical asymmetry and the cell cycle

In many contexts cortical organization is intimately linked with the cell cycle. This connection is particularly important for process such as asymmetric cell division, which ultimately regulates progenitor cell populations (Morin and Bellaiche 2011). Our studies highlight a cell cycle correlated restriction of Ezrin prior to S phase (Figure 2.1D). Notably, Cdk5 is not required for the dynamic restriction of Ezrin, but rather for Ezrin activation and membrane localization prior to S phase. This mechanism is independent of Ezrin activation and localization to the cleavage furrow during cytokinesis. Cdk5 is a serine/threonine kinase that belongs to the cyclin-dependent kinase (Cdk) family (Dhavan and Tsai 2001). While classical Cdks bind cyclins for their activation and are master regulators of cell cycle progression (Morgan 1997), Cdk5 is activated by the non-cyclin proteins p35 and p39, whose expression is restricted to postmitotic neurons (Dhavan and Tsai 2001). Though Cdk5 activity is not known to be regulated in a cell cycle dependent manner, expression of the retinoblastoma protein pRB in cells that lack it (SAOS-2 cells) leads to Cdk5 activation in a p35 dependent fashion (Mao and Hinds 2010). Therefore, Cdk5 activity might cycle with pRB activity in G1. If this were true, it would fit well with our observation of Cdk5 dependent activation of Ezrin in G1. It is also worth noting that Cdk5 phosphorylates Ezrin on the FERM domain at residue T235, which is distinct from phosphorylation of the C-terminal threonine residue (T567) that is thought to be activating (Yang and Hinds 2003). In this regard, it will be important to determine how phosphorylation of other residues within ERMs might be involved in either promoting or preventing ERM activation.

Ezrin as a positional cue for the centrosome

Our studies have identified Ezrin as a critical cue to position the interphase centrosome. In fact, the centrosome remains positioned beneath the Ezrin-decorated cortex during the progressive, cell-cycle correlated restriction of Ezrin (Figure 4A). These observations fit well with studies showing that cues associated with Ezrin cortical patches are critical for correct positioning of the mitotic spindle (Thery et al. 2005). Briefly, Thery *et al* demonstrated, using ECM micropatterning, that rounded mitotic cells maintain memory of their ECM attachments via retraction fibers and cortical Ezrin, which guides orientation of the subsequent mitotic spindle (Thery et al. 2005). Astral microtubules connect centrosomes to the cell cortex and apply pulling forces to the cortical cytoskeleton during mitosis (Manneville and Etienne-Manneville 2006; Kunda and Baum 2009; Vaughan and Dawe 2010). This raises the important question of whether the centrosime mediates restriction of cortical Ezrin via astral microtubules or whether the centrosome uses astral microtubules to associate with the cortical Ezrin cap. Our studies suggest the latter and are consistent with a model wherein Ezrin locally stabilizes actin, providing a force-generating platform for astral microtubule-mediated centrosome positioning.

The mechanism by which the centrosome interacts with enriched cortical Ezrin and actin is unclear. Indeed, evidence suggests crosstalk between microtubules and the actin cytoskeleton is important for a number of biological processes including spindle orientation during mitosis (Lasserre and Alcover ; Kunda and Baum 2009). Recently, studies have demonstrated that prior to nuclear envelope breakdown (NEB) in the *D. melanogaster* embryo, proper centrosome

separation does not require myosin II but requires dynamic actin rearrangements at the growing edge of the interphase cap (Cao et al.). Interestingly, they and others demonstrated that APC2 provides an important physical link between spindles and cortical actin (Cao et al. ; McCartney et al. 2001) suggesting that APC2 may link the Ezrin cap to the centrosome via astral microtubules in CaCo2 cells. Indeed, preliminary evidence shows that APC2 is required for centrosome association with the Ezrin cap. Interestingly, we noted that during mitosis one centrosome remains associated with the Ezrin cap while the other migrates to the opposite end of the cell. In that regard, we aim to investigate how differences in mother vs. daughter centrosomes might impact their association with the Ezrin decorated cortex.

Novel role for Merlin and ERMs in tumorigenesis

Current understanding of Merlin as a tumor suppressor

Despite extensive analyses of Merlin function over almost two decades, it is still unclear how it functions as a tumor suppressor. There is abundant evidence in both flies and mice that Merlin regulates growth factor receptor abundance and/or availability at the cell surface to control proliferation. In *D. melanogaster* Merlin functions with the FERM-domain-containing tumor suppressor, Expanded, (McCartney et al. 2000; Maitra et al. 2006) such that loss of both Merlin and Expanded yield increased surface abundance of EGFR, Notch and Patched suggesting that Merlin might promote receptor clearance or inhibit receptor recycling. In support of the notion that receptor abundance can lead to activation and

overproliferation, a downstream reporter of EGFR signaling is upregulated in mutant cells (Maitra et al. 2006). Additionally, studies from our lab demonstrate that loss of Merlin yields persistent EGFR internalization and signaling at high cell density, which does not occur in confluent wild-type cells, indicating that Merlin normally prevents EGFR endocytosis and signaling upon cell:cell contact (Curto et al. 2007). Although the mechanism by which Merlin might regulate receptor abundance and activation is not known, my work suggests that Merlin and Ezrin could work together to define cortical domains to/from which receptors are differentially trafficked. This could represent a fundamental intersection between cell polarity and receptor trafficking.

It is also not clear whether deregulation of receptor activity is the only or even the major driver of tumorigenesis in Merlin deficient cells. Though human patients develop benign Schwann cell tumors upon biallelic inactivation of *Nf2,* mouse models reveal an unexpectedly broad role for Merlin in many different cell types (McClatchey et al. 1997; Giovannini et al. 2000; Kalamarides et al. 2002). Indeed, heterozygous *Nf2* mutation leads to the development of a range of highly metastatic tumors including osteosarcomas and hepatocellular carcinomas (McClatchey et al. 1998).

Potential role for Merlin in promoting genomic stability

My work suggests that Merlin deficiency may contribute to tumor progression via a different mechanism. In Chapter 2 I showed that a key function for Merlin is to restrict cortical Ezrin, which is critical for proper centrosome

positioning, spindle orientation and tissue architecture. Notably, these features are often perturbed in cancer cells. In many cancer cells supernumerary centrosomes are clustered such that cells retain the ability to form bipolar spindles. The mechanisms controlling centrosome clustering are not well understood but recent studies suggest a key role for the force-generating properties of the cortical actin cytoskeleton (Kwon et al. 2008). In line with our observations we note that loss of Merlin yields unclustered centrosomes and multipolar spindles in several types of cells that harbor supernumerary centrosomes.

Aberrant centrosome clustering could affect genome stability (Kwon et al. 2008). For example, transient defects in centrosome clustering can promote chromosome missegregation and aneuploidy (Ganem et al. 2009). Indeed, inactivation of *NF2* is found in an increasing number of sporadic malignant human cancers including mesothelioma and renal adenocarcinoma, both of which are often aneuploid (Musti et al. 2006; Dalgliesh et al. 2010). Preliminary evidence from our lab indicates that Merlin deficiency in both mesothelioma and renal cell lines correlates with unclustered centrosomes and multipolar spindles, which can be rescued by exogenous Merlin. Alternatively, loss of spindle pole clustering can also decrease cell viability due to mitotic castrophe (Ganem et al. 2009). Thus in some contexts loss of Merlin could actually favor tumor genome stability, as displayed by the benign schwannomas and meningiomas that NF2 patients predominantly develop. A major goal will be to determine if failure to restrict Ezrin at the cortex in the context of *Nf2* deficiency promotes tumorigenesis via mitotic defects and chromosomal instability.

It will be particularly interesting to investigate the role of centrosome unclustering in Nf2-deficient renal tumors. Our lab has demonstrated that targeted deletion of *Nf2* in the mouse kidney yields hyperplastic lesions throughout the kidney that exhibit ectopic Ezrin localization and progress to eventually become invasive adenocarcinomas by 6 months of age (Morris and McClatchey 2009). Interestingly, a key causative factor for renal cancers in humans is mutation of the von Hippel Lindau (*VHL*) tumor suppressor gene. Familial *VHL* patients that harbor heterozygous germline inactivating VHL mutation are predisposed to developing renal tumors and cysts. The best studied function of the VHL protein, pVHL, is a component of a ubiquitin ligase complex that targets the transcriptional activator hyoxia-inducible factor (*HIF*) for degradation. In the absence of pVHL active HIF allows tumor cells to adapt to the low oxygen environment that occurs in many tumors (Kaelin 2009). However, pVHL is also an efficient microtubule-stabilizing protein, which in turn, has been linked to pVHL-mediated control of mitotic spindle orientation, chromosome stability and cilium formation (Frew and Krek 2007; Thoma et al. 2007; Thoma et al. 2009; Thoma et al. 2010). While about half of sporadic renal tumors harbor inactivating *VHL* mutations, little is known about other driving mutations. Indeed, genes that are commonly mutated in other cancers, including *Ras, ErbBs, p53* and *Rb*, are not mutated frequently in renal cancer.

Our lab has demonstrated that deletion of *Nf2* in the proximal convoluted tubule (PCT) of the mouse kidney leads to a rapid, multifocal and fully penetrant model of renal adenocarcinoma (Morris and McClatchey 2009). In addition, we

identified two *Nf2* mutations in renal cancers in the COSMIC database and Dalgleish *et al* identified 7 *Nf2* mutations in a large panel of human renal carcinoma samples and cell lines which do not contain *VHL* mutations or exhibit a hypoxic signature (Dalgliesh et al. 2010). Thus, *Nf2* deficiency might contribute to *VHL* independent renal cancers for which little is known. Evidence suggests that certain cell types or cellular contexts are differentially sensitive to loss of specific Merlin activities and the molecular basis for this is not understood. The kidney is one setting that appears particularly sensitive to the organizational/mitotic spindle defects observed upon loss of Merlin or pVHL function. Therefore, an understanding the molecular relationship between Merlin and pVHL in the kidney would be highly beneficial for determining which specific functions of Merlin are most critical for different cell types and contexts.

Treating Nf2 deficient human cancers

Molecular studies over the years have identified an array of receptors and signaling pathways that Merlin can regulate. Despite this knowledge there are currently no effective treatments for neurofibromatosis type 2 patients. For example, studies from our lab have shown that Merlin can negatively regulate EGFR signaling upon cell contact (Curto et al. 2007). Furthermore, we have demonstrated that pharmacologic inhibition of EGFR blocks the proliferation of *Nf2* deficient liver progenitors in vitro and in vivo (Benhamouche et al. 2010). However, treatment of NF2 patients with the EGFR inhibitor erlotonib showed inconsistent effects (Plotkin et al. 2010). The development of targeted therapies relies heavily on a clear

molecular understanding of disease pathology, in this case *Nf2* deficiency. However, my studies suggest that there is much more that we need to understand about Merlin before we can begin to effectively treat NF2 patients. Clearly, this is a call for more basic research.

Considering that Merlin plays such a fundamental role in orchestrating an array of cellular activities it is difficult to imagine how a simple, strait forward therapeutic approach might be effective. Indeed, attempts to treat patients by targeting signaling pathways downstream of Merlin have been ineffective. To continue this strategy would be to ignore what we now understand about Merlin function and would likely lead to failure. In the case of NF2, the best alternative might be to re-introduce a functional version of Merlin. Unfortunately, this is not yet technically feasible and therefore requires a different approach.

My studies and others have shown that Merlin function is highly cell type and cell context specific. Cells express specific receptor types, are exposed to different receptor ligands, they interact with a number of different cell types and display specific cell architectures. In addition, my studies suggest that different mutations in *Nf2* could affect discrete Merlin functions. Therefore, depending on a given cell type, tumor context, and *Nf2* mutation we can expect that our approach to treatment will need to be just as specific. Clearly, this will require a personalized medicine approach. With the advent of rapid next-gen sequencing technologies individual patient and tumor information may be readily available in the near future.

In thinking how we might treat the typical NF2 patient that develops schwannomas following biallelic inactivation of *Nf2*, my studies suggest an exciting

new possibility. Both *in vitro* and *in vivo* I have shown that loss of Merlin and ERM function together is detrimental to cells. Therefore, we expect that Merlin deficient schwannomas in NF2 patients would be particularly sensitized to loss of ERM function. To this end, we might imagine developing a pharmacologic inhibitor that locks the ERM proteins into an inactive confirmation or prevents their binding to actin or membrane receptors. It is not known if the ERMs are easily "druggable", therefore, an alternative might be to target the kinases known to activate the ERMs. Indeed, inhibitors to Rho kinase are already available.

Distinct from the typical schwannomas that NF2 patients develop, inactivation of *NF2* is found in an increasing number of sporadic malignant human cancers including mesothelioma and renal adenocarcinoma, both of which are often aneuploid (Musti et al. 2006; Dalgliesh et al. 2010). We have recently found in a small set of *NF2* deficient mesothelioma cells containing supernumerary centrosomes fail to properly cluster their centrosomes to maintain a bipolar spindle. This one case where we might therapeutically target *Nf2* deficient cells differently. In this case, loss of Merlin may perturb spindles as a result of unclustered centrosomes leading to aneuploidy. Perhaps treatment with nocodazole, which also affects clustering, could be synthetically lethal here by pushing the cell into mitotic catastrophe. Along these lines, Aurora kinase inhibitors may also be effective treatments as they are essential for proper centrosome separation (Glover et al. 1995). Indeed, a plethora of Aurora kinase inhibitors have been described (Taylor and Peters 2008), and recently the Aurora kinase inhibitor ZM447439 was shown to inhibit cell growth in all mesothelioma cell lines tested

(Crispi et al. 2010). Though the basis for sensitivity to this drug is unknown, we speculate that it may involve *Nf2* deficiency. Consequently, this is one example where cell context might be an important consideration for how we treat *Nf2* deficient tumors.

References

Benhamouche, S., Curto, M., Saotome, I., Gladden, A.B., Liu, C.H., Giovannini, M., and McClatchey, A.I. 2010. Nf2/Merlin controls progenitor homeostasis and tumorigenesis in the liver. *Genes Dev* **24**(16): 1718-1730.

Cao, J., Crest, J., Fasulo, B., and Sullivan, W. Cortical actin dynamics facilitate early-stage centrosome separation. *Curr Biol* **20**(8): 770-776.

Charras, G.T., Hu, C.K., Coughlin, M., and Mitchison, T.J. 2006. Reassembly of contractile actin cortex in cell blebs. *J Cell Biol* **175**(3): 477-490.

Cole, B.K., Curto, M., Chan, A.W., and McClatchey, A.I. 2008. Localization to the cortical cytoskeleton is necessary for Nf2/merlin-dependent epidermal growth factor receptor silencing. *Mol Cell Biol* **28**(4): 1274-1284.

Coscoy, S., Waharte, F., Gautreau, A., Martin, M., Louvard, D., Mangeat, P., Arpin, M., and Amblard, F. 2002. Molecular analysis of microscopic ezrin dynamics by two-photon FRAP. *Proc Natl Acad Sci U S A* **99**(20): 12813-12818.

Crispi, S., Fagliarone, C., Biroccio, A., D'Angelo, C., Galati, R., Sacchi, A., Vincenzi, B., Baldi, A., and Verdina, A. 2010. Antiproliferative effect of Aurora kinase targeting in mesothelioma. *Lung Cancer* **70**(3): 271-279.

Curto, M., Cole, B.K., Lallemand, D., Liu, C.H., and McClatchey, A.I. 2007. Contact-dependent inhibition of EGFR signaling by Nf2/Merlin. *J Cell Biol* **177**(5): 893-903.

Dalgliesh, G.L., Furge, K., Greenman, C., Chen, L., Bignell, G., Butler, A., Davies, H., Edkins, S., Hardy, C., Latimer, C. et al. 2010. Systematic sequencing of renal carcinoma reveals inactivation of histone modifying genes. *Nature* **463**(7279): 360-363.

Dhavan, R. and Tsai, L.H. 2001. A decade of CDK5. *Nat Rev Mol Cell Biol* **2**(10): 749-759.

Fehon, R.G., McClatchey, A.I., and Bretscher, A. 2010. Organizing the cell cortex: the role of ERM proteins. *Nat Rev Mol Cell Biol* **11**(4): 276-287.

Frew, I.J. and Krek, W. 2007. Multitasking by pVHL in tumour suppression. *Curr Opin Cell Biol* **19**(6): 685-690.

Ganem, N.J., Godinho, S.A., and Pellman, D. 2009. A mechanism linking extra centrosomes to chromosomal instability. *Nature* **460**(7252): 278-282.

Giovannini, M., Robanus-Maandag, E., van der Valk, M., Niwa-Kawakita, M., Abramowski, V., Goutebroze, L., Woodruff, J.M., Berns, A., and Thomas, G. 2000. Conditional biallelic Nf2 mutation in the mouse promotes manifestations of human neurofibromatosis type 2. *Genes Dev* **14**(13): 1617-1630.

Gladden, A.B., Hebert, A.M., Schneeberger, E.E., and McClatchey, A.I. 2010. The NF2 tumor suppressor, Merlin, regulates epidermal development through the establishment of a junctional polarity complex. *Dev Cell* **19**(5): 727-739.

Glover, D.M., Leibowitz, M.H., McLean, D.A., and Parry, H. 1995. Mutations in aurora prevent centrosome separation leading to the formation of monopolar spindles. *Cell* **81**(1): 95-105.

Gobel, V., Barrett, P.L., Hall, D.H., and Fleming, J.T. 2004. Lumen morphogenesis in C. elegans requires the membrane-cytoskeleton linker erm-1. *Dev Cell* **6**(6): 865-873.

Godinho, S.A., Kwon, M., and Pellman, D. 2009. Centrosomes and cancer: how cancer cells divide with too many centrosomes. *Cancer Metastasis Rev* **28**(1-2): 85-98.

Hamaratoglu, F., Willecke, M., Kango-Singh, M., Nolo, R., Hyun, E., Tao, C., Jafar-Nejad, H., and Halder, G. 2006. The tumour-suppressor genes NF2/Merlin and Expanded act through Hippo signalling to regulate cell proliferation and apoptosis. *Nat Cell Biol* **8**(1): 27-36.

Hao, J.J., Liu, Y., Kruhlak, M., Debell, K.E., Rellahan, B.L., and Shaw, S. 2009. Phospholipase C-mediated hydrolysis of PIP2 releases ERM proteins from lymphocyte membrane. *J Cell Biol* **184**(3): 451-462.

Hughes, S.C. and Fehon, R.G. 2006. Phosphorylation and activity of the tumor suppressor Merlin and the ERM protein Moesin are coordinately regulated by the Slik kinase. *J Cell Biol* **175**(2): 305-313.

Kaelin, W.G., Jr. 2009. Treatment of kidney cancer: insights provided by the VHL tumor-suppressor protein. *Cancer* **115**(10 Suppl): 2262-2272.

Kalamarides, M., Niwa-Kawakita, M., Leblois, H., Abramowski, V., Perricaudet, M., Janin, A., Thomas, G., Gutmann, D.H., and Giovannini, M. 2002. Nf2 gene inactivation in arachnoidal cells is rate-limiting for meningioma development in the mouse. *Genes Dev* **16**(9): 1060-1065.

Kunda, P. and Baum, B. 2009. The actin cytoskeleton in spindle assembly and positioning. *Trends Cell Biol* **19**(4): 174-179.

Kunda, P., Pelling, A.E., Liu, T., and Baum, B. 2008. Moesin controls cortical rigidity, cell rounding, and spindle morphogenesis during mitosis. *Curr Biol* **18**(2): 91-101.

Kwon, M., Godinho, S.A., Chandhok, N.S., Ganem, N.J., Azioune, A., Thery, M., and Pellman, D. 2008. Mechanisms to suppress multipolar divisions in cancer cells with extra centrosomes. *Genes Dev* **22**(16): 2189-2203.

Lallemand, D., Curto, M., Saotome, I., Giovannini, M., and McClatchey, A.I. 2003. NF2 deficiency promotes tumorigenesis and metastasis by destabilizing adherens junctions. *Genes Dev* **17**(9): 1090-1100.

Lallemand, D., Manent, J., Couvelard, A., Watilliaux, A., Siena, M., Chareyre, F., Lampin, A., Niwa-Kawakita, M., Kalamarides, M., and Giovannini, M. 2009. Merlin regulates transmembrane receptor accumulation and signaling at the plasma membrane in primary mouse Schwann cells and in human schwannomas. *Oncogene* **28**(6): 854-865.

Lasserre, R. and Alcover, A. Cytoskeletal cross-talk in the control of T cell antigen receptor signaling. *FEBS Lett* **584**(24): 4845-4850.

Lutchman, M. and Rouleau, G.A. 1995. The neurofibromatosis type 2 gene product, schwannomin, suppresses growth of NIH 3T3 cells. *Cancer Res* **55**(11): 2270-2274.

Luxenburg, C., Pasolli, H.A., Williams, S.E., and Fuchs, E. 2011. Developmental roles for Srf, cortical cytoskeleton and cell shape in epidermal spindle orientation. *Nat Cell Biol* **13**(3): 203-214.

Maitra, S., Kulikauskas, R.M., Gavilan, H., and Fehon, R.G. 2006. The tumor suppressors Merlin and Expanded function cooperatively to modulate receptor endocytosis and signaling. *Curr Biol* **16**(7): 702-709.

Manneville, J.B. and Etienne-Manneville, S. 2006. Positioning centrosomes and spindle poles: looking at the periphery to find the centre. *Biol Cell* **98**(9): 557-565.

Mao, D. and Hinds, P.W. 2010. p35 is required for CDK5 activation in cellular senescence. *J Biol Chem* **285**(19): 14671-14680.

McCartney, B.M., Kulikauskas, R.M., LaJeunesse, D.R., and Fehon, R.G. 2000. The neurofibromatosis-2 homologue, Merlin, and the tumor suppressor expanded function together in Drosophila to regulate cell proliferation and differentiation. *Development* **127**(6): 1315-1324.

McCartney, B.M., McEwen, D.G., Grevengoed, E., Maddox, P., Bejsovec, A., and Peifer, M. 2001. Drosophila APC2 and Armadillo participate in tethering mitotic spindles to cortical actin. *Nat Cell Biol* **3**(10): 933-938.

McClatchey, A.I. 2003. Merlin and ERM proteins: unappreciated roles in cancer development? *Nat Rev Cancer* **3**(11): 877-883.

McClatchey, A.I. and Fehon, R.G. 2009. Merlin and the ERM proteins--regulators of receptor distribution and signaling at the cell cortex. *Trends Cell Biol* **19**(5): 198-206.

McClatchey, A.I., Saotome, I., Mercer, K., Crowley, D., Gusella, J.F., Bronson, R.T., and Jacks, T. 1998. Mice heterozygous for a mutation at the Nf2 tumor suppressor locus develop a range of highly metastatic tumors. *Genes Dev* **12**(8): 1121-1133.

McClatchey, A.I., Saotome, I., Ramesh, V., Gusella, J.F., and Jacks, T. 1997. The Nf2 tumor suppressor gene product is essential for extraembryonic development immediately prior to gastrulation. *Genes Dev* **11**(10): 1253-1265.

Morgan, D.O. 1997. Cyclin-dependent kinases: engines, clocks, and microprocessors. *Annu Rev Cell Dev Biol* **13**: 261-291.

Morin, X. and Bellaiche, Y. 2011. Mitotic spindle orientation in asymmetric and symmetric cell divisions during animal development. *Dev Cell* **21**(1): 102-119.

Morris, Z.S. and McClatchey, A.I. 2009. Aberrant epithelial morphology and persistent epidermal growth factor receptor signaling in a mouse model of renal carcinoma. *Proc Natl Acad Sci U S A* **106**(24): 9767-9772.

Munro, E., Nance, J., and Priess, J.R. 2004. Cortical flows powered by asymmetrical contraction transport PAR proteins to establish and maintain anterior-posterior polarity in the early C. elegans embryo. *Dev Cell* **7**(3): 413-424.

Musti, M., Kettunen, E., Dragonieri, S., Lindholm, P., Cavone, D., Serio, G., and Knuutila, S. 2006. Cytogenetic and molecular genetic changes in malignant mesothelioma. *Cancer Genet Cytogenet* **170**(1): 9-15.

Pilot, F., Philippe, J.M., Lemmers, C., and Lecuit, T. 2006. Spatial control of actin organization at adherens junctions by a synaptotagmin-like protein Btsz. *Nature* **442**(7102): 580-584.

Plotkin, S.R., Halpin, C., McKenna, M.J., Loeffler, J.S., Batchelor, T.T., and Barker, F.G., 2nd. 2010. Erlotinib for progressive vestibular schwannoma in neurofibromatosis 2 patients. *Otol Neurotol* **31**(7): 1135-1143.

Rauzi, M. and Lenne, P.F. 2011. Cortical forces in cell shape changes and tissue morphogenesis. *Curr Top Dev Biol* **95**: 93-144.

Roch, F., Polesello, C., Roubinet, C., Martin, M., Roy, C., Valenti, P., Carreno, S., Mangeat, P., and Payre, F. 2010. Differential roles of PtdIns(4,5)P2 and phosphorylation in moesin activation during Drosophila development. *J Cell Sci* **123**(Pt 12): 2058-2067.

Roubinet, C., Decelle, B., Chicanne, G., Dorn, J.F., Payrastre, B., Payre, F., and Carreno, S. 2011. Molecular networks linked by Moesin drive remodeling of the cell cortex during mitosis. *J Cell Biol* **195**(1): 99-112.

Rouleau, G.A., Merel, P., Lutchman, M., Sanson, M., Zucman, J., Marineau, C., Hoang-Xuan, K., Demczuk, S., Desmaze, C., Plougastel, B. et al. 1993. Alteration in a new gene encoding a putative membrane-organizing protein causes neuro-fibromatosis type 2. *Nature* **363**(6429): 515-521.

Saotome, I., Curto, M., and McClatchey, A.I. 2004. Ezrin is essential for epithelial organization and villus morphogenesis in the developing intestine. *Dev Cell* **6**(6): 855-864.

Sherr, C.J. 2004. Principles of tumor suppression. *Cell* **116**(2): 235-246.

Taylor, S. and Peters, J.M. 2008. Polo and Aurora kinases: lessons derived from chemical biology. *Curr Opin Cell Biol* **20**(1): 77-84.

Thery, M., Racine, V., Pepin, A., Piel, M., Chen, Y., Sibarita, J.B., and Bornens, M. 2005. The extracellular matrix guides the orientation of the cell division axis. *Nat Cell Biol* **7**(10): 947-953.

Thoma, C.R., Frew, I.J., Hoerner, C.R., Montani, M., Moch, H., and Krek, W. 2007. pVHL and GSK3beta are components of a primary cilium-maintenance signalling network. *Nat Cell Biol* **9**(5): 588-595.

Thoma, C.R., Matov, A., Gutbrodt, K.L., Hoerner, C.R., Smole, Z., Krek, W., and Danuser, G. 2010. Quantitative image analysis identifies pVHL as a key regulator of microtubule dynamic instability. *J Cell Biol* **190**(6): 991-1003.

Thoma, C.R., Toso, A., Gutbrodt, K.L., Reggi, S.P., Frew, I.J., Schraml, P., Hergovich, A., Moch, H., Meraldi, P., and Krek, W. 2009. VHL loss causes spindle misorientation and chromosome instability. *Nat Cell Biol* **11**(8): 994-1001.

Tikoo, A., Varga, M., Ramesh, V., Gusella, J., and Maruta, H. 1994. An anti-Ras function of neurofibromatosis type 2 gene product (NF2/Merlin). *J Biol Chem* **269**(38): 23387-23390.

Trofatter, J.A., MacCollin, M.M., Rutter, J.L., Murrell, J.R., Duyao, M.P., Parry, D.M., Eldridge, R., Kley, N., Menon, A.G., Pulaski, K. et al. 1993. A novel moesin-, ezrin-, radixin-like gene is a candidate for the neurofibromatosis 2 tumor suppressor. *Cell* **75**(4): 826.

Van Furden, D., Johnson, K., Segbert, C., and Bossinger, O. 2004. The C. elegans ezrin-radixin-moesin protein ERM-1 is necessary for apical junction remodelling and tubulogenesis in the intestine. *Dev Biol* **272**(1): 262-276.

Vaughan, S. and Dawe, H.R. 2010. Common themes in centriole and centrosome movements. *Trends Cell Biol* **21**(1): 57-66.

Yang, H.S. and Hinds, P.W. 2003. Increased ezrin expression and activation by CDK5 coincident with acquisition of the senescent phenotype. *Mol Cell* **11**(5): 1163-1176.